A Thesis on

THE KINETICS of CRYSTALLISATION and DISSOLUTION of SPARINGLY SOLUBLE SALTS in AQUEOUS SOLUTIONS.

by

NEIL PURDIE B.Sc. Supervisor, Dr. G.H.NANCOLLAS.

presented for the degree of DOCTOR of PHILOSOPHY.

to

The UNIVERSITY of GLASGOW. October, 1961.

SUMMARY.

In a kinetic study of the crystallisation of sparingly soluble salts from supersaturated solutions the dependence of crystal nucleation in spontaneous growth on such effects as the geometry of the apparatus, the purity of the solutions, the previous history of the water etc., warrants the use of the more reproducible method of growth by inoculation with seed crystals. This method is used in the present work.

In an adsorbed layer theory suggested by Davies and Jones, growth and dissolution are described as non-reciprocal processes. The theory has been su successfully tested in growth and in dissolution work on silver chloride, a 1-1 electrolyte and silver chromate, a 2-1 electrolyte.

In the first part of this thesis the study of the dissolution of silver chloride was extended to solutions of non-equivalent ionic concentrations. These conditions effectively alter the ion distribution in the layer, the ion in excess in solution being in excess in the adsorbed layer. As in equivalent ionic concentration conditions, good first order kinetic plots were observed in accordance with the theory of diffusion control in dissolution reactions.

Parts 2a. and 2b. were designed to test the adequacy of the theory to include 2-2 electrolytes. Magnesium oxalate, a fairly soluble salt, forms a very stable complex in solution,

$$Mg^{2+} + Ox^{2-} \rightleftharpoons MgOx.$$

The theory of growth requires that a second order rate equation in ionic concentrations should be obeyed,

$$-\frac{dm}{dt} = k(m - m_o)^2.$$

and in spite of this complex formation, growth was explained by the theory at equivalent and non-equivalent concentrations and in the presence of adsorbates. Considerable retardation was observed in presence of adsorbates and from a Langmuir adsorption isotherm treatment of results the observed rate constant approached a limiting value as adsorbate concentration was increased, illustrating that adsorption accurred only at specific crystal sites. Crystallisation was followed by conductivity, titrimetric and photographic techniques. Spontaneous crystallisation was observed at supersaturations above a certain limit, but could be eliminated by increasing the seed concentration, The rate of growth was independent of the increasing

PREFACE.

This work was carried out from October, 1958 to October, 1961, at the University of Glasgow in the Department of Physical Chemistry, which is under the supervision of Professor J. Monteath Robertson, F.R.S.

A reprint from the Transactions of the Faraday Society is appended, dealing with the work on silver chloride dissolution; the work on the crystallisation of magnesium oxalate has been accepted for publication in the same journal.

Thanks are due to the Department of Scientific and Industrial Research for a maintenance grant during the first two years of this work. I am also indebted to Messrs. Unilever for providing the Transformer Ratio Arm Bridge, to Mr. J. Leslie who constructed the conductivity cells, to Dr. H.F. Steedman for the use of the photomicroscope, and to Dr. H.S. Dunsmore for computation of results.

Above all I would like to record my sincere gratitude to Dr. G.M. Nancollas for the keen interest, encouragement and patience which he has shown at all times throughout this work.

CONTENTS.

Kinetic Studies of the Precipitation and Dissolution of Sparingly Soluble Salts.

GENERAL INTRODUCTION:

At first sight the growth and dissolution of crystals may be considered to be exactly reciprocal processes. That this is not the case becomes apparent on referring to the relevant literature. On the contrary both phenomena are individualistic and so complex that many conflicting ideas and theories at present prevail.

Both processes are heterogeneous in character and a general approach to the possible features involved in the mechanisms has been outlined by Bircumshaw and Riddiford [1]. These authors consider the steps at a crystal solid-solution interface to be five fold, and either crystal growth or dissolution occurs depending upon the relative rates of these

steps. The steps involved are:-

1) Transport of solute to the interface.
2) Adsorption of solute at the interface.
3) Chemical reaction at the interface.
4) Desorption of products from the interface.
5) Transport of solute from the interface to the bulk of the solution.

Steps 2, 3 and 4 have been combined to give one overall interface step by Davies and Jones [2]; so that in crystallisation, 2 is faster than 4 and vice versa for dissolution. This three step mechanism is used throughout the present work. Bircumshaw and Riddiford elaborate upon the relative rates of step 1 with respect to 2 for crystallisation. If 1 is faster then the rate of the reaction is controlled by the slow interface step, and diffusion is the controlling step if 2 is very much faster than 1. A direct analogy can be drawn for dissolution if the relative rates of steps 2 and 3 are compared.

Assimilation of the solute units into the crystal lattice during growth and the reverse process in dissolution is not considered, but it is generally

accepted that suitable sites for growth or dissolution are kinks in dislocations or molecular terraces as described by Burton, Cabrera and Frank [3]. For example more rapid growth after etching lithium fluoride crystals, which may be considered to introduce dislocations, was described by Sears [4]: and in the growth of barium titanate, whose crystal structure is of a butterfly wing, de Vries and Sears [5] observed thickening on only the side of the crystal which was etched. Johnson and O'Rourke [6] and Nielsen [7] however, describe and prefer a process of two dimensional surface nucleation which had previously been outlined by Becker and Döring [8]. This theory does not consider growth to proceed continuously by a screw dislocation, but rather by fresh nucleation on low index planes of the crystals.

Apart from the mechanism occurring on the surface, and necessarily involved in step 2, there is considerable controversy about the mechanism of deposition and removal of solute across the interfacial boundary. This aspect is of importance because of its direct application to quantitative inorganic analysis. Consequently the bulk of the work has been done on

precipitations which involve spontaneous crystallisation.

Ostwald [9.] originally described two regions of supersaturation: a metastable region where crystallisation occurred only by inoculation with seed crystals, and a labile region wherein spontaneous crystallisation was rapid. Precipitations from the labile region followed kinetically, often show an induction period where nucleus formation is proceeding. It was concluded by von Weimarn [10.] that the rate of precipitation and the number of particles was proportional to the degree of supersaturation at the time of precipitation. A similar idea suggested by Christiansen and Nielsen [11.] was that the time of crystallisation varied inversely as some significant power of the initial concentration.

However these ideas are considered to be inadequate. and other factors must affect the rate. Turnbull [12.] suggests that the rate is highly dependent on the size of the initial particles, and Fischer [13.] stresses the importance of induced nucleation. Such items as dust, mechanical shock, age of solutions [14.], previous history of the water used in preparation of solutions [15.] and the physical state of the container all affect the

time of nucleation of particles. Fischer goes as far as to say that pure homogeneous nucleation cannot be achieved.

If we consider spontaneous crystallisation to occur purely by homogeneous nucleation and growth, then the problem is whether or not these mechanisms exist concurrently or consecutively. Collins and Leineweber [16.] in a kinetic study of homogeneous precipitation of barium sulphate by conductivity and light scattering techniques, favour the consecutive timeing of the mechanism. Nucleation, they say, occurs in an initial burst and is subsequently followed by diffusion controlled growth. This view is shared by Turnbull [12.] but subsequent growth he describes as being interface controlled. Dunning and Notley [17.] describe a method for arresting nucleation and following the two consecutive mechanisms individually in the growth of cyclonite crystals. On the other hand, Christiansen, Nielsen, Johnson and O'Rourke, and Kolthoff prefer to describe the nucleation and growth mechanisms as concurrent, nucleation being gradually eliminated as the supersaturation is depleted by the growth mechanism.

Johnson and O'Rourke [6.] by evaluating a chronometric

integral for both mechanisms working simultaneously arrive at a fourth order kinetic equation, a result which is in agreement with experimental results on barium sulphate precipitation observed by Nielsen [7]. Earlier work by Christiansen and Nielsen [18] had described the rate of nucleation alone of barium sulphate as an eighth order reaction,

$$k = t.c_o^8 \qquad \text{\_\_\_\_\_ (1)}$$

where $\underline{t}$ = time of precipitation

c_o = initial concentration.

and the power of eight was explained as being the number of ion species present in the crystal nucleus or germ, which could withstand thermal effects etc. and initiate the growth process. That equation)1) was general was proved by applying it to results for silver chromate (Christiansen and Nielsen) and for calcium fluoride from experimental results obtained by Tovberg Jensen [19] when the significant numbers of ions in the germ and in the equation were 6 and 9 respectively.

Work by Kolthoff [20] on growth of lead sulphate crystals describes a phenomenon of self induction whereby nuclei formed in the earlier stages of the

precipitation can promote the formation of new nuclei before nucleation is completely suppressed. A similar effect has been observed in the present work, that even when seed crystals are added to inoculate growth, nucleation can be induced if the concentration of the seed is insufficient to accommodate the initial growth surge.

Everything considered it would appear that elucidation of the kinetics of spontaneous crystallisation is extremely difficult, without considering the consequences of induced nucleation. Reproducibility is very difficult if not impossible, and a more systematic method of studying crystal growth would be to eliminate nucleation entirely by inoculating solutions of supersaturation in the metastable region by addition of suitable seed crystals.

This method has been exploited by C.W. Davies and his co-workers on the kinetics of crystallisation of silver chloride from supersaturated solutions, at equivalent and non-equivalent ionic concentrations [2.], at different temperatures [21.], under the effect of foreign ions [22.], and a study of the delayed crystallisation in the presence of these foreign ions [23.]

Howard and Nancollas [24]. studied the precipitation of silver chromate, and these results compare favourably with the observations made in the silver chloride work in which a surface reaction is probably the rate controlling step.

This thesis is in three parts. The latter two parts deal with the kinetics of crystallisation of magnesium oxalate and barium sulphate to test the adequacy of the existing theories of inoculated growth.

Dissolution is much simpler and the mechanism is one of the solute units in the crystal lattice acquiring, at the interface, a solvation sheath and their subsequent diffusion away from the crystal. This phenomenon has been observed for many years, and results show the mechanism to be diffusion controlled. In the general picture of heterogeneity, step 1 would be slow compared to step 2, and hence rate controlling.

As a test for this theory part one of the current work was done. It deals with the dissolution of silver chloride into subsaturated solutions, at equivalent and non-equivalent ionic concentrations.

Apparatus and Experimental Techniques.

The crystal growth of magnesium oxalate and barium sulphate from supersaturated solutions, and the dissolution of silver chloride crystals into sub-saturated solutions were studied by the change in conductivity observed when the appropriate seed crystals were added.

In addition, the crystallisation of magnesium oxalate was followed by a titrimetric technique, using standard potassium permanganate or disodium ethylene-diamine tetraacetate, and by a photographic technique.

Measurement of Resistance.

Resistances were measured on an a-c screened Wheatstone Network of the type described by Jones and Joseph [25.] and Shedlovsky [26.] and modified to minimise inductance and capacitance effects in the construction of various parts of the bridge circuit (fig. 1).

R_1 was the conductivity cell and R_2, a Sullivan non-reactive resistance box reading from 0.1 to 10,000 ohms. The ratio arms R_3 and R_4 were supplied by a 100 ohm Sullivan non-reactive slide resistance, and the total resistance was subdivided into 10^5 parts

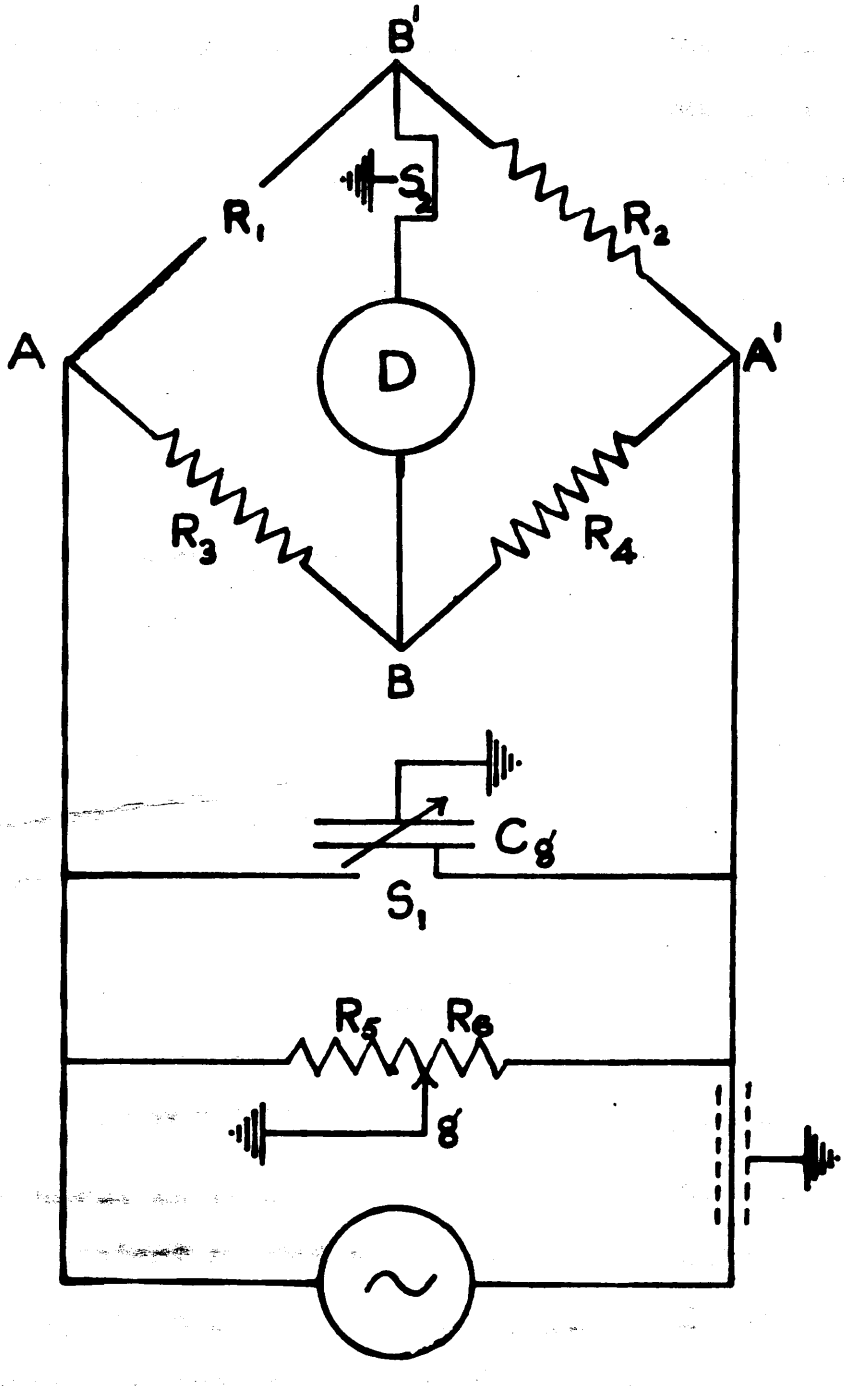

FIG. 1

by two concentric dials. The output from the bridge was amplified before passing to the ear-phones by a two stage high gain mains operated Sullivan amplifier. A mains operated oscillator, (Advance model H-1) was used at a frequency source of 1000 cycles per second, being the optimum frequency for aural detection. Leads from the oscillator to a balanced and screened Sullivan transformer were screened and earthed. The transformer was designed to screen the supply source from the bridge without upsetting the balance of the latter to earth. Further screened, earthed leads connected the transformer to the bridge. The sharpness of the sound minimum in the detector was improved considerably by earthing the bridge. A modified Wagner earth described by Jones and Joseph [25]. ensured the telephone earpeice being maintained at ground potential, thus eliminating any leakage of current due to the capacity between the telephone coils and the operator. The Wagner earth is represented by the resistances Rg, Rf, the contact g, and the variable condenser Cg. The bridge was balanced in the usual way, and the detector D was connected to ground by switch Sg, B was then brought to ground potential by adjustment of the

contact g. The bridge was again balanced and the process repeated until no change in the sound minimum was observed, between successive measurements.

The cell itself behaves as a condenser, and capacity effects arising from interaction between the electrodes, and between the electrodes and the cell wall were eliminated by balancing out against a Sullivan decade stable mica condenser reading from 0 to 0.01 μF, connected across either R_1 or R_2.

The cell was brought into circuit via two copper leads stretching from the platinum - mercury contacts of the electrodes to mercury cups supported in the thermostat. The copper leads were of equal length to compensate for resistance effects, as were the copper leads from the mercury cups to the resistance box R_2. The mercury cups were maintained at the same temperature as the cell to prevent heat interchange between the room and the cups. The connections to the cell and the resistance box could be interchanged by means of a mercury commutator of the rocking type. When water and solutions of high resistance were being measured, a 10,000 ohm, non-reactive, standard resistance was connected in parallel with the cell.

In practice, the setting of the Wagner earth once found, could be kept constant and any slight deviations from balance could be easily compensated by the mica condenser.

Because of the relatively high solubility of magnesium oxalate compared to silver chloride and barium sulphate, it was necessary to prepare solutions of high concentration in the cell. The Wheatstone network described was inaccurate in solutions of such low resistance, and a transformer ratio arm bridge [27]. (Wayne Kerr Universal Bridge B221) was used. Hereafter referred to as T.R.A. bridge.

The basic circuit of the T.R.A. bridge is shown in figure 2.

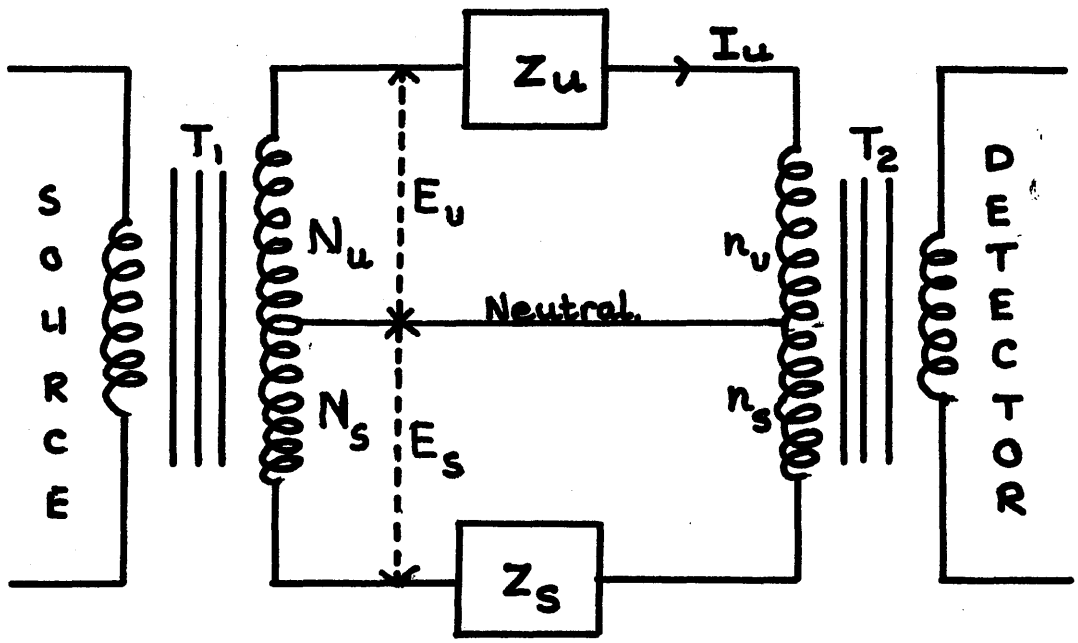

FIG. 2.

Z_u is an unknown impedance, and Z_s a variable standard impedance. T_1 is a voltage transformer, to the primary of which the source of a.c. is connected. The secondary winding is tapped to give sections having N_u and N_s turns. T_2 is a current transformer, the primary of which is tapped to give n_u and n_s turns and the secondary of which is connected to the detector.

Assuming that the transformers are ideal, Z_s is adjusted to give null indication in the detector. The detector is a tuned two-stage amplifier incorporating a sensitivity control, with a double - shadow "magic eye" associated with each stage. Balance is indicated by maximum shadow.

Under these conditions zero flux is produced in the current transformer, and there is therefore no voltage drop across its windings. The detector sides of both the unknown and standard impedances are therefore at neutral potential.

If the voltage across the unknown and standard sides are E_u and E_s respectively, then

$$I_u = \frac{E_u}{Z_u} \quad ; \qquad I_s = \frac{E_s}{Z_s} \quad .$$

For zero core flux in T_2, the algebraic sum of the ampere-turns must be zero.

$$\therefore \quad I_u . N_u = I_s . n_s$$

$$\therefore \quad \frac{E_u}{Z_u} . n_u = \frac{E_s}{Z_s} . n_s$$

$$\therefore \quad Z_u = \frac{E_u}{E_s} . \frac{n_u}{n_s} . Z_s .$$

and for an ideal transformer, the voltage ratio is

equal to the turns ratio,

$$Z_u = \frac{N_u}{N_s} \cdot \frac{n_u}{n_s} \cdot Z_s$$

Thus by suitable tappings on the two transformers, a wide range of measurements can be carried out.

Transformers are not however, ideal, but can be considered to be so for the purpose of the bridge. Transmission loss in the voltage transformer merely reduces the sensitivity of the bridge and can be compensated by increasing the gain of the detector. The windings are precision wound, all the turns embracing the same flux, so the ratio of induced voltages is accurately equal to the turns ratio. Voltage drop in the windings is found to introduce only negligible errors.

Standard impedances are divided into resistive and reactive components. At balance it is necessary for both the "in phase" and "quadrature" ampere-turns to sum algebraically to zero, and so the resistance and reactance standards may be connected to different tappings on the voltage transformer to balance out the currents caused by the unknown impedance.

Tappings are arranged to give four decades, each requiring one reactive and one resistive.

standard. It is possible to add two continuously variable controls : (fig. 3).

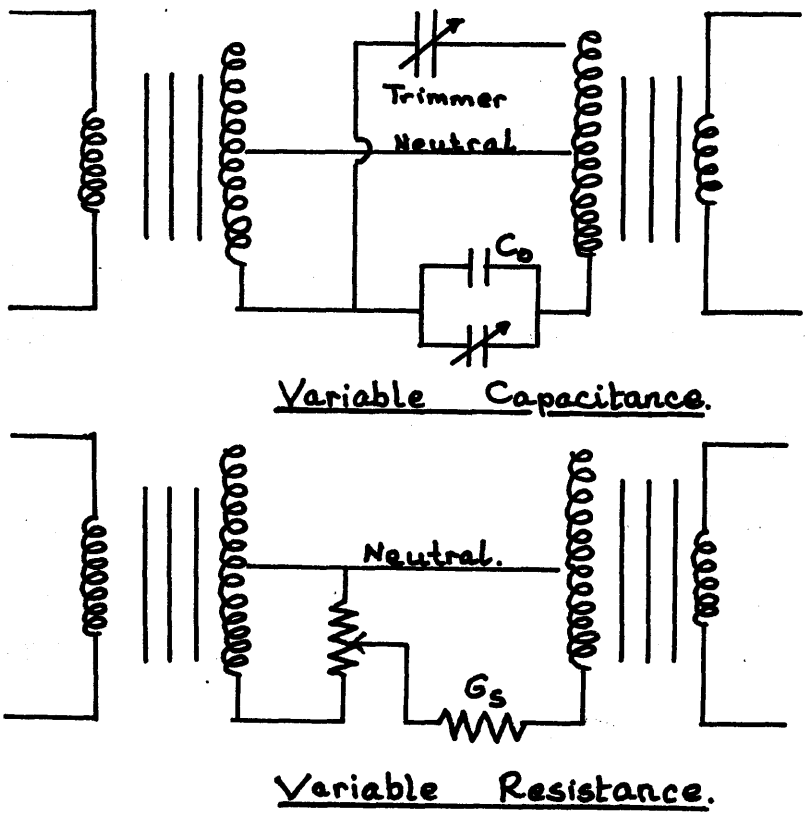

FIG. 3.

Each standard can be made effectively pure. An impure capacitor can be represented by a pure capacitance shunted by a resistance. The effect of the resistance is cancelled by feeding a current equal to that produced by the resistance impurity, through a fixed trimming resistor into the opposite side of

the transformer. The transformer ratios may be used to set the standard in one decade against that in another, so in effect, only two fixed standards of known accuracy are required, one resistive and one reactive.

The conductivity cell is brought into circuit with the T.R.A. bridge by two screened coaxial cables which dip into the mercury cups suspended in the thermostat. Balance is obtained by moving the decade and variable resistances and capacitances until maximum shadow is seen in the two "magic eyes". The bridge gives the impedance of the cell as a parallel combination of resistance and capacitance.

Thermostat and Temperature Control.

The thermostat was a large, earthed and heat insulated metal tank, filled with transformer oil to reduce capacity errors [26]. The oil was stirred by an electrically operated paddle stirrer. A perforated metal tray supported two metal boxes in which pyrex bottles containing seed suspensions were stored at the temperature of the bath. The bottles were immersed in water. The temperature of the bath was regulated by a mercury - toluene spiral regulator, connected inseries with a 60 watt red bulb through a vacuum relay. Control was accurate to $\pm$ 0.005°C. Readings were made on a Beckmann thermometer which had been standarised against a colibrated platinum resistance thermometer.[28] A booster heater was provided for rapid heating of the oil when necessary. Later experiments were done in a constant temperature room thermostated to 25°C. This prevented excessive condensation on the cell cap, but a water cooling system was essential to prevent excessive heating by the bulb.

The thermostat remained in use between runs, so that seed suspensions were stored at the temperature at which they would be used.

The Conductivity Cell.

This was of the Hartley-Barrett type [29]. and was constructed from pyrex glass (plate 1.) The cap was fastened to the pot by a slightly greased B.55 quickfit joint, and carried the electrodes, an aperture to accommodate the stirrer, another to facilitate additions of solutions, and a horizontal side-arm fitted with a three-way stop cock. The electrodes were of greyed platinum and were situated near the wall. They were carried by platinum wires which were fused into glass supports, and held at a fixed distance by four small pyrex glass rivets. It is not possible to seal platinum into glass and a little powdered Araldite epoxy resin was set in the bottom of each support. After fusing and curing at 60°C overnight, then allowing to cool slowly a permanent seal was obtained and leakage of mercury into the cell solution prevented.

The electrode supports were fixed to the cap by two B.10 quickfit joints and sealed in position with Araldite epoxy resin. The cap was placed in the same position relative to the pot for every

PLATE. 1.

The Conductivity Cell.

experiment by aligning scratches on the male and female parts of the joint.

The rotary paddle stirrer described by Howard [30] was replaced by a vibratory stirrer. This consisted of a circular glass disc perforated with conical holes fused to a glass rod, the whole unit being propelled by a vibromix motor (Shandon Scientific Co.). The maximum amplitude of the oscillations was 0.03 in. and the rate of stirring could be varied enormously. This type of stirring was preferred because the blades of the rotary stirrer cut the lines of force which spread out from the electrodes and introduced errors in the measured resistance. The errors varied depending upon the position of the stirrer relative to the electrodes. It was traced by using other materials in place of the glass stirrer. Stainless steel had a very large effect of reducing the resistance between the electrodes, and when it was coated with a resin, the effect was reversed and the resistance between the electrodes was effectively increased. The vibrating stirrer did not suffer from these disadvantages since it was fixed in position with respect to the

electrodes. When resistance readings were being taken, the cell motor and the thermostat stirrer motor were stopped. In some experiments a dust cap was attached to the vibrating rod but equilibration of the cell solutions took much longer, consequently in the majority of cases the dust cap was absent but a fast stream of purified air was passed through the cell. The aperture through which additions were made was always sealed with a dust cap. The side arm was used to introduce carbon dioxide free air into the cell.

The carbon dioxide free air supply.

The available compressed air supply was filtered by passing it through a jar of cotton wool, then passed through 2N sulphuric acid to remove ammoniacal vapours. Carbon dioxide was removed in 30% potassium hydroxide as the air passed through three tubes, then three towers packed with glass beads. This was followed by a water scrubber and a column of distilled water. Before entering the cell the air bubbled through conductivity water, a preheating tube and a glass wool pad all supported in the thermostat, to

saturate it with water vapour at 25°C.

Preparation of Conductivity Water.

Distilled water was deionised by passing it over a mixed bed resin [31]. The resins were Amberlite IR 120(H) acid resin and Amberlite IRA 140 basic resin mixed in a proportion of 1:2 by volume. An intimate mixture is essential so that H^+ ions liberated from the acid resin by exchange of cation impurities are neutralised by OH^- anions from the basic resin by exchange with anion impurities. Water of specific conductivity about 0.1×10^{-6} ohm^{-1} was obtained for periods of about a year by this method before renewal of the column which contained 40 ml. of wet resin. The water was collected and stored in a pyrex flask fitted with a soda lime guard tower.

Preparation of Stock and Cell Solutions.

All glass apparatus used in the preparation of solutions was pyrex. Pipettes and burettes were grade A glassware. Flasks required for stock solutions

were cleaned with cleaning mixture and steamed out before use. If stored they were filled with distilled water.

The cell solution was prepared by weight from dilute solutions which would give the appropriate subsaturated or supersaturated solution in the cell. (e.g. silver nitrate and potassium chloride were used to prepare silver chloride cell solutions).

The dilute solutions were freshly prepared each time from stock solutions, and the concentrations of the former solutions were such that, 10 ml. added from a calibratted pipette to about 250 g. of conductivity water in the cell, would give the predetermined cell solution concentration. The dilute solutions were prepared by weight in exactly the same way from the stock solutions. All solutions were made up by weight from conductivity water using a Sartorius balance of 2 kg. capacity and weights which had been calibrated by the method of Kohlrausch [32]. The balance was sensitive to 0.005g.

Analar salts were used throughout. The potassium chloride used in cell constant determinations was

recrystallised four times from conductivity water. Solids were weighed in pyrex sample tubes using a Stanton Model S.M.1 balance and platinum plated weights, calibrated as before [32]. All weights were vacuum corrected [33]. The preparation of solutions for low ionic strength experiments in the crystallisation of magnesium oxalate and barium sulphate are dealt with separately in the appropriate sections.

A typical experiment therefore involved cleaning and filling the cell, and allowing it to equilibrate in the thermostat. Dilute solutions were added individually; the second one being added very slowly over a period of five to ten minutes to prevent spontaneous nucleation of crystals from very high local concentrations of the electrolyte. After each addition the cell was allowed to reach equilibrium again. Carbon dioxide was removed rom the seed suspension before adding it to the cell by passing a rapid stream of nitrogen gas over it for about an hour. Rapid additions were made from a pipette with a sawn off tip, and the time of half delivery of the suspension was taken as the zero time for the reaction.

Determination of cell constant.

The cell constant was determined by the method of Frazer and Hartley [34]. The cell was weighed dry then about 240g. of conductivity water added. It was then allowed to equilibrate in the bath as described. Equilibrium was attained in about three hours and the resistance readings remained constant for periods up to 3 hours. Before use the recrystallised potassium chloride was heated to a dull red heat in a platinum crucible for several minutes and allowed to cool in a desiccator. The stock solution was approximately decinormal, and additions to the cell were made from a weight burette. Resistances were measured when equilibrium was reached usually after 15 to 30 minutes after addition. The resistance box R_2 was adjusted until the bridge readings for both positions of the commutator were close together. A slightly different value of R_2, of about two to five ohms, gave a further two readings on the ratio arms. The average conductivity value calculated from both pairs of ratio arms readings

was corrected for the water resistance. Further additions from the weight burette were made until the concentration of potassium chloride in the cell was about 0.001N. The cell was removed and after cleaning and drying its outer surface, it was weighed full and weighed again after emptying and drying with acetone. The weight of water in the cell was evaluated from the known weights of potassium chloride solution added. Evaporation during the run was negligible.

The cell constant was then calculated by comparing each measured value with the conductivity values derived by Shedlovsky [35], at the same concentrations, using the interpolation formula

$$\Lambda = 149.92 - 93.05\ c^{\frac{1}{2}} + 50c.$$

Where Λ is the equivalent conductivity of potassium chloride at normality c.[36]. The value of the cell constant for each cell used in the subsequent work was evaluated from at least twelve determinations (three series).

Cell A, had a cell constant of 0.09060 ± 0.05%

Cell B, had a cell constant of 0.08174 ± 0.05%

Cell C, had a cell constant of 0.07692 ± 0.05%

The conductivity technique described was used in all parts of this work; further techniques of titration and photographic methods for following the kinetics are outlined in part 2a.

PART 1. Dissolution of Silver Chloride into subsaturated solutions at various ionic ratios.

The Dissolution of Silver Chloride into Subsaturated Solutions.

Introduction.

In the past considerable discussion had centred around the question whether growth and dissolution are strictly reciprocal processes: A good account is given by Buckley [37].

The data obtained from the study of many dissolution reactions laid the foundation of Nernst's diffusion theory of heterogeneous reactions. Noyes and Whitney [38] found that for dissolution of benzoic acid and lead chloride, an equation involving the first order of the subsaturation was followed.

$$\frac{dc}{dt} = k_d(C_o - C). \qquad \text{——— (1).}$$

Similar observations were made by King and Brawdzman [39], King and Schaok [40] and Nernst [41] for the dissolution of many metals in acids.

Nerst's theory of heterogeneous reactions envisaged a stationary layer, the Nernst layer, at

the interface of a stirred solution. Efficient agitation was visualised as extending down to this layer, and a linear concentration gradient extending across the layer. The rate of the reaction would be determined by the rate of diffusion of the solute across the layer; which can be described by Fick's equation

$$k = \frac{D}{\delta}(C_o - C) \qquad \text{\_\_\_\_\_(2).}$$

D is the diffusion coefficient of the solute and δ the thickness of the Nernst layer. The rate constant k_d, equation (1), is therefore equal to D/δ , equation (2).

Step 3 in the Davies, Jones mechanism for heterogeneous reactions i.e. diffusion away from the interface, would therefore be rate controlling. Factors which affect the diffusion of solute would also affect the rate of the heterogeneous reaction. That step 2., the reaction at the interface, must be very fast in comparison is a necessary corollary.

The dimensions of δ can be altered by varying

the rate of stirring if the geometry of the system is kept constant. Several workers [39-46] have found that the rate constants of dissolution reactions depend on the rate of stirring as follows:

$$k_d \propto (r.p.m.)^a.$$

and values of a varied from 0.56 to 1. Conversely the rate of dissolution of some metals in acid observed by Centnerszwer and Zablocki [47] and of glass in alkali [48] was found to be independent of the rate of stirring, if stirring were fast enough. In contrast however, Marc in a series of publications [49-52] on crystallisation in which step 1 (i.e. diffusion of solute to the interface) would be rate controlling if Nerust's theory were correct, observed that the rate of reaction was independent of the rate of stirring.

If δ depended only upon the geometry of the system and the rate of stirring, then by keeping these variables constant, the rate of a chemically different reaction could be calculated. Brunner [42] calculated δ from dissolution of benzoic acid in water ($\delta = 3 \times 10^{-3}$ cm.) and successfully used it to calculate the rate of solution of magnesia in a variety of acids. Moelwyn - Hughes [53] however, considers a stationary layer of

such dimensions improbable, and Fage and Townend [54]. using an ultra microscope technique observed fluid motion down to much shorter distances, in the region of 0.6×10^{-4}cm. from the surface. The Nernst layer must be considered therefore to be mobile, and the linear function of concentration with distance an approximation.

The observed rate must also depend upon the diffusion coefficient of the solute in the solution. This varies inversely as the viscosity of the solution, so if the viscosity of the aqueous medium were increased, say by adding gelatin or soluble resins, than the observed rate would fall. This was indeed found by several workers [39,55-59]. Results from experiments on the dissolution of magnesium cylinders in acids showed that with δ assumed constant, since the theory requires δ to be a function of the geometry of the system and the rate of stirring this is possible that

$$k_d \propto D^x$$

where D = diffusion coefficient

and x varied from 0.66 to 0.75 depending upon the

experimental conditions of flow [60-62].

The effect of temperature on dissolution reactions has been observed by van Name [63] and on evaluating the energy of activation from the Arrhenius equation

$$k_d = A.e^{-E/RT},$$

values of the order of magnitude for the energy of activation for diffusion were obtained $\Delta E \sim$ 4. K.Cal. $Mole^{-1}$. Davies and Nancollas [21] studying crystallisation and dissolution of silver chloride found that the energy of activation for the former was zero, but for the latter was in the theoretical range for diffusion control. A value of 4.5 k.cal. $mole^{-1}$ was also found by Howard, Nancollas and Purdie [64] for dissolution of silver chloride seed crystals into subsaturated solutions. Moelwyn Hughes [53] calculated E_a = 16 K.cal. $mole^{-1}$ for the kinetics of the decomposition of sodium hypochlorite catalysed by a cobalt peroxide suspension and this surely means that step 1 is not rate determining but step 2, (i.e. some interface mechanism) is dominant.

From consideration of the above conflicting

observations, it is apparent that the Nerust theory for describing all types of hetrogeneous reactions is very limited. Although it may be theoretically possible for step 2 or step 3 to be in complete control in dissolution, the ideal cases are not met in practice. Experimental techniques based upon the above observations are applied to each case in an effort to explain the mechanism. A mechanism for interface control is described in part 2.

Nerust's theory of diffusion control may be applicable to heterogeneous reactions involving dissolution, with certain reservations. It cannot, however, be applied generally to describe crystallisation reactions where the theory of an adsorbed phase [2]. is preferred and an interface controlling step is dominating. The reciprocity of dissolution and crystallisation would not therefore appear to exist.

Experimental.

Preparation of Seed Suspension.

5g. of silver chloride were precipitated by mixing equivalent concentrations of analar silver

nitrate and analar potassium chloride. The precipitate was washed free from chloride with distilled water and distributed over five 5 l. pyrex beakers covered by clock glasses and filled with distilled water. The solutions were boiled for one to two hours then filtered through double fluted filter papers into pre-heated 5 l. round bottom flasks, lagged with cotton wool. The filter funnels had been thoroughly cleaned and pre-heated.

Slow crystallisation of silver chloride occurred on cooling slowly. The crystals from all the flasks were combined and washed about 10 to 15 times with distilled water by centrifugation and decantation, and finally about 6 to 10 times with conductivity water before being transferred to a blackened, waxed pyrex stock bottle. The neck and stopper of the bottle were not painted to avoid accidental contamination of the suspension, but instead a small beaker, blackened only on the outside and waxed, was inverted over the stopper. The was was added to prevent the paint from peeling after long submersion in the water thermostat. Seed suspensions were allowed to age for one month before use: their total

volume varied from 50 to 100 ml.

All operations were carried out under photographic "safety" lights.

The "ageing" process is one of crystallisation of the larger crystals, which were usually 5 to 10 microns in length, at the expense of the smaller ones. The process is described classically as Ostwald "ripening", and is important in that it smooths off the surfaces of the larger crystals and removes all of the smaller crystals which show an enhanced solubility [65,66]. Kolthoff and Bowers [67] have made a detailed study of silver bromide using (a) dye adsorption (b) exchange of radio-active bromide ion (c) electron microscope techniques and describe a three step ageing mechanism involving (i) ionic exchange over the first few minutes followed by (ii) Ostwald dilution over several days completed by (iii) crystal coagulation. Solubility values are functions of the size, of the interfacial tension and the specific surface area of the crystals, [68,69] and more recently results by Turkevich [70] have shown that the solubility is controlled by the size of the smallest crystals present. He reports that

crystals less than 1 micron in size are capable of recrystallisation; those greater than 1 micron are not, so there will be a minimum equilibrium size reached on "ageing".

Concentrations of Seed Suspensions:

Table 1.

Seed	Conc. ($mg.ml^{-1}$).
A	3.06
B	1.25
C	0.50

The length of crystals in each case were no smaller than 2 micron and no larger than 7 micron; the average of a hundred measurements was around 5 micron.

Preparation of Cell Solution.

10 ml. portions of the dilute solutions of silver nitrate and potassium chloride were added to the cell as previously described, P.26, and dissolution was followed after the addition of around 4-6 mg. of seed crystals in suspension by measuring the change in resistance readings with time.

Results:

A single crystallisation experiment was done first of all to compare the effect of turbulent stirring with respect to rotary stirring. Results identical with previous conclusions were observed, and are included in the appendix.

A number of dissolution experiments have been done at 25°C at equivalent and non equivalent concentration.

Solubility of Silver Chloride.

The solubility was taken as 1.337×10^{-5} g. equivalent l^{-1}, the value found by Davies and Jones, since the seed crystals were prepared in a similar manner and were of similar dimensions [70].

Ionic Mobilities and Equivalent Conductivity.

The equivalent conductivity of an electrolyte is obtained from the Onsager equation if the value at infinite dilution and the concentration of the solution are known. For a uni-univalent electrolyte, the Onsager equation becomes:

$$\Lambda = \Lambda^{o} - (0.2277\ \Lambda^{o} + 59.86)\ c^{\frac{1}{2}} \qquad \text{\_\_\_\_\_(1).}$$

at 25°C. For silver chloride Λ^{o} is equal to 138.26.

The equivalent conductivity can by evaluated in another way from measured conductivity values and the cell constant

$$\Lambda = \frac{1000 \times 1/R \times \text{cell constant}}{d} \qquad \text{\_\_\_\_(2).}$$

where R is the resistance of the solution corrected for the resistance of water. On evaluating Λ by equations (1) and (2) the results agreed to within 0.5% for all cell solutions. This gives an independent check on the accuracy with which cell solutions were prepared.

During dissolution the ionic strength $I = 4 \times 10^{-5}$ of the solution changed only very slightly, and a constant value for the equivalent conductivity was used throughout. Solubility dependence on changing ionic strength was likewise neglected.

Experiments at Equivalent Concentration.

The change in concentration of solid Δg after

a given time was calculated from measured resistance values, using equation (2)

$$\Delta c = \frac{1000 \times \Delta 1/R \times \text{cell constant}}{\Lambda}$$

Δ 1/R is the difference between the initial and instantaneous conductivity readings. Conductivity at zero time is obtained by extrapolating the curve of 1/R against time to the ordinate. The instantaneous concentration is therefore given by $C = C_I \pm \Delta C$, where C_I is equal to the initial concentration.

Typical smooth curves of 1/R against time are shown in Fig. 1. The initial concentrations, percentage subsaturations and rate constants are shown in Table 2. The measured gradients $\frac{\Delta\ 1/R}{\Delta\ t}$ converted to dc/dt by multiplying by the factor $\frac{.10^3 \times \text{cell constant}}{\Lambda_{AgCl}}$ and graphs of dc/dt against (c_0-c) are given in Figs. 2 and 3, where good straight lines corresponding to 96% of the reaction were obtained. The data for

the construction of these graphs are given in Tables 3 and 4. Reproducibility of the method is illustrated by agreement between runs 28 and 29. The results show therefore that for dissolution of silver chloride into subsaturated solutions a first order rate equation

$$dc/dt = k_d(s)(c_o - c)$$

is obeyed.

The factor s included in the rate constant is a surface area factor. The effective surface area participating in the dissolution must decrease with time and the rate equation should be written,

$$\frac{dc}{dt} \cdot \left(\frac{W_1}{W_2}\right)^{\frac{2}{3}} = k_d\,(c_o - c). \qquad \text{\_\_\_\_\_(3).}$$

where W_1 is the initial weight of seed crystals

W_2 is the weight of crystals at time t.

if the seed crystals are assumed cubic. The amount of dissolution was small andthe resultant change in weight amounted to 4% of the total and the correction was neglected.

<u>Experiments at non-equivalent concentrations.</u>

These runs are summarised in Tables 5 to 8, and typical smooth curves of 1/R against time are shown for silver ion in excess in Fig. 4, and for chloride ion in excess in Fig. 5.

These experiments were interpreted in terms of the amount of silver chloride Δ to be dissolved before equilibrium was reached. The instantaneous ion concentrations are therefore given by

$$[Ag^+] = [Ag^+_e] - \Delta \quad \text{and} \quad [Cl^-] = [Cl^-_e] - \Delta$$

or $[Ag^+] + \Delta = [Ag^+_e]$, and $[Cl^-] + \Delta = [Cl^-_e]$.

$[Ag^+_e]$ and $[Cl^-_e]$ are the equilibrium ion concentrations which satisfy the solubility product relationship

$$[Ag^+_e][Cl^-_e] = K_s = 1.788 \times 10^{-10} \quad \text{at } 25^\circ C.$$

Therefore

$$\{[Ag^+] + \Delta\}\{[Cl^-] + \Delta\} = K_s$$

and if the value of Δ is known or can be found, then the intermediate values of $[Ag^+]$ and $[Cl^-]$ could be evaluated. The initial value of Δ can be obtained since the initial values of $[Ag^+]$ and $[Cl^-]$ are known experimentally, and from the change in resistance readings during dissolution the change in Δ can be calculated

$$\delta(\Delta) = \frac{1000 \times \Delta 1/R \times \text{cell constant}}{\Lambda}$$

The rate of solution may be written

$$\frac{dq}{dt} = k_d(s)\ (\Delta)$$

and graphs of $\frac{dq}{dt}$ against Δ are shown in Figs. 5, 6 and 7. The graphs were constructed from the data presented in Tables 6, 7 and 8 and show good straight lines for rather smaller percentages of the total reaction between 25% for experiment 17 and 50% for experiment 10. Analysis of the remainder of the process was attempted using higher order of the rate equation (viz. 2nd order and $\frac{1}{2}$ order) but neither were successful. The rate of dissolution therefore

falls off more rapidly than would be expected for a first order equation, an effect which is more noticeable with Ag^+ ion in excess.

Appendix.

The crystallisation of silver chloride.

Experiment 1 was done and a smooth curve was obtained in Fig. 8a from the data available in Table 9b. The kinetics already reported for the crystallisation of silver chloride[2] was second order according to the equation

$$-\frac{dc}{dt} = k\ (s)\ (c-c_0)^2$$

This experiment employed turbulent stirring, as opposed to rotary stirring, [64] and from Fig. 8b a good straight line was obtained for the graph of $\frac{dc}{dt}$ against $(c-c_0)^2$. Second order kinetics for growth, therefore, is independent of the mode of stirring as expected by the theory of growth explained in Part 2.

Discussion of Results:

Nernst's theory for heterogeneous reactions cannot be used to explain crystallisation experiments, where rate equations with higher orders than unity have been observed. However dissolutions, which furnished the experimental data on which the theory was based, are considered to be first order.

In the case of the dissolution of silver chloride into water higher orders in the rate equation were reported by Davies and Nancollas [21]. For the general equation of heterogeneous reactions

$$\frac{dc}{dt} = k(\delta)(c_s - c)^n$$

they report $n = 2$ at 35°C and $n = \frac{1}{2}$ at 15°C and 25°C. Contrary to other observations, the rate of dissolution of silver chloride would appear not to be diffusion controlled. Therefore the rate of step 2 (the chemical step at the interface) must be of similar magnitude to step 1 (the diffusion of solute away from the interface), and there is competition for the controlling step. However they pointed out that the detailed analysis was impracticable in

view of the thickness of the diffusion layer surrounding the dissolving crystals, which could be a significant fraction of the distance between crystals in conditions where c/c_o, the ratio of the momentary concentration to its saturation value, was much less than unity.

Howard [30]. studied dissolution into subsaturated solutions and observed first order kinetics. Supporting evidence for diffusion control was obtained by the dependence of the rate constant upon the rate of stirring; and on evaluating the activation energy [64]., the value was of the right order for diffusion control.

The current work at equivalent concentrations using the turbulent type of stirring showed first order kinetics for about 96% of the total reaction. However at non equivalent concentrations, deviation from a first order rate equation was observed.

In solutions of equivalent concentrations the crystal surface may not have exactly equivalent amounts of lattice ions owing to the difference in adsorption affinities: but this difference is likely to be small and is not likely to affect substantially the diffusion of pairs of ions away from the surface.

When non equivalent ion concentrations exist in solution, the surfaces of the crystals are altered by enforced preferential adsorption of the ion in excess. Step 2 in the mechanism would be made much slower and the overall mechanism should go preferentially to an interface control. An electrical potential at the surface, which allows only the passage of ions in stoichiometric proportions is set up and assures that equivalent ion surface conditions cannot be restored at any time throughout the dissolution process. A fuller discussion is included in part 2 for crystallisation under conditions of non-equivalent ion concentrations.

From table 2, the rate constants for runs 28, 29 and 35 agree very well and show the good reproducibility of the method.

The rate constant for experiment 10 of 0.14 shows a considerable reduction from 0.24 in experiment 6, illustrating the effect of using non equivalent concentrations. Runs 30 and 32, which exhibit good reproducibility and have chloride ion in excess, show a reduction of the rate constant from experiment 28 from 0.09 to 0.06. With silver ion in excess, however, the magnitude of the reduction is greater,

TABLE. 2.

Dissolution at 25°C; $[Ag^+]/[Cl^-] = 1$.

Expt. no.	init. conc. (equiv. l^{-1}). $[Ag^+]\times10^5$	$[Cl^-]\times10^5$	$[Ag^+][Cl^-]\times10^{10}$	Seed Susp. (mg. ml^{-1})	% Sub. Satn.	ks (min^{-1}).
6	1.123	1.124	1.262	0.05 (A)	29	0.21
28	1.115	1.115	1.244	0.01 (C)	30	0.09
29	1.114	1.114	1.241	0.01 (C)	30	0.08
30	1.113	1.113	1.238	0.01 (C)	30	0.09

$$\text{Percentage Subsaturation} = \frac{\text{Solubility Product} - \text{Init. Ionic Product}}{\text{Solubility Product.}} \times 100$$

TABLE. 3.

$1/R$ $\times 10^5$	Amt. AgCl dissolved g.equiv.l^{-1}	$[Ag^+]\times 10^5$ g.equiv. l^{-1}.	$[Cl^-]\times 10^5$ g.equiv. l^{-1}.	(c_0-c) $\times 10^6$ g.equiv. l^{-1}	$\Delta 1/R$ / Δt $\times 10^7$	dc/dt $\times 10^7$
Run. 6.						
3.868	0	1.123	1.124	2.13	6.3	4.15
3.908	0.026	1.149	1.150	1.67	5.3	3.49
3.948	0.052	1.175	1.176	1.41	4.3	2.83
3.988	0.078	1.201	1.202	1.14	2.9	1.91
4.028	0.104	1.227	1.228	0.88	1.9	1.25
4.068	0.130	1.253	1.254	0.61	1.2	0.79
4.108	0.156	1.279	1.280	0.35	0.4	0.30
Run. 28.						
3.845	0	1.115	1.115	2.22	2.30	1.52
3.895	0.033	1.148	1.148	1.89	1.90	1.25
3.945	0.066	1.181	1.181	1.56	1.55	1.02
3.995	0.099	1.214	1.214	1.23	1.05	0.69
4.045	0.132	1.247	1.247	0.90	0.60	0.40
4.095	0.165	1.280	1.280	0.57	0.15	0.10
4.145	0.198	1.313	1.313	0.24	0.05	0.03

TABLE. 4.

1/R x 10^5	Amt. AgCl dissolved g.equiv.l^{-1}	$[Ag^+]$x10^5 g.equiv. l^{-1}.	$[Cl^-]$x10^5 g.equiv. l^{-1}.	$(\sigma_0-\sigma)$ x10^6 g.equiv. l^{-1}	$\Delta 1/R$ / Δt x10^7	$d\sigma/dt$ x 10^7
Run. 29.						
3.875	0	1.114	1.114	2.23	2.55	1.68
3.925	0.033	1.147	1.147	1.90	2.17	1.43
3.975	0.066	1.180	1.180	1.57	1.75	1.15
4.025	0.099	1.213	1.213	1.24	1.25	0.84
4.075	0.132	1.246	1.246	0.91	0.78	0.52
4.125	0.165	1.279	1.279	0.58	0.41	0.27
4.150	0.181	1.295	1.295	0.42	0.10	0.08
Run. 35.						
3.744	0	1.113	1.113	2.24	2.88	1.90
3.794	0.033	1.146	1.146	1.91	2.76	1.82
3.844	0.066	1.179	1.179	1.58	2.37	1.56
3.894	0.099	1.212	1.212	1.25	1.61	1.06
3.944	0.132	1.245	1.245	0.92	1.00	0.66
3.994	0.165	1.278	1.278	0.59	0.06	0.39

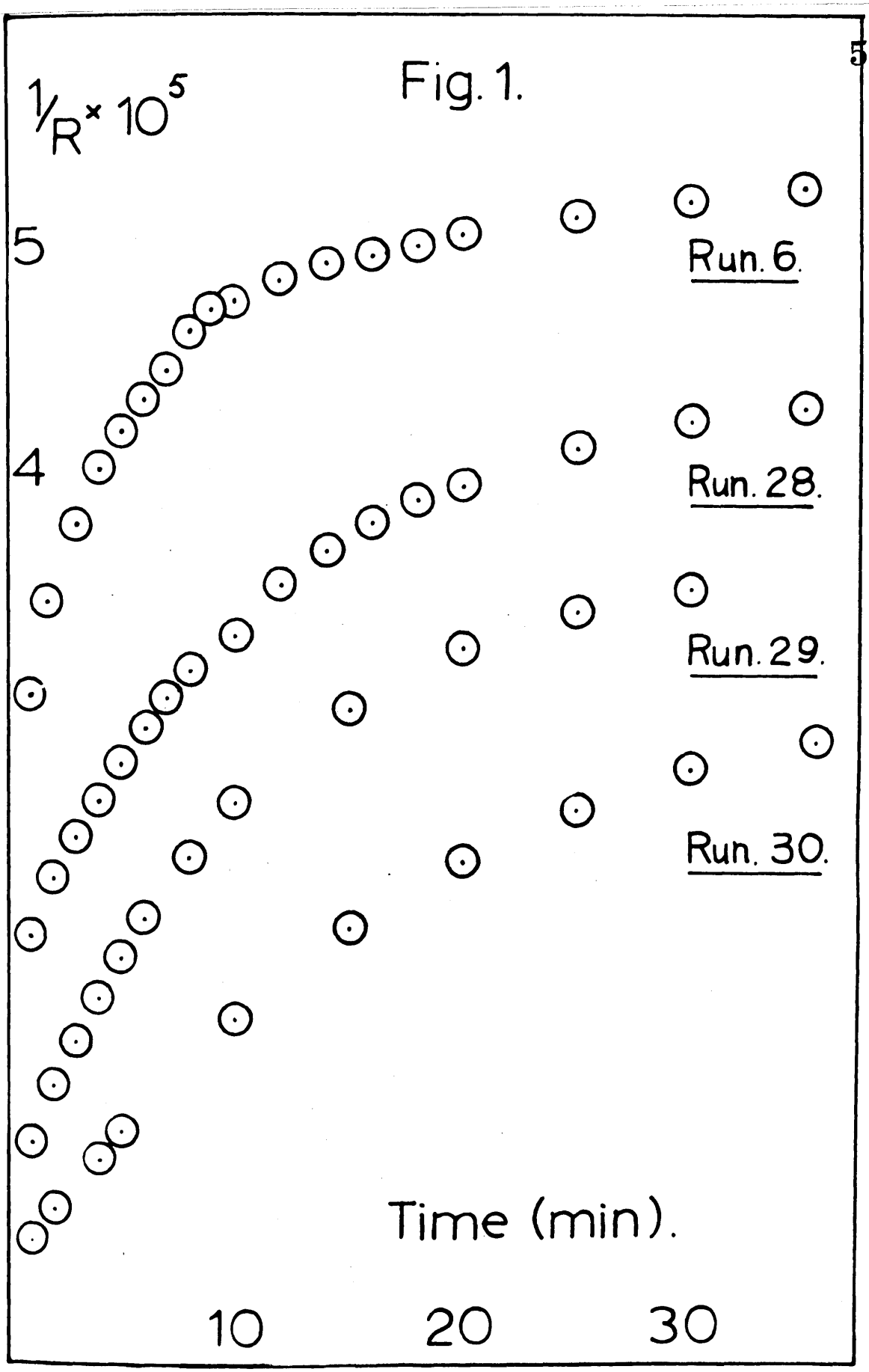
Fig. 1.
1/R × 10^5
5
4
Run. 6.
Run. 28.
Run. 29.
Run. 30.
Time (min).
10
20
30

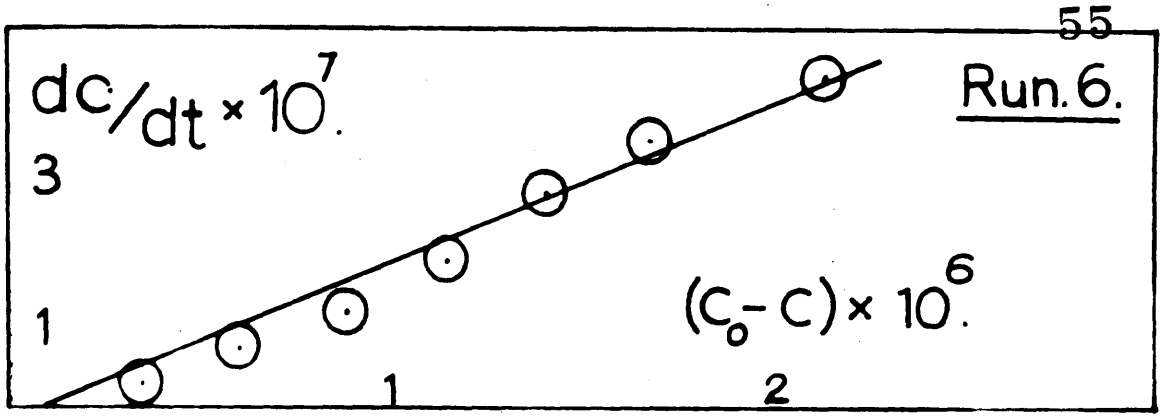
dc/dt × 10^7.
Run. 6.
3
1
(C_o - C) × 10^6.
1
2

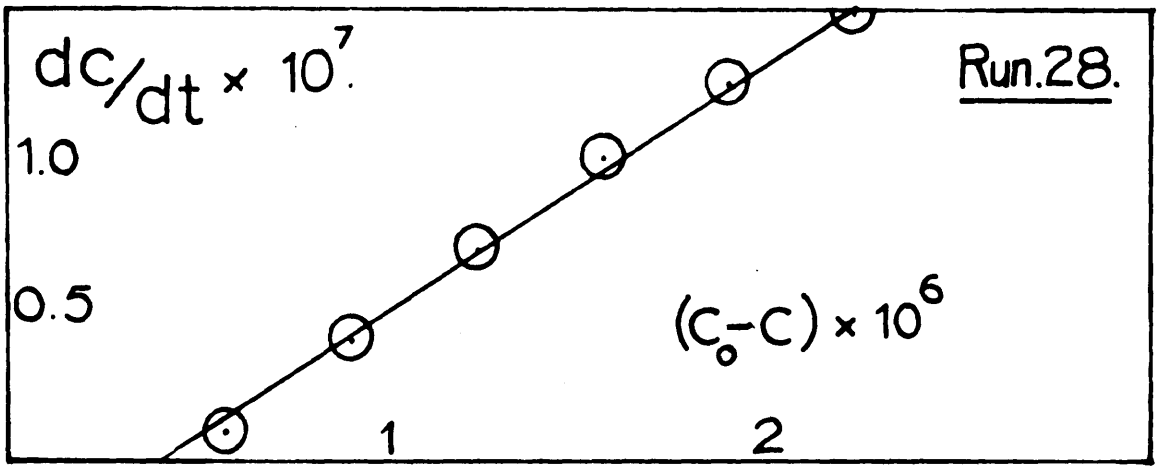
dc/dt × 10^7.
Run. 28.
1.0
0.5
(C_o - C) × 10^6
1
2

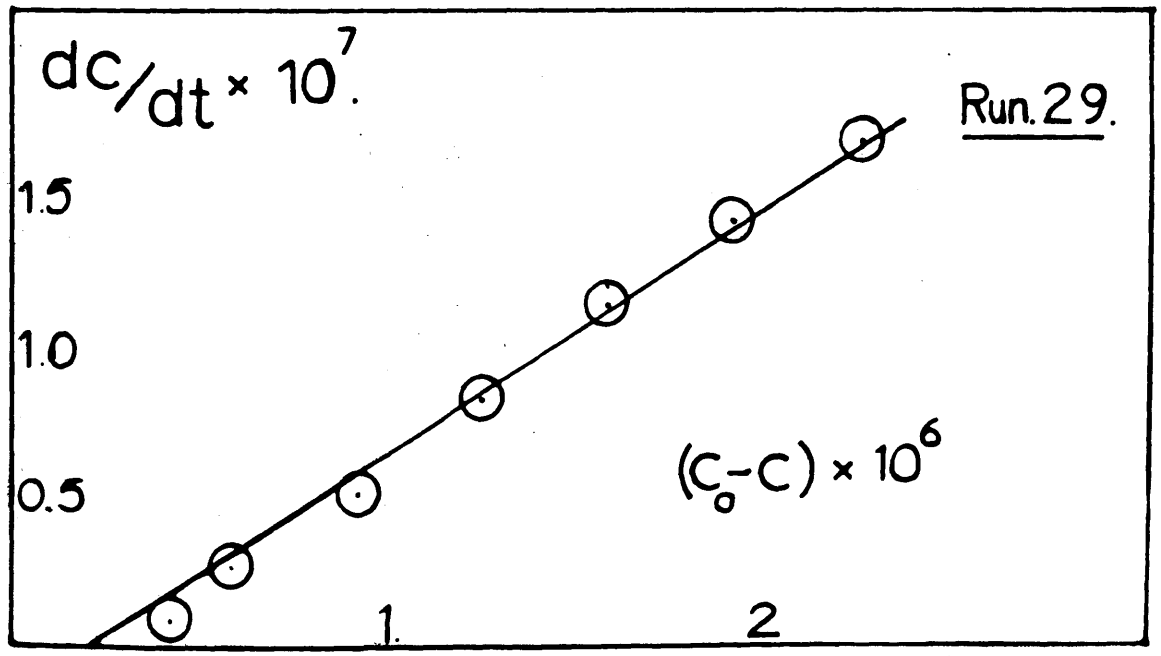
dc/dt × 10^7.
Run. 29.
1.5
1.0
0.5
(C_o - C) × 10^6
1.
2

Fig. 2.

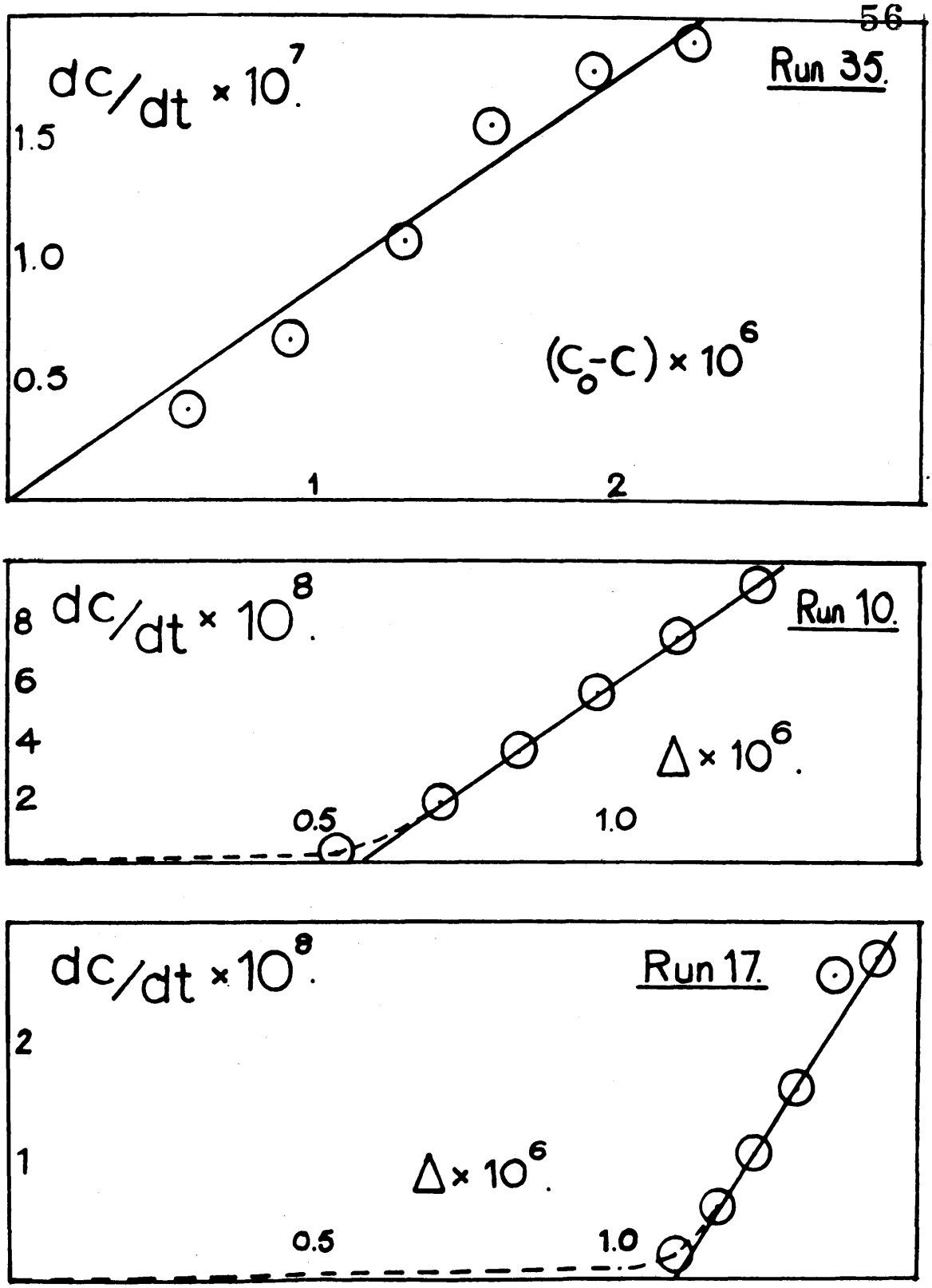
dc/dt × 10^7.
Run 35.
1.5
1.0
0.5
(C_o-C) × 10^6
1
2
dc/dt × 10^8.
Run 10.
8
6
4
2
Δ × 10^6.
0.5
1.0
dc/dt × 10^8.
Run 17.
2
1
Δ × 10^6.
0.5
1.0

Fig. 3.

TABLE. 3.

Dissolution at 25°C.; $[Ag^+]/[Cl^-] \neq 1$.

Expt. no.	Initial Concentration (equiv. l^{-1}) $[Ag^+] \times 10^5$	$[Cl^-] \times 10^5$	$[Ag^+][Cl^-] \times 10^{10}$	Ionic Ratio.	Seed Susp. ($mg.ml^{-1}$)	% Sub Satn.	$ks(min^{-1})$
10	1.696	0.859	1.458	2.0	(A) 0.5	18	0.14
17	2.048	0.680	1.392	3.0	(B) 0.2	22	0.08
20	0.592	2.366	1.400	0.25	(B) 0.2	21	0.12
21	0.592	2.366	1.400	0.25	(B) 0.2	21	0.10
30	0.652	1.930	1.258	0.33	(C) 0.1	30	0.06
32	0.652	1.930	1.258	0.33	(C) 0.1	30	0.05
33	1.577	0.789	1.244	2.0	(C) 0.1	30	0.03
34	2.231	0.558	1.248	4.0	(C) 0.1	30	0.03

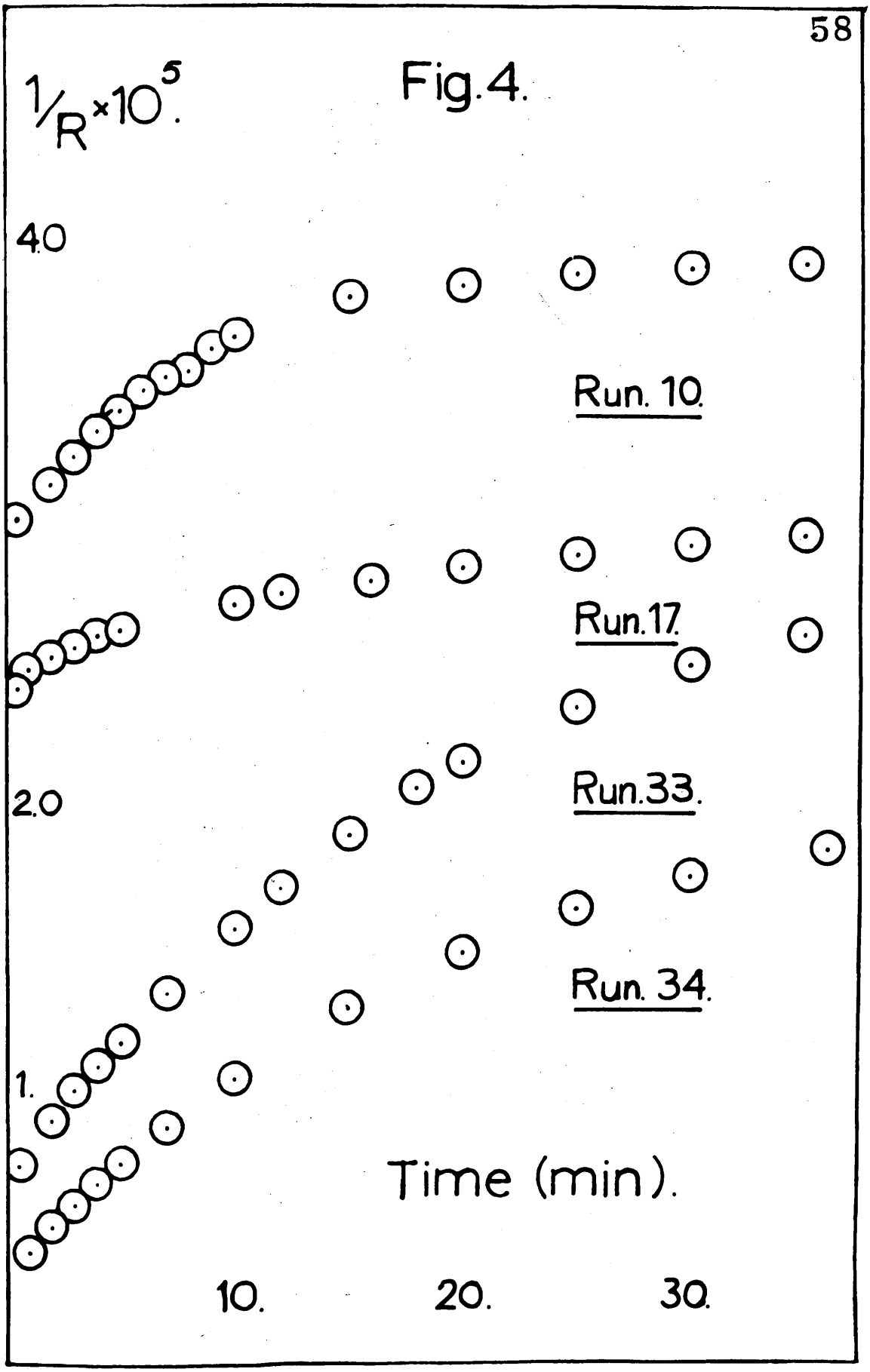
1/R × 10^5.
Fig. 4.
4.0
2.0
1.
Run. 10.
Run. 17.
Run. 33.
Run. 34.
Time (min).
10.
20.
30.

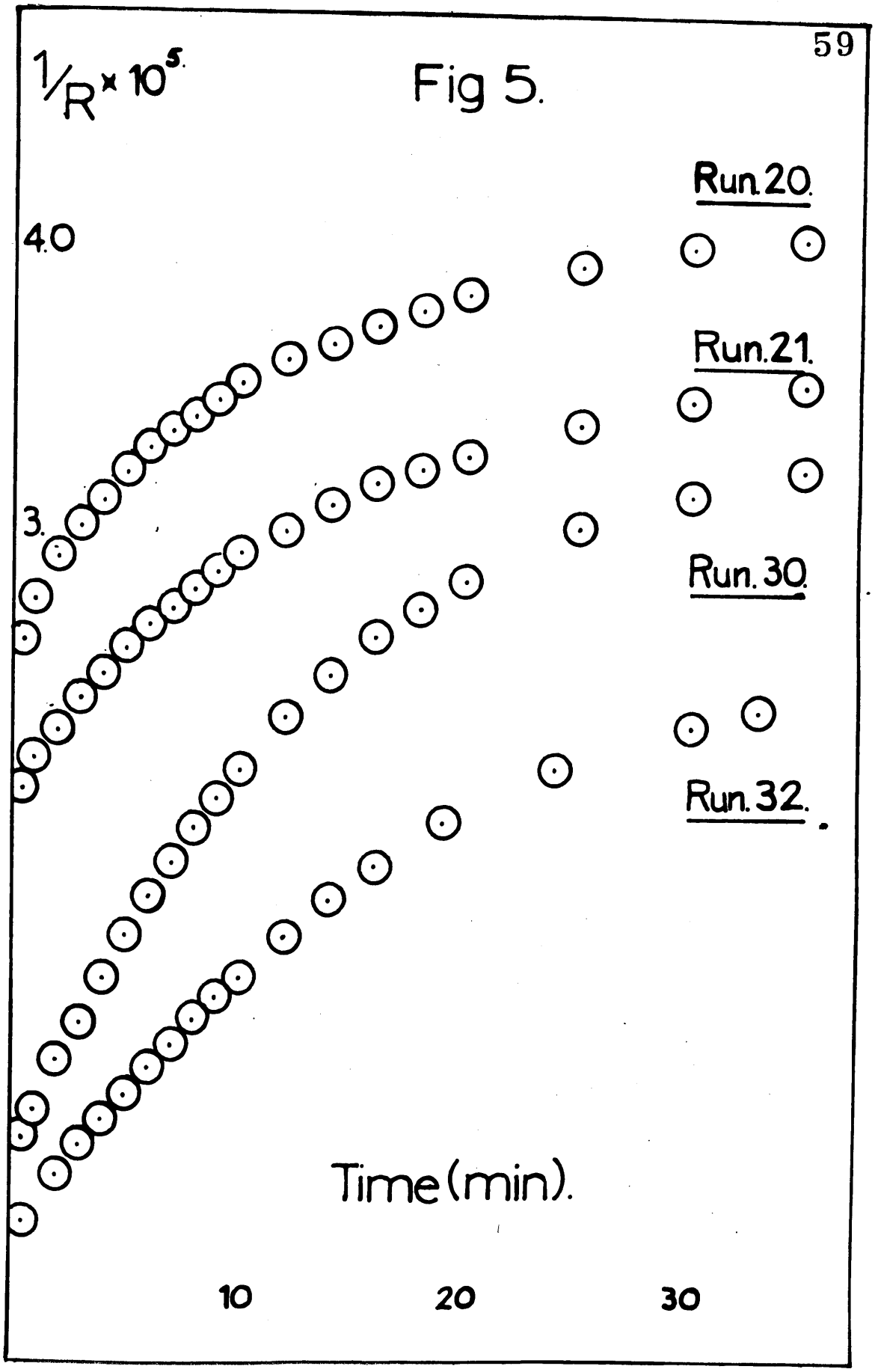
1/R × 10^5.
Fig 5.
Run.20.
Run.21.
Run.30.
Run.32.
4.0
3.
Time (min).
10
20
30

TABLE. 6.

1/R $\times 10^5$	Amt. AgCl dissolved g.equiv.l^{-1}	$[Ag^+] \times 10^5$ g.equiv. l^{-1}.	$[Cl^-] \times 10^5$ g.equiv. l^{-1}.	Δ $\times 10^6$ g.equiv l^{-1}	$\frac{\Delta 1/R}{\Delta t}$ $\times 10^8$	da/dt $\times 10^8$
Run. 10.						
4.547	0	1.696	0.859	1.23	14.0	9.22
4.567	0.013	1.709	0.872	1.10	11.3	7.43
4.587	0.026	1.722	0.885	0.97	8.5	5.59
4.627	0.052	1.748	0.911	0.71	3.0	1.98
4.647	0.065	1.761	0.924	0.58	0.4	0.26
Run. 17.						
4.662	0	2.048	0.680	1.43	4.1	2.70
4.682	0.014	2.062	0.694	1.30	2.4	1.58
4.692	0.021	2.069	0.701	1.23	1.6	1.05
4.702	0.028	2.076	0.708	1.17	0.9	0.59
Run. 20.						
6.458	0	0.592	2.366	1.30	15.3	10.08
6.498	0.026	0.618	2.392	1.03	10.7	7.03
6.518	0.039	0.631	2.405	0.90	7.2	4.74
6.538	0.052	0.644	2.418	0.77	5.6	3.69
6.558	0.065	0.657	2.431	0.64	3.8	2.50
6.618	0.104	0.696	2.470	0.25	0.8	0.53

TABLE. 7.

1/R x10^5	Amt. AgCl dissolved g.equiv.l^{-1}.	$[Ag^+]$x10^5 g.equiv.l^{-1}.	$[Cl^-]$x10^5 g. equiv. l^{-1}.	Δ x 10^6 g.equiv.l^{-1}	$\frac{\Delta 1/R}{\Delta t}$ x 10^3	dc/dt. x 10^8
Run. 21.						
5.444	0	0.592	2.366	1.30	12.5	8.23
5.464	0.013	0.605	2.379	1.16	10.7	7.04
5.484	0.026	0.618	2.392	1.03	9.1	5.98
5.504	0.039	0.631	2.405	0.90	7.3	4.81
5.524	0.052	0.644	2.418	0.77	5.5	3.62
5.544	0.065	0.657	2.431	0.64	3.7	2.44
5.564	0.078	0.670	2.444	0.51	2.6	1.71
5.584	0.091	0.683	2.457	0.38	1.4	0.92
5.604	0.104	0.696	2.470	0.25	0.8	0.53
Run. 30.						
4.450	0	0.652	1.930	1.87	17.0	11.19
4.500	0.033	0.685	1.963	1.54	15.0	9.87
4.550	0.066	0.718	1.996	1.21	12.5	8.22
4.600	0.099	0.751	2.029	0.88	9.5	6.25
4.650	0.132	0.784	2.062	0.55	5.0	3.29
4.700	0.165	0.817	2.095	0.22	2.0	1.32

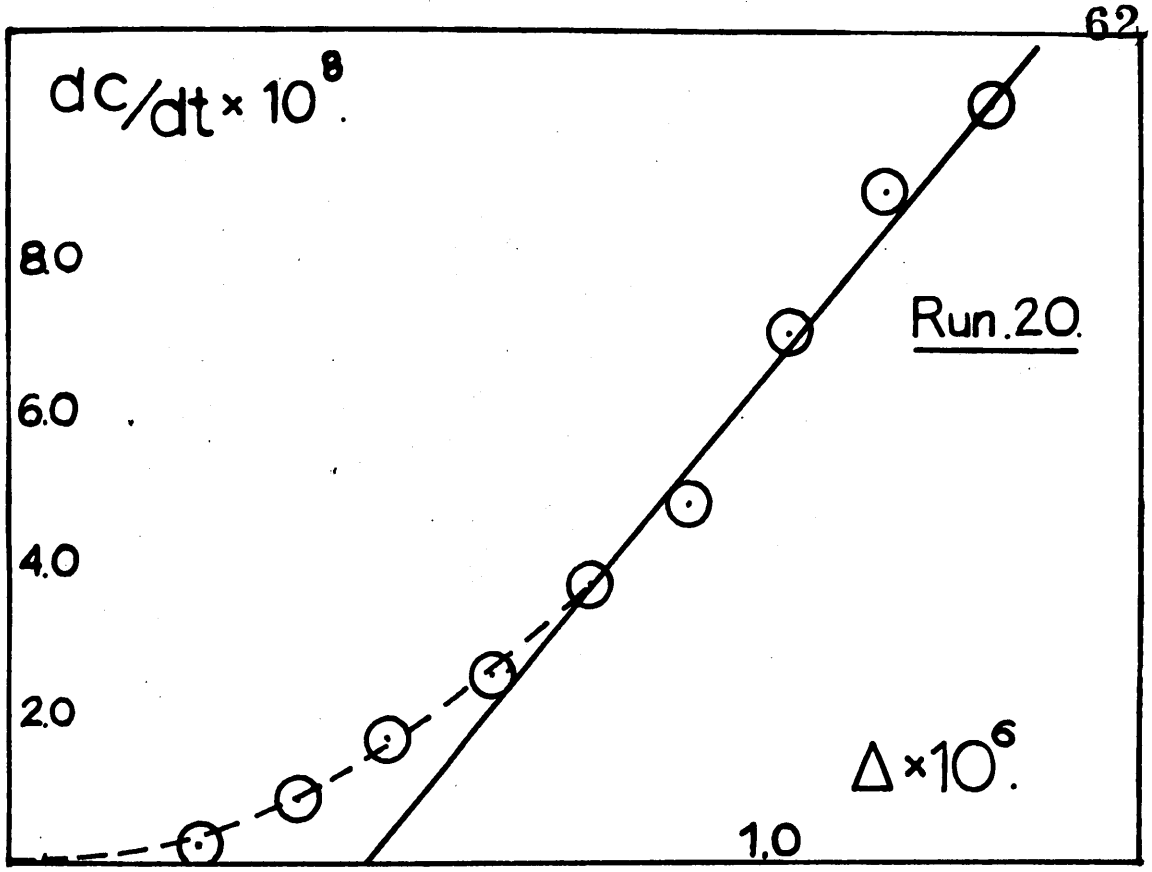
dc/dt × 10⁸.
8.0
6.0
4.0
2.0
Run.20.
Δ×10⁶.
1.0

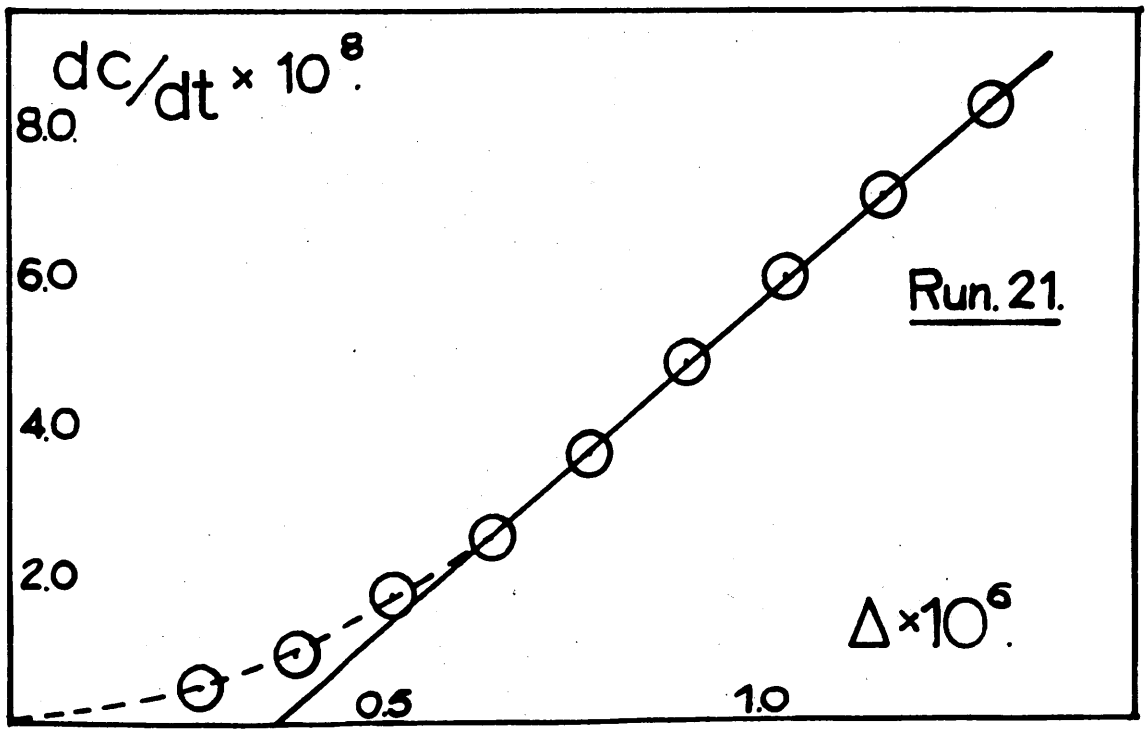
dc/dt × 10⁸.
8.0
6.0
4.0
2.0
Run.21.
Δ×10⁶.
0.5
1.0

Fig.6.

TABLE. 8.

1/R x10^5	Amt. AgCl dissolved g.equiv.l^{-1}.	$[Ag^+]$x10^5 g.equiv. l^{-1}.	$[Cl^-]$x10^5 g.equiv. l^{-1}.	Δ x 10^6 g.equiv l^{-1}	$\frac{\Delta 1/R}{\Delta t}$ x 10^8	da/dt x 10^8
Run. 32.						
4.746	0	0.652	1.930	1.87	11.4	7.50
4.796	0.033	0.685	1.963	1.54	9.6	6.34
4.846	0.066	0.718	1.996	1.21	7.1	4.67
4.896	0.099	0.751	2.029	0.88	4.0	2.64
4.946	0.132	0.784	2.062	0.55	1.5	0.99
Run. 33.						
3.946	0	1.577	0.789	2.11	10.9	7.17
3.996	0.033	1.610	0.822	1.78	8.8	5.79
4.046	0.066	1.643	0.855	1.45	6.7	4.41
4.096	0.099	1.676	0.888	1.12	3.9	2.56
4.146	0.132	1.709	0.921	0.79	1.6	1.05
Run. 34.						
4.513	0	2.231	0.558	1.83	8.3	5.46
4.563	0.033	2.264	0.591	1.50	6.5	4.28
4.613	0.066	2.297	0.624	1.17	4.0	2.63
4.663	0.099	2.330	0.657	0.85	1.6	0.99

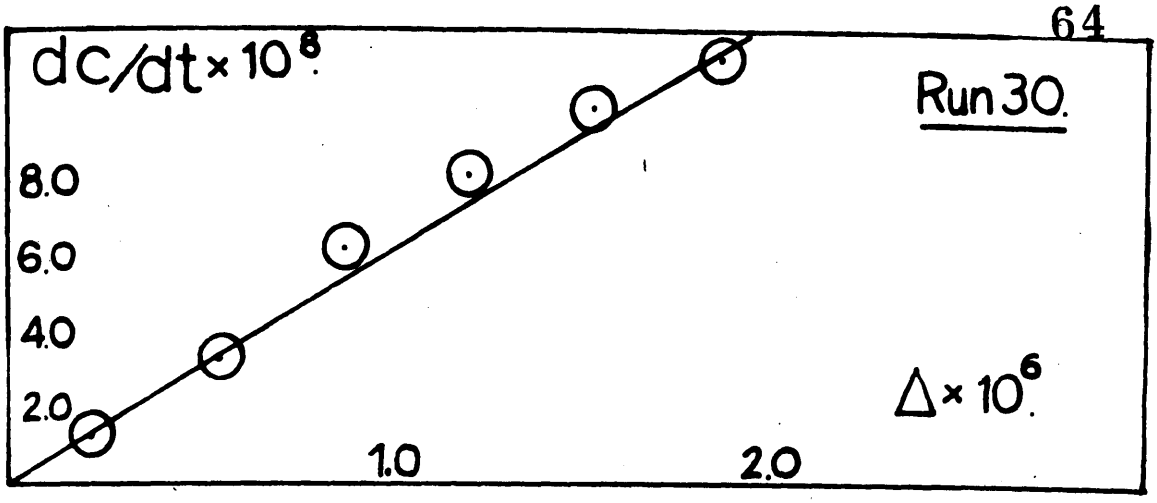
dc/dt × 10⁸
Run 30.
8.0
6.0
4.0
2.0
1.0
2.0
Δ × 10⁶

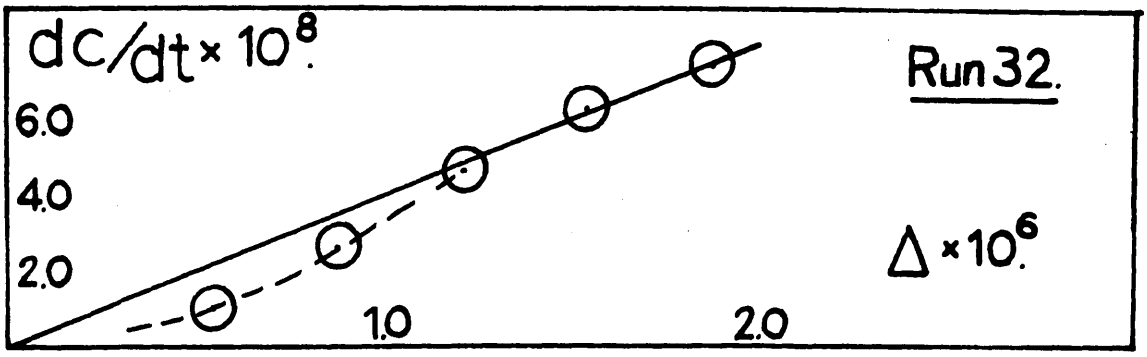
dc/dt × 10⁸
Run 32.
6.0
4.0
2.0
1.0
2.0
Δ × 10⁶

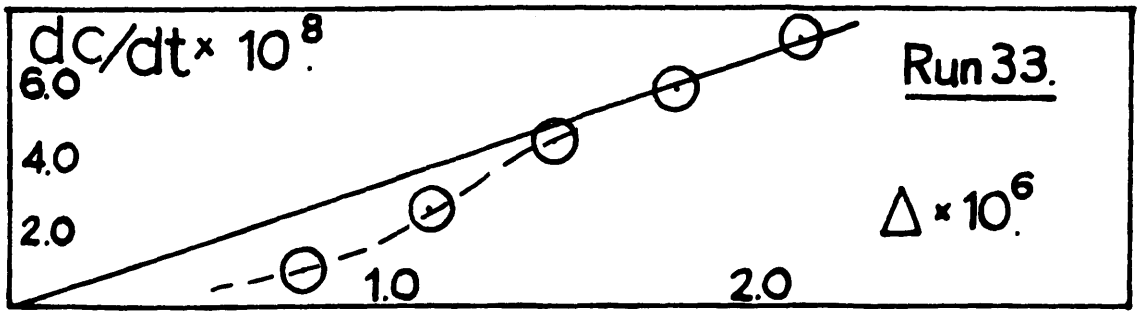
dc/dt × 10⁸
Run 33.
6.0
4.0
2.0
1.0
2.0
Δ × 10⁶

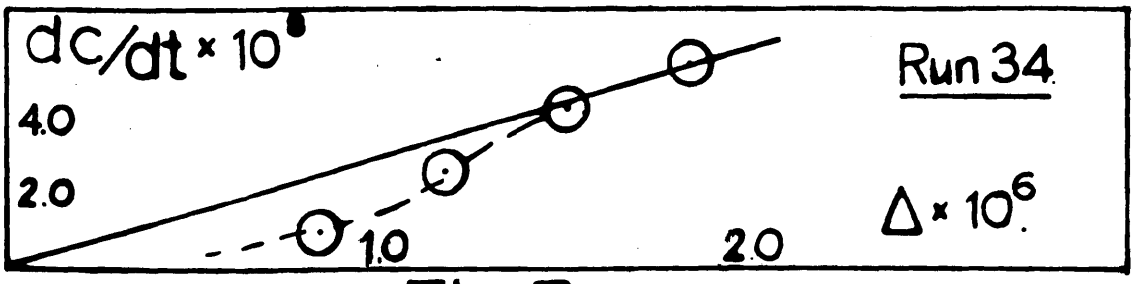
dc/dt × 10⁸
Run 34.
4.0
2.0
1.0
2.0
Δ × 10⁶

Fig. 7.

TABLE. 9a.

Crystallisation at 25°C.; $[Ag^+]/[Cl^-] = 1$.

Expt. no.	Init. concns. (g.equiv.)l^{-1}. $[Ag^+]\times10^5$	$[Cl^-]\times10^5$	$[Ag^+][Cl^-]\times10^{12}$	Seed Susp. (mg.ml^{-1})	% Super Sat.	ks(min^{-1}) $l.mole^{-1}$
1	1.454	1.460	2.121	(A) 0.5	19	0.04

Percent. Super-Saturatn. = $\frac{\text{Init. Ionic Product-Solubility Product}}{\text{Solubility Product.}} \times 100$.

TABLE. 9b.

1/R $\times10^5$	Amt. AgCl deposited g.equiv.l^{-1}.	$[Ag^+]\times10^5$ g.equiv.l^{-1}.	$[Cl^-]\times10^5$ g.equiv.l^{-1}.	(c_0-c) g.equiv.l^{-1}	$\frac{\Delta 1/R}{\Delta t}$ $\times10^8$	da/dt $\times10^8$
Run. 1.						
4.840	0	1.457	1.457	1.59	8.3	5.50
4.820	0.013	1.444	1.444	1.14	5.9	3.89
4.800	0.026	1.431	1.431	0.88	5.0	3.29
4.780	0.039	1.418	1.418	0.66	3.7	2.44
4.760	0.052	1.405	1.405	0.46	2.5	1.65
4.750	0.059	1.398	1.398	0.37	2.0	1.32
4.730	0.072	1.385	1.385	0.23	1.7	1.12

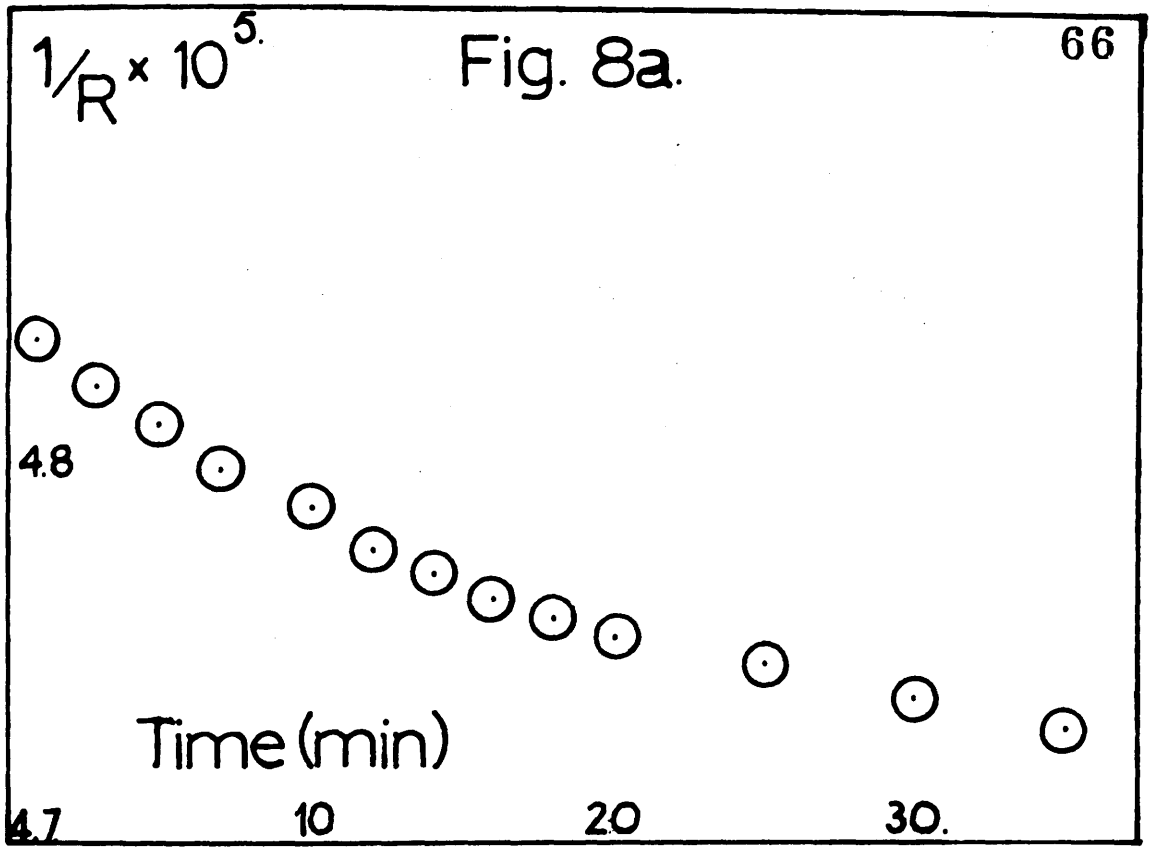
1/R × 10^5.
Fig. 8a.
4.8
Time (min)
4.7
10
20
30.

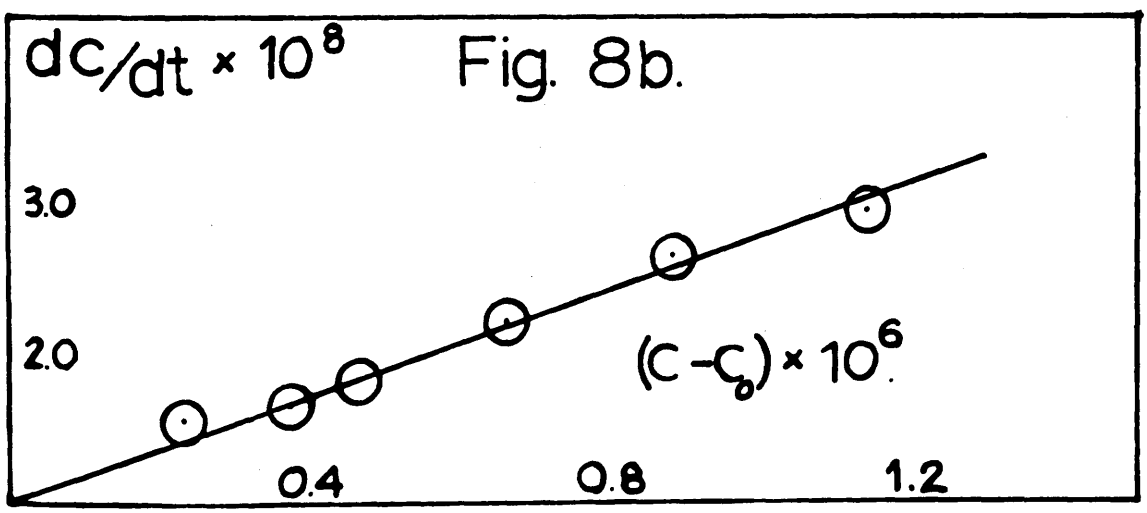
dc/dt × 10^8
Fig. 8b.
3.0
2.0
(C - C_0) × 10^6.
0.4
0.8
1.2

the observed rate in run 33, where $[Ag^+]/[Cl^-] = 3$, is 0.03. That this effect is general is shown by runs 20 and 21 which have chloride ion in excess and an observed rate constant of 0.12, whilst run 17 with silver ion in excess has a rate constant of 0.08. Furthermore the observed deviation from the first order rate equation is greater and occurs earlier when silver ion is in excess.

This reduction of the rate constants would suggest that some surface effect is becoming important, reducing the rate of step 2, the interface step, relative to step 3, the diffusion step. Knowledge of the rates of adsorption for the silver ion and the chloride ion on silver chloride solid might yield some useful information. Adsorption of the ion in excess will begin immediately on adding the seed crystals to the subsaturated solution. Since it is unlikely that adsorption equilibrium will be maintained during the reaction, the process of dissolution will be opposed by that of adsorption and the surface will not be allowed to attain the potential necessary for the optimum release of Ag^+ and Cl^- ions in equal numbers. The result is a lowering of the rate of

dissolution. Differences in the relative rates of adsorption of Ag^+ and Cl^- ions at the surface may account for the much larger lowering of dissolution rate when Ag^+ ions are in excess. In crystallisation of silver chloride, Davies and Nancollas [22]. observed that the rates at non equivalent concentrations were slower and with Ag^+ ion in excess the reduction in magnitude of the rate constant was smaller than that with Cl^- ion in excess. This would support the rate of adsorption dependance theory.

Summarising therefore, the agreement with a diffusion controlled mechanism for dissolution of silver chloride in subsaturated solutions of equivalent ion concentrations [30]., did not persist entirely when tested in solutions of non equivalent ion concentrations. Instead a tendency to some surface controlling step of uncertain mechanism is likely, with the effect illustrated by a deviation from the first order rate equation.

RESULTS AND DISCUSSION.

Part 2. Crystallisation of Sparingly Soluble Salts in Aqueous Solutions.

2a. Magnesium Oxalate.

2b. Barium Sulphate.

GENERAL INTRODUCTION.

The simple first order rate equation suggested by the Nernst theory for heterogeneous reactions has been seen in many cases to be inadequate to explain crystal growth. The more general equation should be accepted:

$$-\frac{dc}{dt} = kS(c-c_o)^n$$

Values of n of 2, 3, 4 and even as high as 8 have been found, and each one explained in a mechanism of crystal growth. The value of 8 was given by Christiansen and Nielsen[11.] for barium sulphate crystallisation, but their experiments were designed to study only nucleation. Nielsen[7,69.] later suggested for growth of barium sulphate a value of n = 4 which changed to 2 as the growth proceeded. Analogous results were obtained for calcium oxalate precipitation[92.]. The mechanism proposed was one of diffusion control together with two dimensional surface nucleation on the nuclei produced by spontaneous growth. The growth of potassium perchlorate[91.] could not be described in this way and a concept of convection control was introduced.

Values of n of 6 for calcium fluoride[19.] and 2 for silver chromate[18.] have already been mentioned, but like the value of 8 for barium sulphate it was confined to the nucleation process in spontaneous growth. Collins and Leinewaber[16.], and Johnson and O'Rourke[6.] suggested n = 4 was correct for precipitation of barium sulphate but they did not agree on the mechanism. The former favoured nucleation followed by diffusion controlled growth and the latter nucleation and a surface controlled step. A theory which should embrace all growth processes was proposed by Davies and Jones[2.].

In their study of growth of silver chloride on seed crystals, Davies and Jones observed a value of n = 2 and suggested that an interface step was controlling. The mechanism for interface control postulates an adsorption layer and the kinetics are formulated in terms of a stationary concentration of ions in the adsorbed phase with the following two assumptions:

(1) a crystal in contact with an aqueous solution always tends to be covered with a monolayer of hydrated ions. Secondary adsorption on this monolayer is negligible. Crystallisation, which is the incorporation of further units into the crystal lattice, can only occur of the resulting configuration satisfies this condition.

(2) Crystallisation of an electrolyte occurs through the simultaneous dehydration of cations and anions in staichiometric proportions.

A saturated solution exists when the rate of adsorption of ions from solution becomes just sufficient to maintain the monolayer of hydrated ions intact, and it must be assumed that every ion striking the surface enters this mobile adsorbed layer. Then the rate of adsorption of cations = $k_1 s [M_o^{m+}]$, and of anions = $k_1 s [X_o^{y-}]$. The subscript zero indicates the solubility value of each ion species M^{m+} and X^{y-}. From a supersaturated solution, all the cations reaching the surface do not enter the monolayer, and the remainder, $([M^{m+}]-[M_o^{m+}])$ are available for deposition. A similar fraction of anions will be available for deposition in solutions of equivalent concentrations viz. $([X^{y-}]-[X_o^{y-}])$. This fraction either suffers elastic collision with the monolayer, or if the ions arrive simultaneously in stoichiometric proportions at sites suitable for growth, then the respective underlying ions can become dehydrated and be incorporated in the crystal lattice. For a symmetrical electrolyte (i.e. m=y) like silver chloride, magnesium oxalate or barium sulphate, the rate equation would then become:

$$-\frac{dc}{dt} = k([M^{m+}]-[M_o^{m+}])([X^{y-}]-[X_o^{y-}])$$
$$= k\,(c-c_o)^2 . \qquad \text{(1).}$$

The transfer of ions on dehydration from the absorbed phase to the suitable growth sites may occur by one of two mechanisms suggested by Doremus[72]. In model A he considers the ions to come together to form a crystal "molecule" which by surface diffusion reaches the growth site. Energetically this is unfavourable because of possible dehydration to form the "molecule" and partial hydration at the site with water molecules of crystallisation. The mechanism is explained in a third order rate equation. Model B considers the direct assimilation of the ions into the lattice from the adsorbed phase immediately above a kink on partial or complete dehydration and the overall mechanism is second order.

The rate of step 1 (in crystallisation, the important diffusion step is transport of solute to the crystal) in the general picture of heterogeneous reactions is considered very fast compared to the interface step 2. This latter step is not controlled by any diffusion mechanism and the rates of crystallisation experiments should be unaltered by changing stirring speed, apparatus structure (fluid dynamics), diffusion coefficient etc.

"Negative" tests, such as these, are useful in ascertaining that diffusion has no part in controlling the rate of crystallisation. Alterations to the surface of the crystals however, should influence the rate constants, if not the rate equation. Surface active reagents reduce the rate of growth[22], and in some cases even arrest it completely. Habit modifying effects have been seen in other cases[57,73-77], when specific adsorption has occurred on particular faces leaving the remaining faces free to participate in the normal growth mechanism. Qualitatively the rate is considered to be reduced by mechanical blocking of active sites at kinks by the large molecules of adsorbate[78].

The surface can also be altered by using non-equivalent ionic concentrations in solution. Under conditions of equivalent concentrations the resultant small potential difference between the crystal and the solution due to the preferential adsorption of one of the lattice ions is probably too small to have an effect upon the mechanism of growth. However, when seed crystals are immersed in a solution in which $[M^{m+}]/[X^{y-}] = r$, where $1\ r \geqslant 1$, then more M^{m+} ions will be adsorbed and a potential difference ψ will be established between the crystal and the solutions.

An electrical double layer now surrounds the crystals and the value of ψ is such that it allows cations and anions to enter the adsorbed layer in equal numbers. The former equations must be replaced by,

availability of M^{m+} ions at the surface

$$= k_1 s[M^{m+}] \exp. (-\psi/RT)$$

availability of X^{n-} ions at the surface

$$= k_1 s[X^{y-}] \exp. (\psi/RT).$$

Since these are equal when $n = y$ then

$$\exp. (\psi/RT) = [M^{m+}]^{\frac{1}{m}}/[X^{y-}]^{\frac{1}{n}} = r^{\frac{1}{m}}.$$

The number of ions of each type entering the monolayer in unit time is as before C_o, and the rate of crystallisation becomes,

$$-\frac{dn}{dt} = ks([M^{m+}]r^{-\frac{1}{m}} - C_o)([X^{y-}]r^{-\frac{1}{n}} - C_o).$$

$$= ks([M^{m+}]^{\frac{1}{m}}[X^{y-}]^{\frac{1}{n}} - C_o)^2$$

which reduces, under conditions of equivalent concentrations to equation (1).

For crystallisation of symmetrical electrolytes therefore, $n = 2$ in the rate equation would be expected. A shift from diffusion to interface control is possible

when the rate of step 2 becomes progressively slower with respect to step 1, by increasing the rate of the ions in the adsorbed phase, and if the rate of 2 was originally comparable to the rate of 1 in equivalent conditions, then a mechanism change may be possible. Therefore, the mechanism in conditions of non equivalent concentrations must not automatically be considered to be that in solutions of equivalent concentrations.

In the crystallisation of silver chromate, Howard and Nancollas [24] obtained a value $n = 3$. This is compatible with the above results in that silver chromate is a uni-bivalent electrolyte, so the concentration term in the equation will be a function of the third power of the concentration.

Part 2a of this work deals with the crystallisation of magnesium oxalate in equivalent and non equivalent concentrations and in the presence of added surface active agents. The growth of the seed crystals is followed by conductivities at various ionic strengths, by titration using standard potassium permanganate or standard disodium ethylene diamine tetraacetate solutions and by a photomicroscopic technique.

The results illustrate an agreement with the theory, second order kinetics existing throughout, in some cases after an initial induction period. The rate of growth is independent of the increase in surface area during growth; a possible effect already reported by Doremus[72]. It is seen that the induction period is due to spontaneous crystallisation initiated when the seed crystals are added, and this effect can be eliminated by adding sufficiently high concentration of seed.

Part 2b is a report on the growth of barium sulphate under conditions of equivalent and non equivalent ionic concentrations. A value of $n = 2$ is observed after an abnormally fast initial portion.

Part 2a.

Crystallisation of Magnesium Oxalate from Supersaturated Aqueous Solutions.

In solutions of magnesium oxalate there are present appreciable amounts of a very stable complex, MgOx,

$$Mg^{2+} + Ox^{2-} \rightleftharpoons MgOx. \qquad \text{\_\_\_\_\_(a).}$$

Pedersen [79.] has shown that this was the only complex formed in solutions of equivalent concentrations of Mg^{2+} and Ox^{2-} ions. From solubility and conductivity results he was able to distinguish between MgOx and another complex $Mg(Ox)_2^{2-}$ [80,81,82.] given by the equilibrium.

$$Mg^{2+} + 2Ox^{2-} \rightleftharpoons Mg(Ox)_2^{2-}. \qquad \text{\_\_\_\_\_(b).}$$

A value for the thermodynamic dissociation constant of reaction (a) given by

$$K = \frac{[Mg^{2+}][Ox^{2-}]\, f_2^2}{[MgOx]} = 3.7 \times 10^{-4}\ \text{l. mole}^{-1}. \qquad \text{\_\_\_\_\_(c).}$$

was reported by Davies [83.].

With such a stable complex present in solution very high supersaturations could be maintained without spontaneous growth for long periods. The critical

concentration for spontaneous growth was very high and concentrations about five times the solubility value were used, the solutions being stable for periods up to six hours.

The theory of growth requires the simultaneous deposition of ions and it was interesting to see if this condition was maintained even when a complex existed in solution. As ions were removed during growth, the equilibrium would be re-established and the instantaneous ionic concentration could be evaluated at any time. Measurement of changes in conductivity could therefore be used to follow growth. A conductivity method was used by Brescia and Peisach,[84] who observed no change in conductivity during growth. This is clearly wrong and probably their conductimetric technique was not sufficiently sensitive to detect the changes of the ionic concentration. Consequently they used a titration technique to follow large changes in concentration and found that growth was first order with respect to total oxalate. i.e.

$$-\frac{d\,Tm}{dt} = k_2 s\,(Tm - Tm^0). \qquad \text{\_\_\_\_\_(2).}$$

From a thermodynamic treatment of results, Lichstein and Bressoin [85.] provided evidence for growth being diffusion controlled from calculated energy of activation and from the effects of stirring.

The growth of calcium oxalate has been followed by Nielsen [92.] and a fractional value of n between 4 and 2 obtained. The solubility is very much less that for magnesium oxalate, but a similar complex, CaOx, is formed in solution

$$Ca^{2+} + Ox^{2-} \rightleftharpoons CaOx.$$

Growth was followed after spontaneous nucleation and the rate equation was given as

$$-\frac{d[CaOx]}{dt} = Ks\,[CaOx]^{4}$$

or

$$-\frac{dm}{dt} = Ks\,([Ca^{2+}]^{2}[Ox^{2-}]^{2}).$$

Nielsen considers that a nucleus of four complex units or eight ions is required before growth can proceed without further nucleation. This size is critical in that it is energetically more favourable for the nucleus to add ions than to lose them.

EXPERIMENTAL.

Preparation of solutions.

Analar grade reagents were used throughout and all glass apparatus was pyrex. Cell solutions for the experiments at high ionic strength were prepared by mixing together magnesium chloride and potassium oxalate of known concentration. The second solution was added very slowly over a period of five to ten minutes. Conductivity water was used in the titration experiments because other divalent ions, if present, would complex with ethylene diamine tetra acetate anion to give erroneous titration results. Magnesium chloride crystallises with six waters molecules so all stock solutions were estimated by titration. Analar potassium oxalate was used without further treatment.

The inaccuracies which the high concentration of potassium chloride produced in the resistance measurements, using the Wheatstone Bridge network, could be improved if this supporting electrolyte were removed i.e. if solutions of low ionic strength could be prepared in which the current was carried entirely by the Mg^{2+} and Ox^{2-} ions. Magnesium oxide and magnesium carbonate were too insoluble in oxalic acid to be of practical use and magnesium hydroxide, being gelatinous, was

difficult to handle. Solutions of magnesium oxalate of low ionic strength were prepared by exchanging Mg^{2+} ions for $2K^{+}$ ions in a potassium oxalate solution by passage through a resin in the magnesium form. The resin was prepared from an Amberlite IR 120(H) resin, by passing through a 2M hydrochloric acid solution, then a 2M magnesium chloride solution until the pH of the eluant rose to around 7. The column was then washed free from chloride ions with distilled water. Solutions were collected directly into the cell and weighed, a column of about 17 cm. length and 2 cm. diameter was sufficient to exchange about 250 ml. of 3.0×10^{-2}M in oxalate ion concentration completely. The optimum flow rate was ~~each~~ *ca.* 0.5 ml. per minute. When solutions were tested for Ox^{2-} ion concentration before and after cation exchange, no loss of salt by precipitation in the resin was observed.

Titrimetric Technique.

The apparatus consisted of a round bottom bolt-neck flask with smaller stoppered side arms for making the necessary additions to the cell. The central wide neck carried a rubber stopper through which the stirrer passed. Both rotary stirring and vibratory stirring were used with this apparatus. The flask was supported

in a water thermostat regulated to 25.0 ± 0.1 °C with a toluene-mercury regulator.

The constancy of titrations of portions of the supersaturated cell solutions over an hour indicated that spontaneous crystallisation had not occurred before adding the seed crystals. Crystallisation was followed by removing portions of the stirred cell suspension and separating the crystals from the mother liquor by filtration through a No.4 sinter stick or by rapid centrifugation. Centrifugation was preferred since it was much more rapid, the normal time of transfer from cell to titration vessel being ninety seconds. The decrease in concentration during the time of extraction was negligible. Aliquot portions (usually 4 ml.) of the filtrate were analysed by titration for total oxalate against standard potassium permanganate after the addition of sulphuric acid [86]. Analysis for total magnesium was done with standard disodium ethylenediamine tetraacetate using Eriochrome Black - T as indicator in the presence of an ammonium hydroxide - ammonium chloride buffer of pH = 10 [87]. Grade A Burettes were used in experiments of high initial total oxalate concentration. In experiments of low initial total oxalate concentration a micrometer syringe with

a very fine needle was used to make the small additions during titrations. The total volume of potassium permanganate required for oxidation of the oxalate ion was less than 0.5 ml. but the volume could be read to four decimal places giving an accuracy of about 0.5%.

Photographic Technique.

Because of the very large concentration changes during growth, the increase in crystal dimensions were sufficient to allow growth to be followed microscopically. Electron micrographs did not yield the required evidence since they tended to show too few crystals with too much detail. A Ziess photo-microscope, simply an optical microscope fitted with a camera, was used at magnifications of 50 x and 320 x. The photographs were taken on Ilford H.P.3 film; the contrast between the crystals and the substrate was improved by inserting a x 2 Ilford green filter. Crystal dimensions were measured from printed enlargements (x 1300) of negatives. From the difference in sizes, assuming the crystals to be cubic, the calculated increase in mass of the crystals agreed with the weight deposited to within 10%.

The extraction of samples for investigation was

undesirable in conductivity work and separate experiments were carried out in round bottom flasks agitated by a mechanical shaker in a constant temperature room at 25°C. The growth was followed simultaneously by titration.

Preparation of Seed Crystals.

The usual methods for preparing seed crystals of good uniformity in size and shape, such as crystallisation from boiling saturated solution or slow precipitation yielded only crystals and aggregates of very coarse appearance. Instead, the rapid mixing of almost saturated solutions of magnesium chloride and potassium oxalate with vigorous stirring produced very uniform crystals. The size of the crystal, defined as the length of its longest edge, was an average of 10 micron and all crystals were within the size range 8 to 13μ. The crystals were washed free from chloride ions with distilled water and conductivity water by centrifugation and decantation and stored in pyrex stock bottles in the water thermostat at 25°C. They were allowed to age for at least one month before use: the concentrations of the seed suspensions are given in Table 10.

TABLE 10.

Seed suspension concentrations.

Seed	Conc.($mg.ml^{-1}$).
A	20
B	32
E	30
F	25.

Solubility Value and Solubility Product.

The solubility of magnesium oxalate was estimated in three ways.

a) Crystallisation experiments at high and low ionic strengths were allowed to continue to equilibrium. The concentration of the equilibrium solution was estimated by titration and corrections for the different ionic strengths were applied to give the solubility value.

b) The concentration of the seed suspensions were estimated by titration at various intervals of time over a year. This differs from a) in that saturation was approached from the subsaturated side.

c) Repeated circulation of water and the subsequent magnesium oxalate solutions over a column of seed crystals contained in a thermostated saturator should provide a solution whose concentration does not change on further cycling, and this concentration is the solubility value.

Literature values range from 3.08×10^{-3} to 3.62×10^{-3} mole. l^{-1} [88,89]. expressed as total oxalate and must depend upon the method of preparation of the solid.

From methods a) and b) the solubility value obtained was 3.23×10^{-3} mole. l^{-1}., and the same value within $\pm$ 1.0% was obtained over a period of at least one year. This value compared favourably with 3.20×10^{-3} mole.l^{-1}, obtained by Barney et.al.[82], and the respective thermodynamic solubility products K, given by

$$K = [Mg^{2+}][Ox^{2-}] f_2^2$$

were 7.61×10^{-7} mole^2 l^{-2} and 7.53×10^{-7} mole^2. l^{-2}.

The value of 3.08×10^{-3} mole.l^{-1} was obtained by Wyn Williams[88] by method c), and he reported a maximum value for the solubility which fell with increasing time of contact of solution with solid. This effect was observed, but the value of 3.38×10^{-3} mole.l^{-1}., was discarded in favour of the value obtained by methods used in the quantitative kinetic experiments. It is possible

in the saturator technique that the existence of very small crystallites of dimensions $\ll 1$ micron were present and dissolved to give a supersaturated solution which slowly crystallised, [68]. This could explain the increase in solubility to a maximum and subsequent crystallisation to an equilibrium value.

Growth in the Presence of Adsorbates.

Sodium dodecyl sulphate (kindly given by I.C.I. Ltd.), and sodium eosin were added to the cell solution prior to inoculation. The rate of growth was reduced by both, sodium eosin being much more effective. The upper limit of eosin ion concentration was fixed by the solubility product of magnesium eosin of 9.58×10^{-4} mole^2 l^{-2} [90]. Solutions of high ionic strength in presence of dodecyl sulphate were prepared using sodium oxalate because of the lower solubility product of potassium dodecyl sulphate [91].

The pink colour of the eosin anion interfered with the permanganate and disodium ethylene diamine tetra acetate and points, and only the conductivity technique was used. Quantitative removal of the free eosin acid by precipitation with mineral acid was not possible, presumably owing to occlusion of solution in the

flocculent precipitate. No habit modification was observed on electron microscopic examination.

Measurement of pH.

Measurements were made using a glass electrode with a decimormal calomel reference electrode with a Pye potentiometer and a Vibron Electrometer E.I.L. instrument model 33B., at null indicator. The system was calibrated with two buffer solutions of pH 4.01 and 6.99 respectively (B.D.H. soluble tablets.) . . . Measurements of the pH of the seed suspension, of the cell solution before adding the seed crystals, and of the equilibrium solutions after growth, were made in the presence and in the absence of carbon dioxidem the solutions being stirred to simulate growth conditions. All pH values were in the range 7.3 to 7.6 and at such a high pH the proportion of HOx^- complex ion present would be negligible. The total oxalate concentration in solution was therefore given by,

$$T_{ox} = \left[Ox^{-2}\right] + \left[MgOx\right] \qquad (3).$$

It was also accepted that complexes of the type KOx^- were of negligible importance in solutions of equivalent concentrations.

RESULTS:

a) Equivalent Concentrations.

The concentrations of hydrogen oxalate ion and potassium mono-oxalate ion KOx^- were negligible, so the total oxalate, equal to the total magnesium was given by,

$$T_{Mg} = [Mg^{2+}] + [MgOx] \qquad (3a)$$

$$\text{or } T_{Ox} = [Ox^{2-}] + [MgOx] \qquad (3b)$$

Tmg is equal to TOx, and therefore

$$[Mg^{2+}] = [Ox^{2-}] = m_i.$$

All concentrations are expressed as mole. l^{-1}. The ionic concentrations m_i were obtained from equations (3a, 3b) and the association constant (c) i.e.

$$K = \frac{[MgOx]}{m_i^2 \, f_2^2} \qquad (c)$$

m_i, given by

$$T_{Ox} = 2.7 \times 10^3 . f_2^2 . m_i^2 + m_i \qquad (4)$$

was evaluated by successive approximations of the ionic

strength

$$I = 2\,T_{Ox} + 4\,m_i \;\; (+ [Ads]) \qquad (5)$$

and activity coefficients were calculated by means of the Davies equation [94].

$$\log f_z = -A z^2 \left(\frac{I^{\frac{1}{2}}}{1 + I^{\frac{1}{2}}} - 0.2I \right) \qquad (6)$$

Computations were made at each point during a growth experiment and in the latter part of the work T.I.P. programmes were constructed for use in a Deuce high speed electronic computer. Total concentrations were obtained by titration and ionic concentrations by conductivity experiments, and the kinetic equations

$$-\frac{dmi}{dt} = k_1 (mi - mi^o)^2 \qquad (7)$$

and

$$-\frac{dTm}{dt} = k_2 (Tm - Tm^o)^2 \qquad (2)$$

could be tested for each experiment.

b) <u>Non equivalent ionic concentrations.</u>

The results were expressed as the amount of magnesium oxalate to be deposited before equilibrium was reached, Δ. The mathematical treatment is similar to that in part 1, and the rate equation tested was:

$$-\frac{d\Delta}{dt} = k_3(s).\ \Delta^2 \qquad \text{\_\_\_\_\_(8)}$$

From titration experiments, values of total magnesium and total oxalate were obtained and Δ evaluated by the equation,

$$(mi_{Mg} - \Delta)(mi_{Ox} - \Delta)\ f_2^2 = \text{solubility product} \qquad \text{\_\_\_(9)}$$

and mi_{Mg} obtained by successive approximations from

$$K\ f_2^2.\ mi_{Mg}^2 + mi_{Mg}\left[1 - K\ T_{Mg}\ f_2^2\right] - T_{Mg} = 0. \qquad \text{\_\_\_\_(10)}$$

Once mi_{Mg} was known, from equation (3a), MgOx could be obtained and mi_{Ox} was then obtained from equation (3b).

The more complex quadratic (10) arises from the presence of excess $MgCl_2$ in solution viz.

$$T_{Mg} = mi_{Mg} + [MgOx] \qquad \text{\_\_\_\_\_(3a)}$$

$$T_{Ox} = mi_{Ox} + [MgOx] \qquad \text{\_\_\_\_\_(3b)}$$

From electroneutrality

$$T_{Mg} \mp T_{Ox} + \tfrac{1}{2}[Cl^-] \qquad \text{\_\_\_\_\_(11)}$$

$$\therefore \quad 2mi_{Mg} = 2mi_{Ox} + [Cl^-] \qquad \text{\_\_\_\_\_(12)}$$

Then from equation (c)

$$[MgOx] = K\ mi_{Mg}\ mi_{Ox}\ f_2^2$$

By substitution in (3a)

$$T_{Mg} = mi_{Mg} + K\, mi_{Mg}\, mi_{Ox}\, f_2^2$$

$$= mi_{Mg} + K\, mi_{Mg}\, f_2^2 \left[mi_{Mg} - \frac{[Cl^-]}{2} \right]$$

from equation (12)

i.e. $K\, f_2^2\, mi_{Mg} = mi_{Mg} \left[1 - K.T_{Mg}.\, f_2^2 \right] - T_{Mg} = 0.$

<u>Mobility values.</u>

The equivalent conductivity of magnesium oxalate is given by :

$$\Lambda_{MgOx} = \Lambda^o - b\sqrt{2m_i} \;,$$

the concentration <u>mi</u> being expressed in g. mole. l^{-1}, $\Lambda^o = 127.21.$[95] and <u>b</u> = 471.4 at 25°C for a 2 : 2 electrolyte [95].

Ionic strength corrections were necessary throughout the calculations because of the large change in concentrations. Λ was evaluated for every point and the amount of solid deposited at any time was obtained by means of the equation

$$\Delta m = \frac{1000 \times \Delta 1/R \times \text{cell constant}}{2 \times \Lambda}$$

molar concentrations used.

The amount of solid deposited in experiments at non-equivalent concentrations was given by the exactly analogous equation,

$$\delta(\Delta) = \frac{1000 \times \Delta 1/R \times \text{cell constant}}{2\Delta}$$

where $\underline{\Delta}$ initial was obtained from equation (9).

Surface area corrections.

Whereas in the dissolution of silver chloride the weight dissolved was a very small percentage of the total weight of seed crystals initially added (w_1), the amount of solid deposited in the growth of magnesium oxalate was quite substantial. As the crystals enlarged, the surface area would increase and the rate equation which would include the surface area correction would be written

$$-\frac{dm_1}{dt} = k1\ (s)\ (m_1 - m_1^{o})^2 .$$

Assuming that the seed crystals were uniform cubes and that w_1 mg. of magnesium oxalate were present in the solution at the commencement of the crystallisation process, then

$$v1 = \left(\frac{w_1}{d}\right) \text{ and } a_1 \propto \left(\frac{w_1}{d}\right)^{2/3}$$

where $\underline{d}$ is the density of magnesium oxalate, $\underline{v}_1$ the initial volume of the seed crystals present in the solution, and $\underline{a}_1$, their total surface area. Supposing that at any instant $\underline{w}_2$ mg. of magnesium oxalate is present i.e. $w_2 = w_1$ + weight deposited, then the new surface area is

$$a_2 \propto \left(\frac{w_2}{d}\right)^{2/3}$$

Thus $a_1 / a_2 \propto \left(\frac{w_1}{w_2}\right)^{2/3}$ and to correct the observed rates of crystallisation for changes in surface area caused by crystallisation, they must be multiplied by the factor $(w_2 / w_1)^{2/3}$ since the rate of crystallisation is proportional to the total surface area of seed crystals present.

$$\text{i.e. } -\left(\frac{w_2}{w_1}\right)^{2/3} \times \frac{dm_1}{dt} = k_1 (m_1 - m_1^o)^2 .$$

$$\text{or } -\frac{dm_1}{dt} = k_1 \left(\frac{w_1}{w_2}\right)^{2/3} \times (m_1 - m_1^o)^2 .$$

<u>Experimental Results.</u>

Some crystallisation experiments at 25° C with equivalent ionic concentrations are summarised in

Tables 11 and 16 : C and T refer to conductivity and titration experiments, and subscripts r, t, and s to rotary stirring, turbulent stirring and shaking respectively. Typical conductivity time and total concentration time curves are shown in Figs. 9 to 25. For a given amount of inoculating seed crystals an induction period was observed whenever the initial ionic concentration product rose above a well defined value; for approximately 25 mg. / 100 ml. of added seed crystals, this was 2.9×10^{-5} $mole^2 . l^{-2}$. The duration of the induction period varied between 30 and 220 min. and was approximately inversely proportional to the supersaturation as is seen in Table 16 which contains the results of experiments with high initial concentrations.

For experiments with initial concentrations below this limit, the plots of the integrated form of the equation (6) are good straight lines passing through the origin Figs. 9, 11, 14 and 15.
Experiments 29 Tt and 30 Tt, Fig. 9, show very good agreement for runs at different ionic strength while 31 Tt and 32 Ct show good agreement between conductivity and titration results, Fig.11. The reproducibility of the conductivity method is illustrated by experiments

TABLE. 11.

Crystallisation Experiments. at 25°C. $[Mg^{2+}]/[Ox^{2-}] = 1$.

Low Initial Concentrations.

Expt. no.	Init. $(m_i - m_i^o) \times 10^3$ mole.l^{-1}.	I $\times 10^2$	Seed Susp.	Seed conc. mg./100ml.	k_1 l.mole^{-1}. h^{-1}.
$29T_t$	1.34	1.01	E	24	0.90
$30T_t$	1.33	3.14	E	24	0.95
$31T_t$	1.18	0.96	E	30	0.96
$32O_t$	1.30	0.99	E	30	0.84
$36O_t$	2.07	1.29	F	23	5.81
$37O_t$	3.97	2.06	F	23	7.24
$39O_t$	3.39	1.84	F	23	6.50
$40O_t$	4.17	2.12	F	ca.25	10.00
$66O_t$	2.21	1.35	F	23	-

TABLE. 12.

$T_m \times 10^3$ mole. l^{-1}.	$f_2 \times 10^1$	$m_1 \times 10^3$ mole. l^{-1}.	$(m_1 - m_1^0) \times 10^{-3}$ mole. l^{-1}.	$(m_i - m_i^0)^{-1} \times 10^{-2}$ mole. l^{-1}	$\{(m_i - m_i^0)^{-1} - (m_i - m_i^0)^{-1}_{initial}\} \times 10^{-1}$ mole. l^{-1}	time h.
Run. 29.ft						
9.940	6.581	2.519	1.346	7.430	0	0
9.574	6.612	2.456	1.283	7.798	0.368	1
9.307	6.635	2.409	1.236	8.093	0.663	2
9.294	6.636	2.407	1.234	8.108	0.678	3
9.139	6.650	2.379	1.206	8.292	0.862	4
8.962	6.666	2.348	1.175	8.513	1.083	5
8.752	6.685	2.310	1.137	8.794	1.364	19
8.447	6.714	2.255	1.082	9.241	1.811	24
3.230	7.435	1.173	0	–	–	∞
Run. 30.T_t.						
9.428	5.099	3.050	1.328	7.003	0	0
9.365	5.107	3.005	1.282	7.230	0.227	0.5
9.080	5.117	2.945	1.223	7.557	0.554	2
9.080	5.124	2.945	1.223	7.557	0.554	3
8.900	5.126	2.907	1.185	7.781	0.778	4
8.861	5.127	2.899	1.177	7.832	0.829	4.5
8.818	5.133	2.890	1.168	7.888	0.885	5
8.674	5.377	2.859	1.137	8.085	1.082	5.5

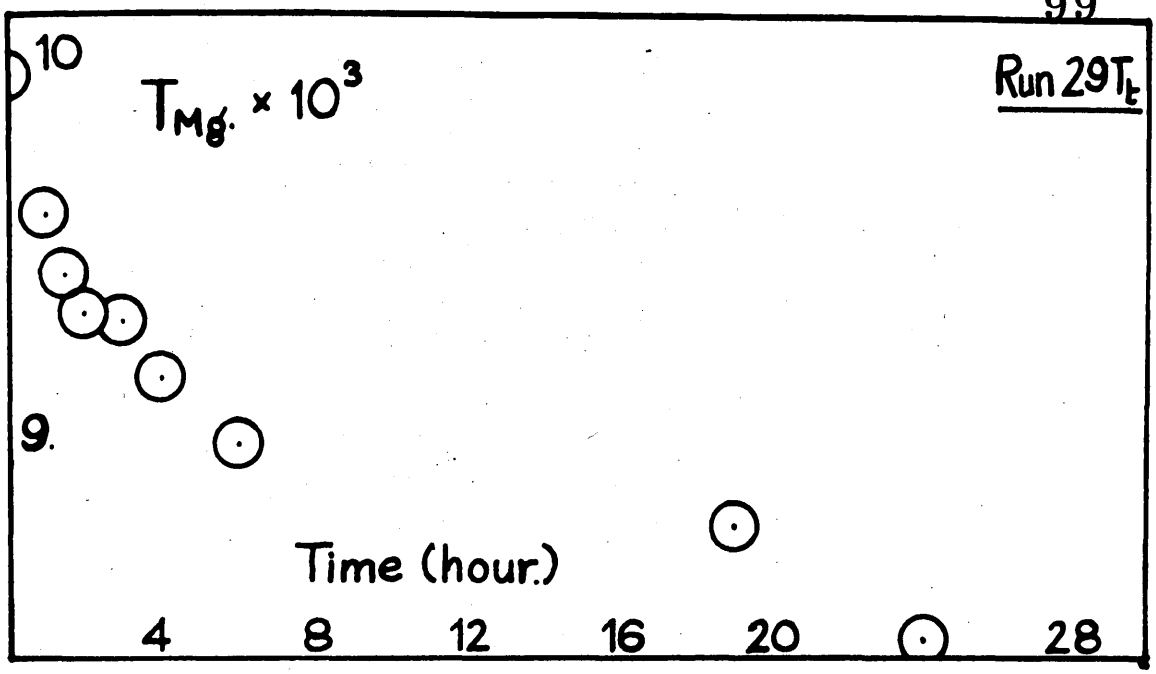
10
$T_{Mg.} \times 10^3$
Run 29T_t
9.
Time (hour.)
4
8
12
16
20
28

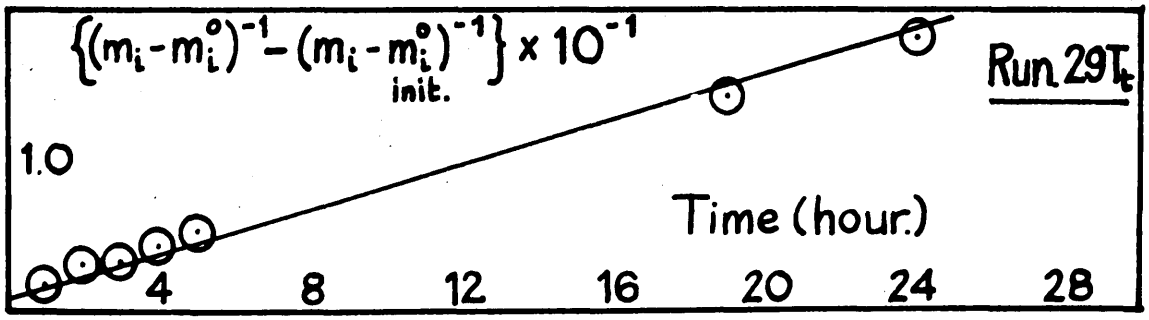
$\{(m_i - m_i^o)^{-1} - (m_i - m_i^o)^{-1}_{init.}\} \times 10^{-1}$
Run 29T_t
1.0
Time (hour.)
4
8
12
16
20
24
28

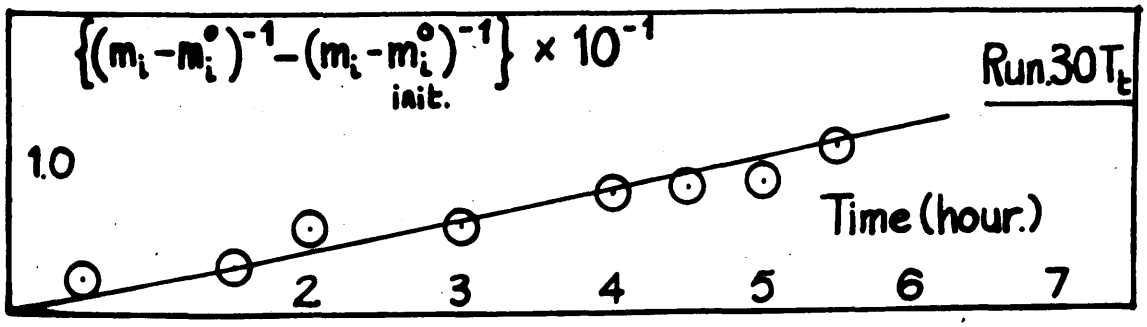
$\{(m_i - m_i^o)^{-1} - (m_i - m_i^o)^{-1}_{init.}\} \times 10^{-1}$
Run 30T_t
1.0
Time (hour.)
2
3
4
5
6
7

Fig. 9.

TABLE. 13.

$T_m \times 10^3$ mole.l^{-1}	$f_z \times 10$	$m_i \times 10^3$ mole.l^{-1}	$(m_i - m_i^o) \times 10^3$ mole.l^{-1}	$(m_i - m_i^o)^{-1} \times 10^{-2}$ mole.l^{-1}	$\{(m_i - m_i^o)^{-1} - (m_i - m_i^o)^{-1}_{initial}\} \times 10^{-2}$ mole.l^{-1}	time h.
RUN. 31 T_c						
8.928	6.642	2.352	1.179	8.387	0	0
8.724	6.688	2.305	1.132	8.833	0.446	1
8.682	6.692	2.298	1.125	8.892	0.505	3
8.618	6.698	2.286	1.113	8.984	0.597	4
8.494	6.710	2.264	1.071	9.169	0.782	5
8.326	6.722	2.235	1.062	9.416	1.029	8
8.262	6.732	2.222	1.049	9.537	1.150	9.5
8.201	6.826	2.092	0.919	10.887	2.500	20
3.230	7.435	1.173	0.0	-	-	∞
$\frac{1}{R} \times 10^3$	Λ					
Run. 32 C_6						
5.6225	103.88	2.470	1.297	7.710	0	0
5.5715	103.96	2.431	1.258	7.949	0.239	1
5.5542	104.05	2.412	1.239	8.071	0.361	2
5.4540	104.26	2.387	1.214	8.237	0.527	5
5.3812	104.40	2.334	1.161	8.613	0.903	8
5.3277	104.52	2.308	1.135	8.811	1.101	11
5.2420	104.77	2.266	1.093	9.149	1.439	17
5.2048	104.92	2.247	1.074	9.311	1.601	20
-	-	1.173	0	-	-	∞

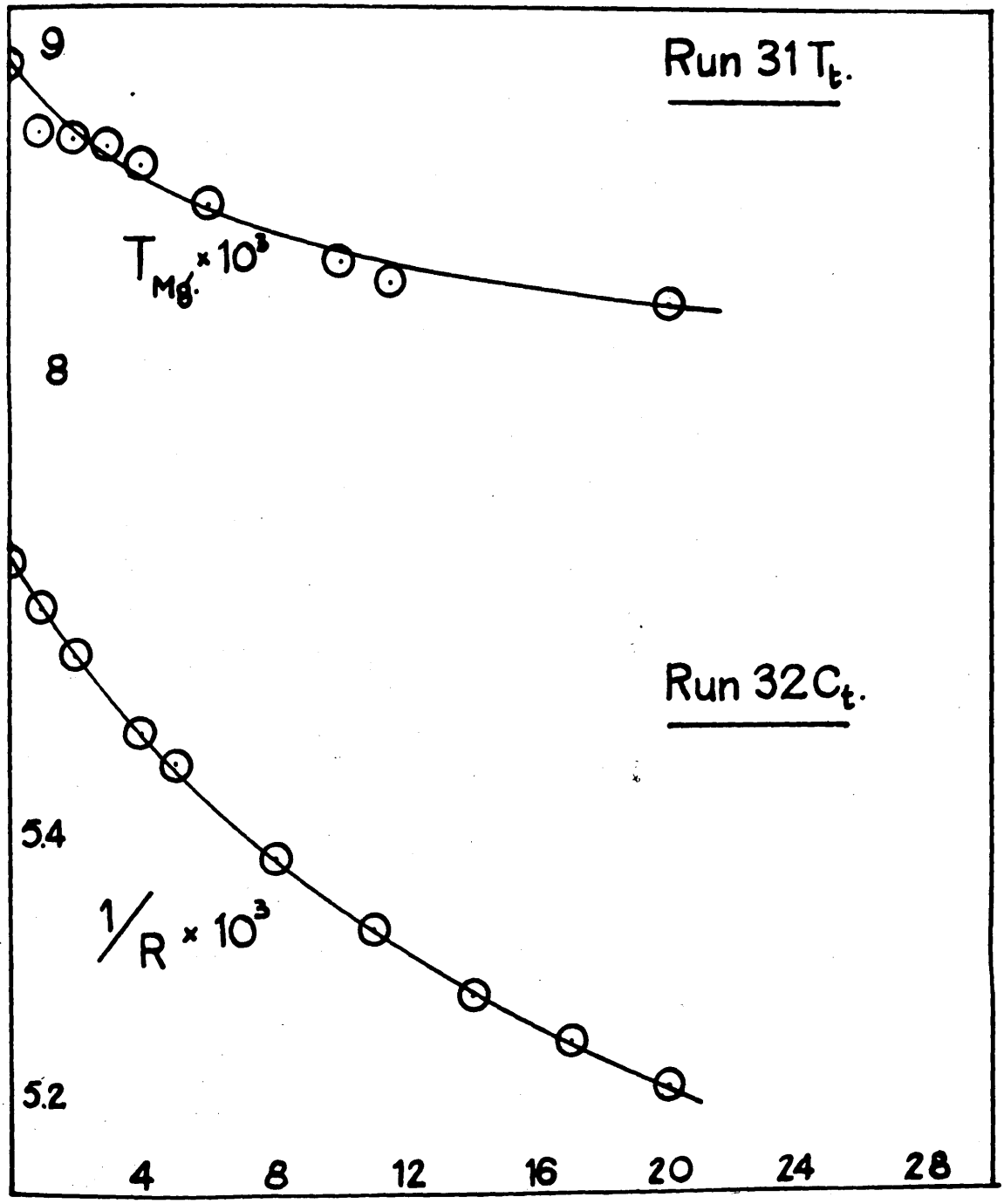

Fig.10.

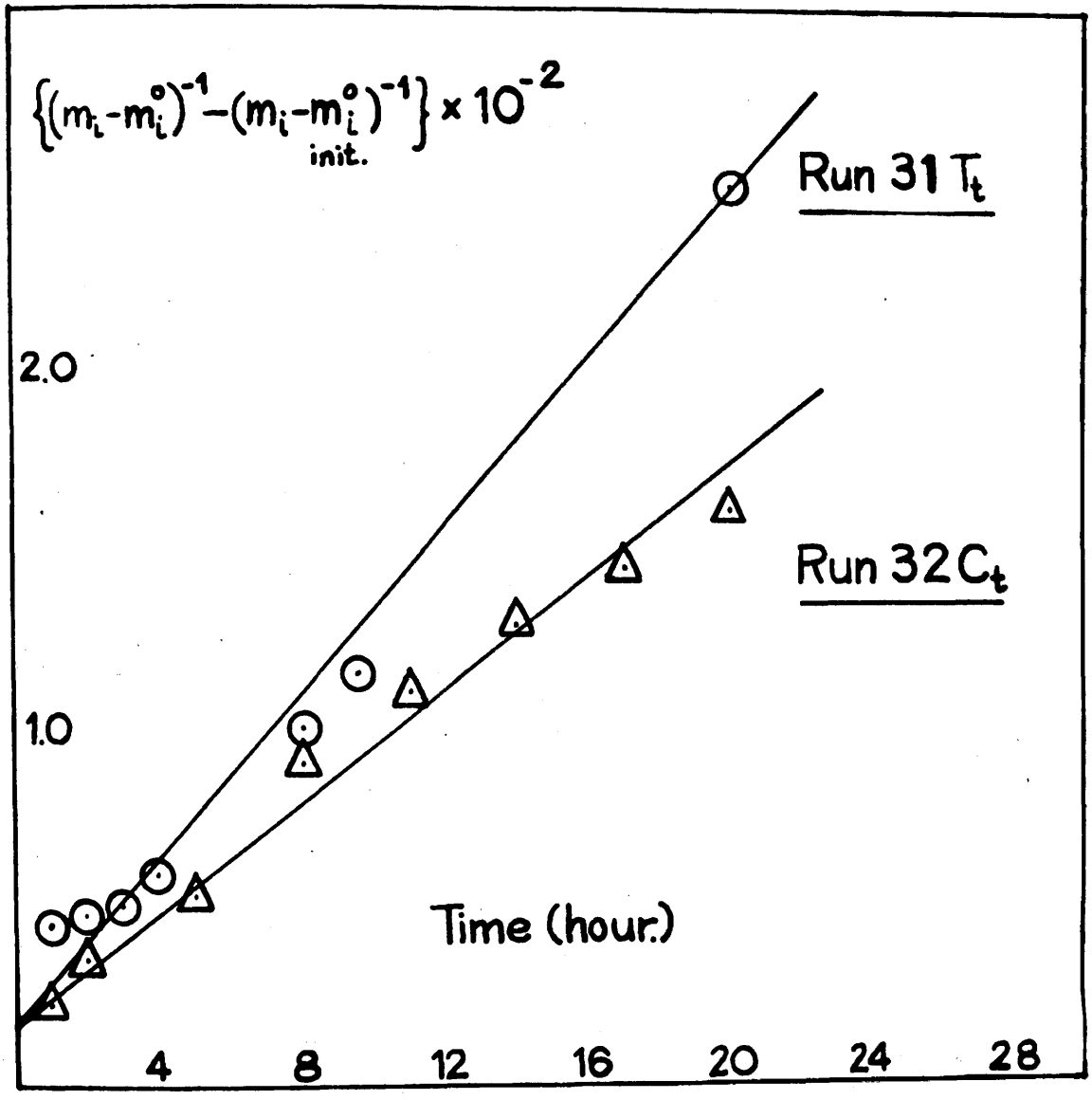
$\{(m_i-m_i^o)^{-1}-(m_i-m_i^o)^{-1}_{init.}\} \times 10^{-2}$
Run 31 T_t
Run 32 C_t
2.0
1.0
Time (hour.)
4
8
12
16
20
24
28

Fig. 11.

$\underline{36C_t}$, $\underline{37C_t}$, $\underline{39C_t}$, and $\underline{40C_t}$. The rate equation requires that the rate constant should be independent of the degree of supersaturation, and $\underline{36C_t}$ and $\underline{39C_t}$, Fig.14, confirm this. The K_1 values for $\underline{37C_t}$ and $\underline{40C_t}$ are slightly higher, and perhaps this is owing to their being just below the limiting conditions and very slight induction effects occurred. The integrated rate plots are given in Fig.15. This adherence to equation (6) persisted for Ca. 50% of the total precipitation corresponding to the duration of most experiments which lasted for 17 hours at least. In experiments followed photographically, growth was seen to take place entirely on the added seed crystals, illustrated in Plate 2 (a,b), in which are shown seed crystals in experiment $\underline{66}$ C_t after 15 minutes and 23 hours.

Above the concentration limit, the time plots show an induction effect, Figs. 16, 18 and 20, and the integrated plots of equation (7) are straight lines which have an intercept on the time axis, Figs. 17, 19, 21. This intercept corresponds to the duration of the induction period estimated by the method of Schierholz[96]. and if the origin is moved to this intersection, then a good second order equation is followed for at least 80% of the total reaction, this

TABLE. 14.

$1/R \times 10^3$	Λ	$(m_i - m_i^0) \times 10^3$ mole. l^{-1}	$m_i \times 10^3$ mole. l^{-1}	$(m_i - m_i^0)^{-1} \times 10^{-2}$ mole. l^{-1}	$\{(m_i - m_i^0)^{-1} - (m_i - m_i^0)^{-1}_{initial}\}$ $\times 10^{-2}$ mole. l^{-1}	time h.
Run. 36 C_t						
7.2188	100.34	2.076	3.249	4.817	0	0
7.1632	100.46	2.058	3.231	4.859	0.042	1
7.1105	100.53	2.031	3.204	4.924	0.107	2
7.0171	100.70	1.983	3.156	5.043	0.226	4
6.9725	100.81	1.960	3.133	5.102	0.285	5
6.9246	100.92	1.936	3.109	5.165	0.348	6
6.4918	101.90	1.710	2.883	5.848	1.031	17
6.4303	102.06	1.681	2.854	5.949	1.132	19
6.3702	102.16	1.652	2.825	6.053	1.236	21
-	-	0	1.173	-	-	∞
Run. 37 C_t						
10.598	93.42	3.967	5.140	2.521	0	0
10.503	93.62	3.909	5.082	2.558	0.037	0.5
10.240	94.05	3.759	4.932	2.660	0.139	2
10.063	94.43	3.654	4.827	2.737	0.216	3
9.899	94.69	3.564	4.737	2.806	0.285	4
9.745	95.08	3.471	4.644	2.881	0.360	5
9.631	95.34	3.399	4.572	2.942	0.421	5.75
8.189	98.24	2.603	3.776	3.842	1.321	16.5
-	-	0	1.173	-	-	∞

TABLE. 15.

$\frac{1}{R}\times10^3$	Λ	$m_i\times10^3$ mole.l^{-1}	$(m_i-m_i^0)\times10^3$ mole.l^{-1}	$(m_i-m_i^0)^{-1}\times10^{-2}$ mole.l^{-1}	$\{(m_i-m_i^0)^{-1}-(m_i-m_i^0)^{-1}_{initial}\}\times10^{-2}$ mole.l^{-1}	time h.
Run. 399$_t$						
9.6038	95.36	4.562	3.389	2.951	0	0
9.4526	95.68	4.475	3.302	3.028	0.077	1
9.3304	95.93	4.406	3.233	3.093	0.142	2
9.2105	96.16	4.338	3.165	3.160	0.209	3
8.9753	96.64	4.206	3.033	3.297	0.346	5
8.8679	96.88	4.147	2.974	3.362	0.411	6
7.6907	99.29	3.509	2.336	4.281	1.330	21
7.6255	99.44	3.474	2.301	4.346	1.395	22
-	-	1.173	0	-	-	∞
Run. 400$_t$						
10.9358	92.77	5.340	4.167	2.400	0	0
10.4403	93.71	5.048	3.875	2.581	0.181	2
9.9485	94.71	4.758	3.585	2.789	0.389	4
9.1597	96.25	4.312	3.139	3.186	0.786	8
8.8345	96.90	4.130	2.957	3.382	0.982	10
8.5474	97.51	3.971	2.798	3.574	1.174	12
7.9869	98.65	3.668	2.495	4.008	1.608	16
7.7214	99.22	3.525	2.352	4.252	1.852	18
7.2646	100.20	3.284	2.111	4.737	2.337	22
-	-	1.173	0	-	-	∞

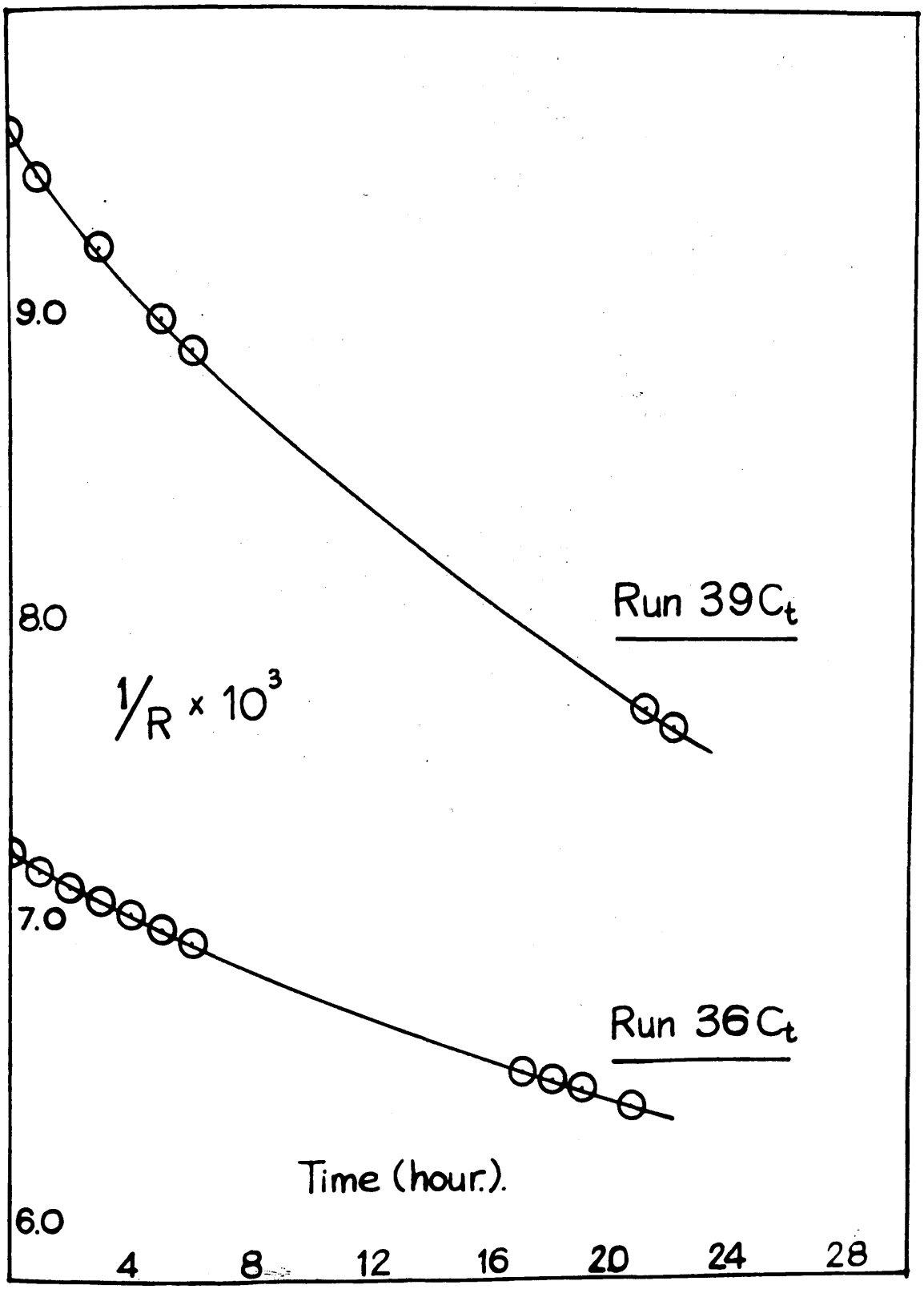

Fig. 12.

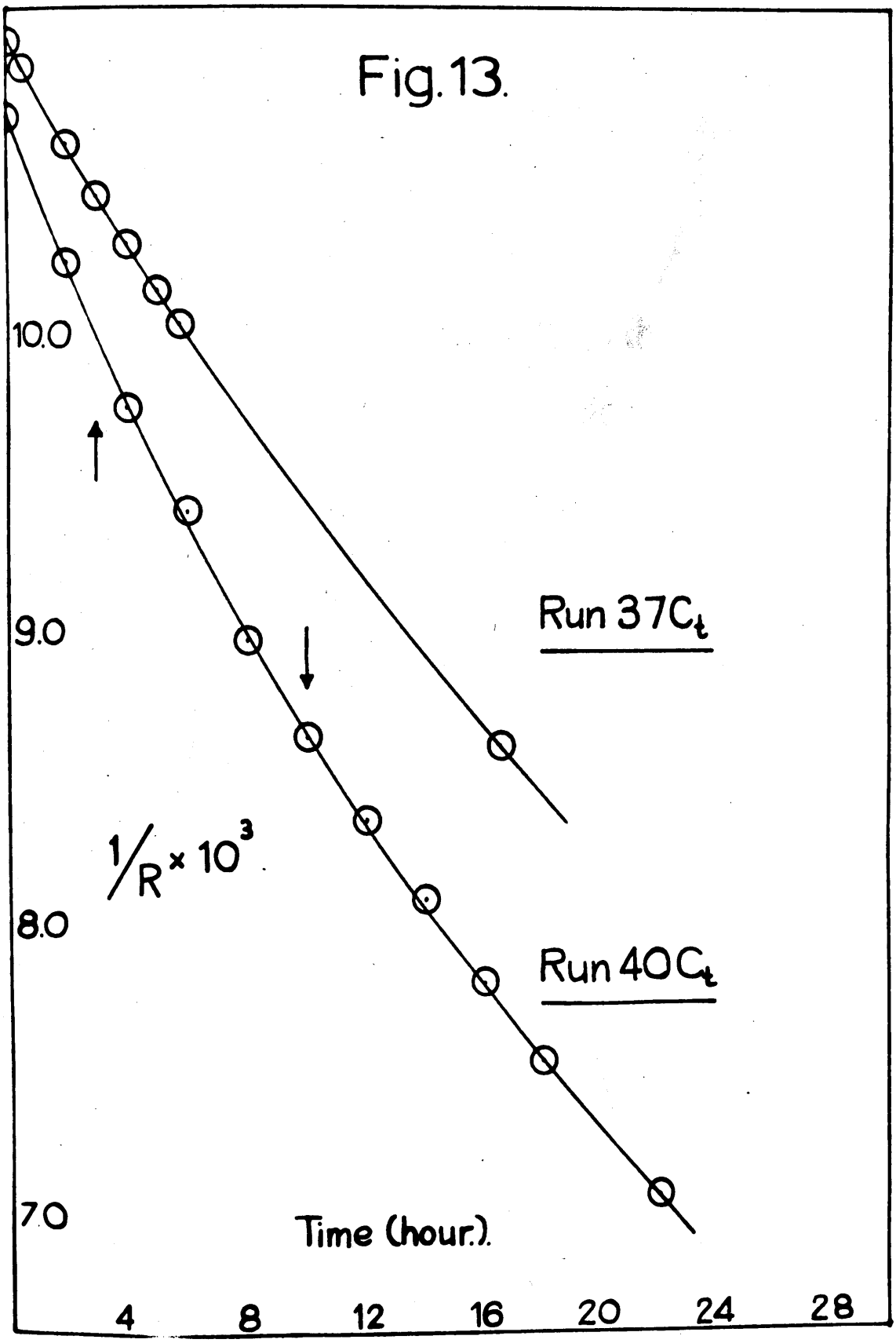
Fig. 13.
10.0
9.0
8.0
7.0
1/R × 10³
Run 37C_t
Run 40C_t
Time (hour.).
4
8
12
16
20
24
28

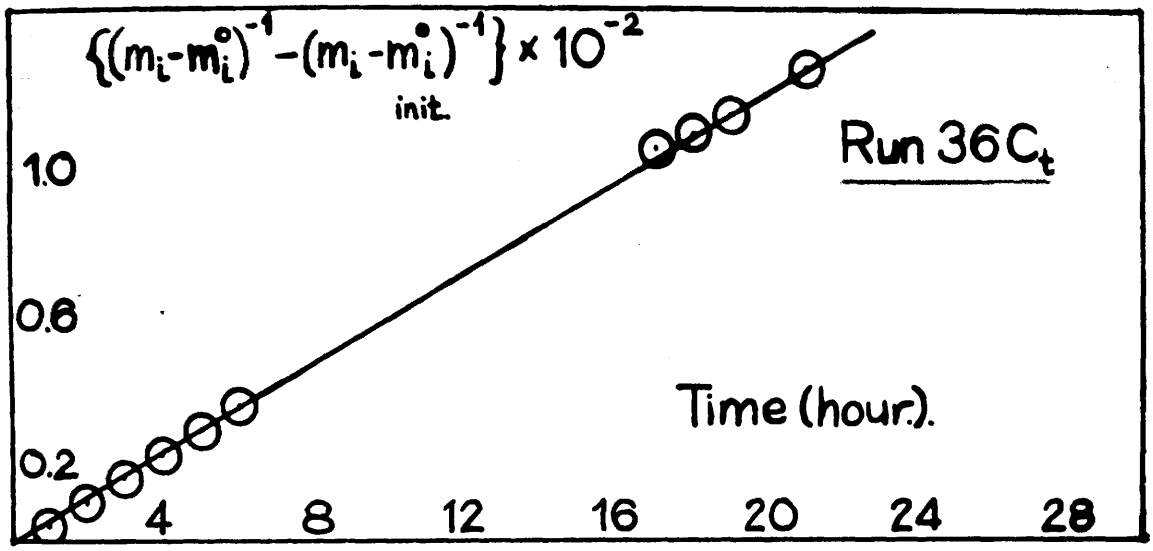
$\{(m_i-m_i^o)^{-1}-(m_i-m_i^o)^{-1}_{init.}\}\times 10^{-2}$
Run 36 C_t
1.0
0.6
0.2
Time (hour.).
4
8
12
16
20
24
28

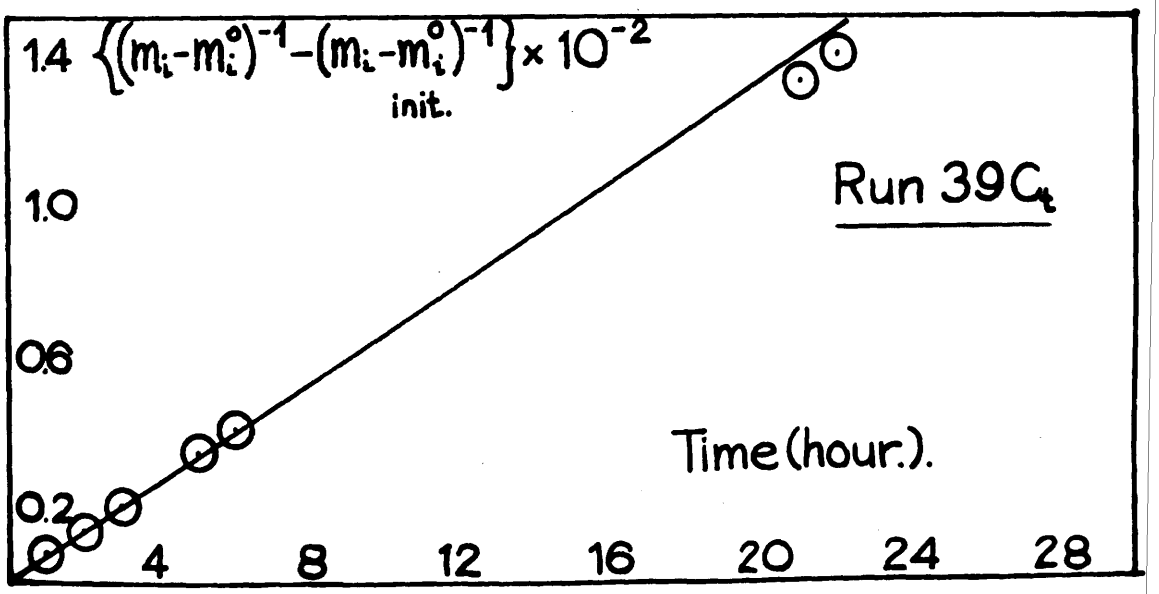
1.4
$\{(m_i-m_i^o)^{-1}-(m_i-m_i^o)^{-1}_{init.}\}\times 10^{-2}$
Run 39 C_t
1.0
0.6
0.2
Time (hour.).
4
8
12
16
20
24
28

Fig. 14.

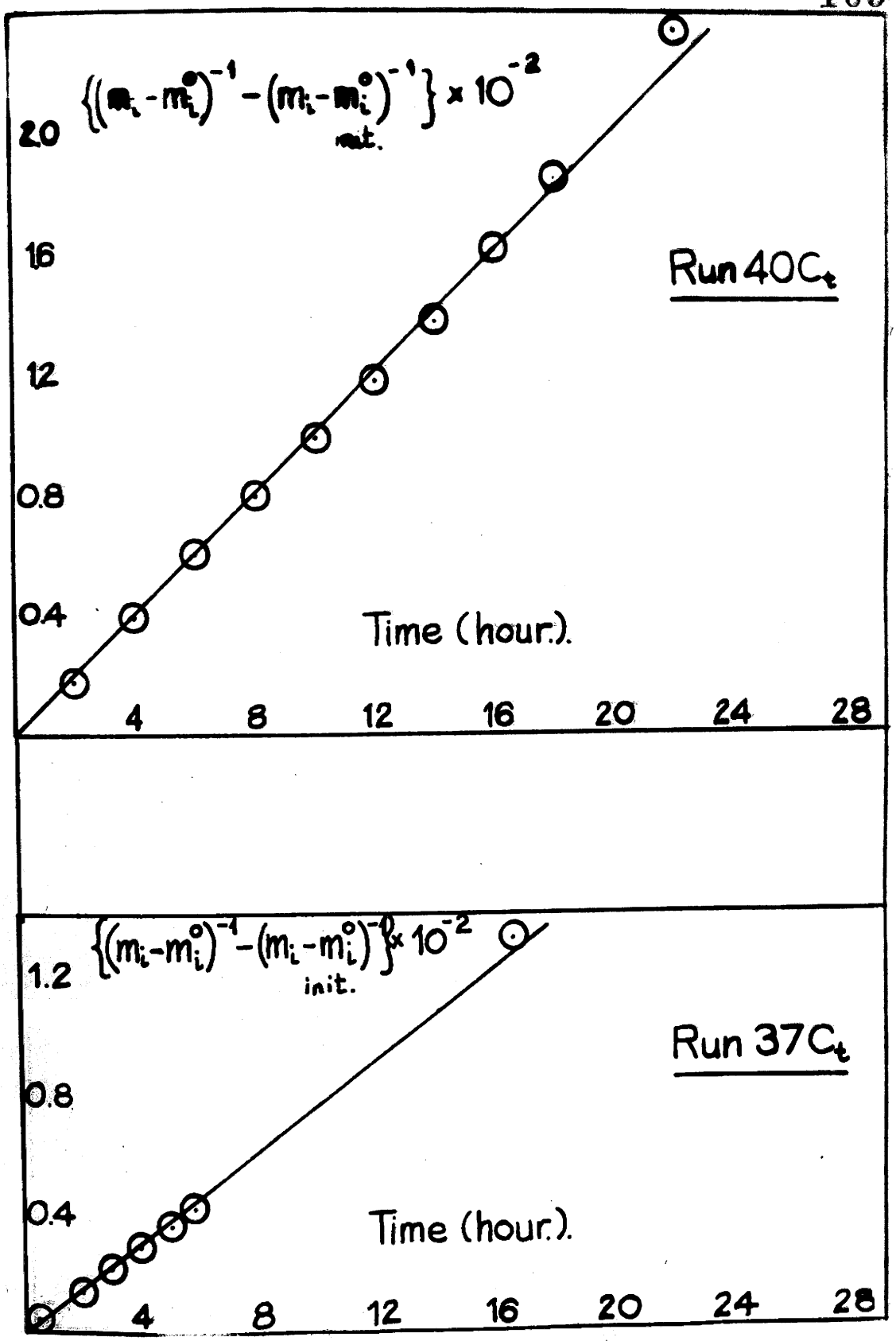
$\{(m_i - m_i^\circ)^{-1} - (m_i - m_i^\circ)^{-1}_{init.}\} \times 10^{-2}$
2.0
1.6
1.2
0.8
0.4
Run 40C$_t$
Time (hour.).
4
8
12
16
20
24
28
$\{(m_i - m_i^\circ)^{-1} - (m_i - m_i^\circ)^{-1}_{init.}\} \times 10^{-2}$
1.2
0.8
0.4
Run 37C$_t$
Time (hour.).
4
8
12
16
20
24
28

Fig. 15.

Plate. 2.

Photographic evidence for the elimination of Spontaneous Growth.

Plate 2.

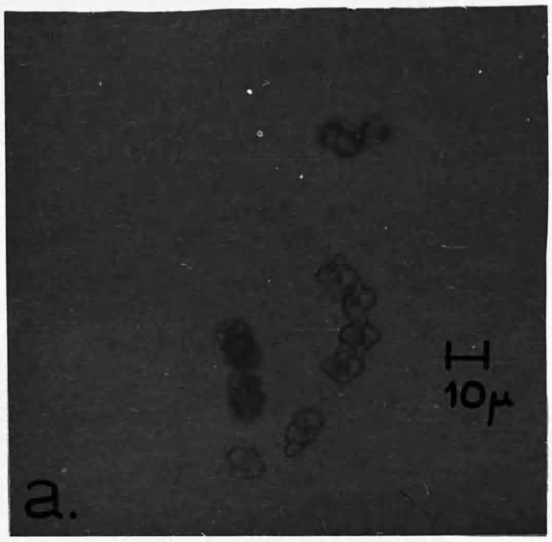

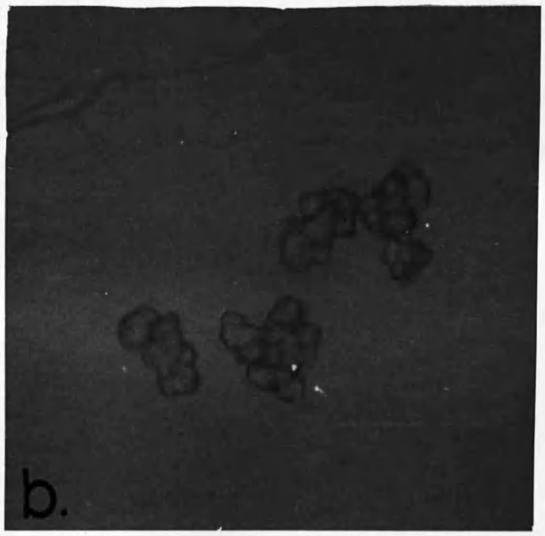

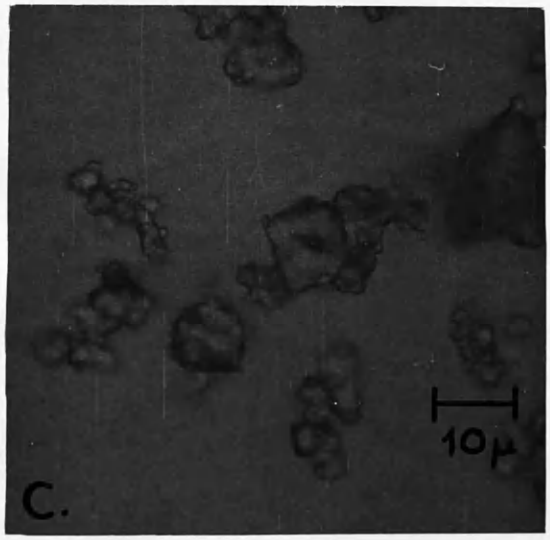

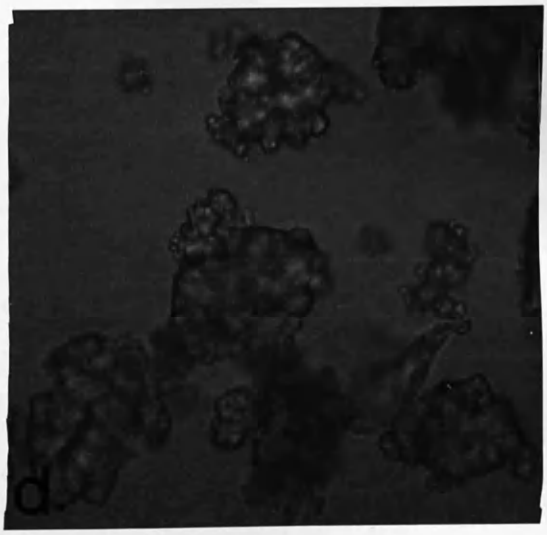

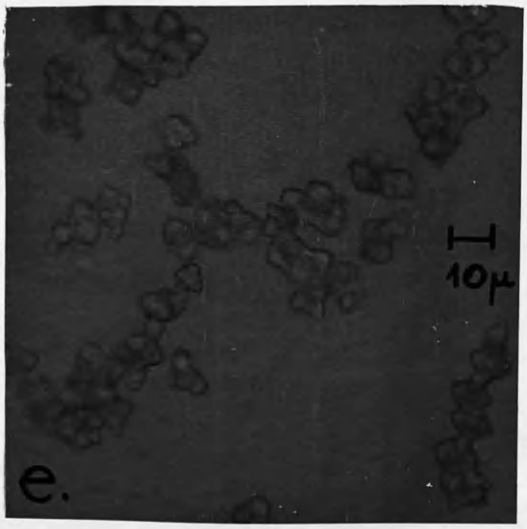

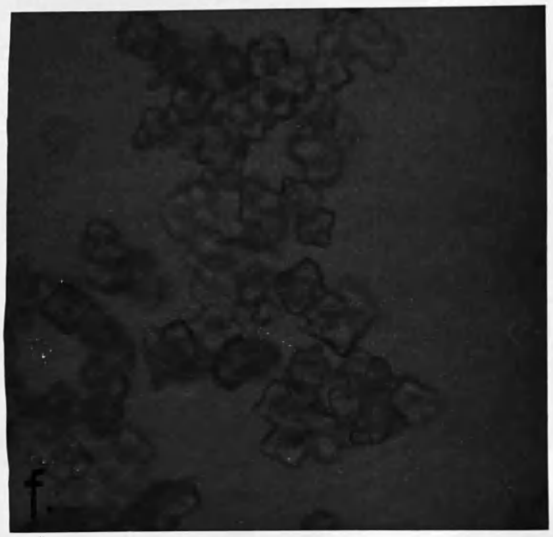

TABLE. 16.

Crystallisation Experiments at 25°C. $[Mg^{2+}]/[Ox^{2-}] = 1$.

High Initial Concentrations.

Expt. no.	Init. $(m_i - m_i^o) \times 10^3$	$I \times 10^2$	Seed Susp.	Seed conc. (mg/100ml)	Ind. Per. (min.)	k_1 l.mole. h^{-1}.
$4T_r$	13.06	20.34	A	18	70	80
$6T_r$	8.90	13.94	B	32	120	77
$7T_r$	8.94	13.94	B	32	120	89
$8T_r$	9.00	13.94	A	18	120	70
$26T_t$	4.17	2.12	E	24	190	28
$27C_t$	4.17	2.12	E	24	190	25
$38C_t$	5.50	2.68	F	23	155	15
$41T_t$	4.24	2.16	F	23	220	16
$42T_t$	5.49	8.90	F	23	220	8
$67T_s$	4.43	2.25	F	83	none	37
$68T_s$	11.55	17.96	F	100	30	37
$69T_s$	6.06	8.18	F	50	none	18
$70T_s$	6.06	8.18	F	100	none	44
$71T_s$	3.81	6.65	F	100	none	42
$72T_s$	3.81	6.65	F	150	none	63

Fig. 16.

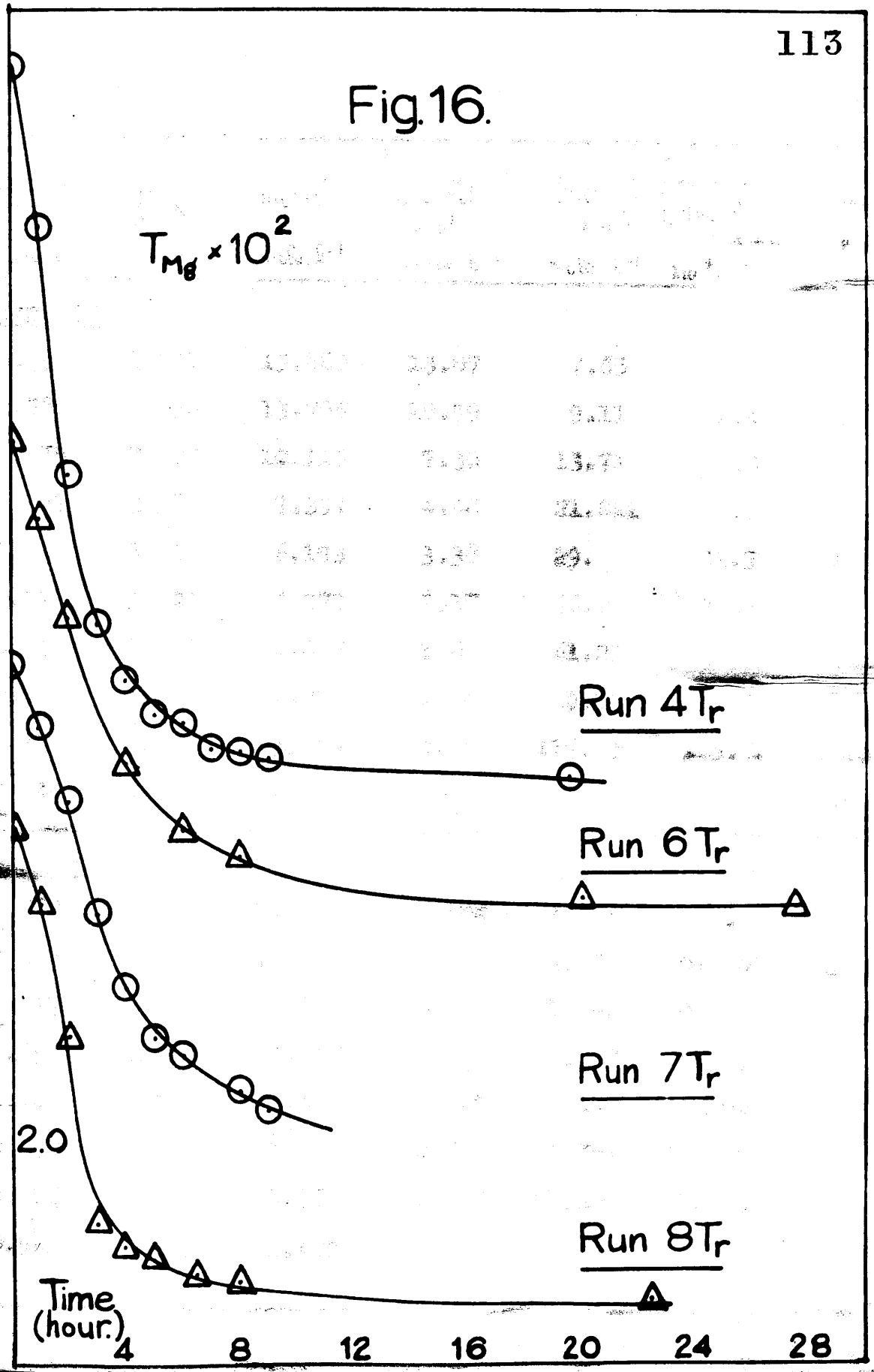
$T_{Mg} \times 10^2$
Run 4 T_r
Run 6 T_r
Run 7 T_r
Run 8 T_r
2.0
Time (hour.)
4
8
12
16
20
24
28

TABLE. 17.

$T_m \times 10^2$ mole.l^{-1}	$f_2 \times 10$	$m_i \times 10^3$ mole.l^{-1}	$(m_i - m_i^o) \times 10^3$ mole.l^{-1}	$(m_i - m_i^o)^{-1} \times 10^{-3}$ mole.l^{-1}	$\{(m_i - m_i^o)^{-1} - (m_i - m_i^o)^{-1}_{initial}\} \times 10^{-3}$ mole.l^{-1}	time h.
Run. 4T$_r$						
6.992	2.817	15.880	13.07	7.65	0	0
5.560	2.854	13.796	10.99	9.11	1.46	1
3.375	2.927	10.110	7.30	13.71	6.06	2
2.057	2.986	7.397	4.58	21.821	14.17	3
1.280	3.014	6.193	3.38	29.60	21.95	4
1.118	3.044	4.979	2.17	46.19	38.45	6
0.944	3.057	4.447	1.63	61.20	53.55	8
0.883	3.062	4.252	1.44	69.52	61.87	9
0.710	3.078	3.665	0.85	117.47	109.82	19.5
0.540	3.101	2.814	0	-	-	∞
Run. 6T$_r$				$\times 10^{-2}$	$\times 10^{-2}$	
4.687	3.186	11.381	[illegible]	1.124	0	0
3.997	3.219	10.297	7.817	1.279	0.155	1
3.117	3.269	8.805	6.325	1.581	0.457	2
1.256	3.412	4.928	2.448	4.087	2.963	6
1.028	3.437	4.322	1.842	5.430	4.306	8
0.642	3.487	3.154	0.674	13.843	12.719	20
0.616	3.491	3.066	0.586	17.065	15.941	27.5
0.541	3.517	2.480	0	-	-	∞

TABLE. 18.

$T_m \times 10^2$ mole.l^{-1}	$f_2 \times 10$	$m_i \times 10^3$ mole.l^{-1}	$(m_i - m_i^o) \times 10^3$ mole.l^{-1}	$(m_i - m_i^o)^{-1} \times 10^{-2}$ mole.l^{-1}	$\{(m_i - m_i^o)^{-1} - (m_i - m_i^o)^{-1}_{initial}\}$ $\times 10^{-2}$ mole.l^{-1}	time h.
Run. 7T$_r$						
4.707	3.182	11.421	8.937	1.119	0	0
4.159	3.208	10.567	8.083	1.237	0.118	1
3.497	3.243	9.476	6.992	1.430	0.311	2
2.485	3.306	7.638	4.154	1.940	0.821	3
1.841	3.354	6.311	3.827	2.613	1.494	4
1.236	3.410	4.881	2.397	4.172	3.053	6
0.925	3.445	4.035	1.551	6.448	5.329	8
0.764	3.465	3.551	1.067	9.368	8.249	9
0.541	3.512	2.484	0	-	-	∞
Run. 8T$_r$						
4.745	3.173	11.499	9.009	1.110	0	0
4.081	3.205	10.460	7.970	1.255	0.145	1
2.918	3.270	8.469	5.979	1.672	0.562	2
1.240	3.402	4.800	2.310	4.150	3.040	3
0.956	3.433	4.131	1.641	6.095	4.985	5
0.827	3.449	3.751	1.261	7.929	6.819	6.5
0.749	3.459	3.510	1.020	9.803	8.693	8
0.638	3.490	2.800	0.310	30.175	29.065	22.5
0.540	3.503	2.490	0	-	-	∞

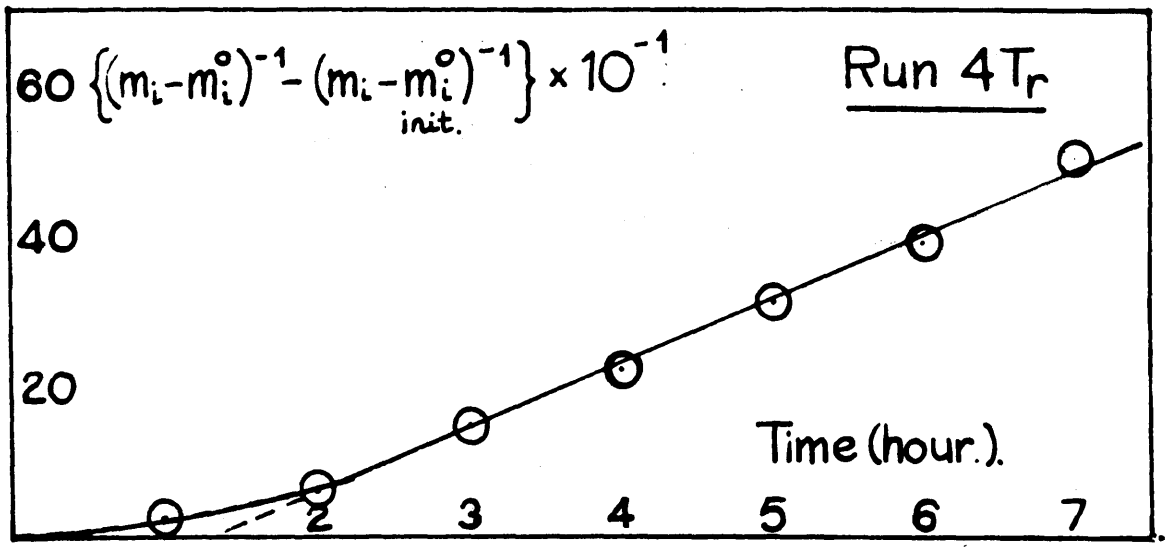
60 {(m_i-m_i^o)^-1-(m_i-m_i^o)_init.^-1} x 10^-1
Run 4Tr
40
20
Time (hour.).
2
3
4
5
6
7

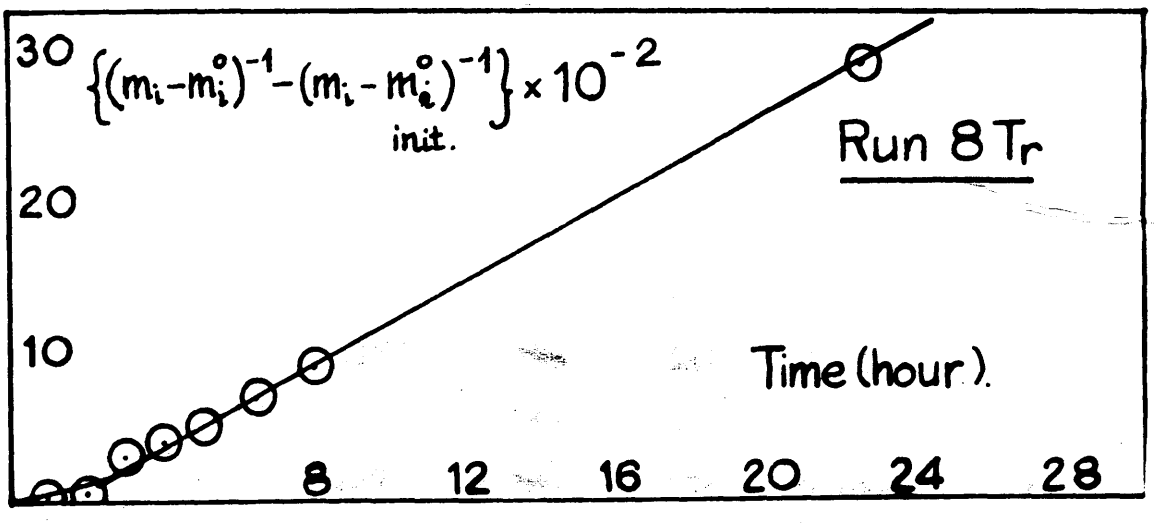
30 {(m_i-m_i^o)^-1-(m_i-m_i^o)_init.^-1} x 10^-2
Run 8Tr
20
10
Time (hour).
8
12
16
20
24
28

Fig. 17.

TABLE. 19.

$T_m \times 10^2$ mole. l^{-1}	$f_2 \times 10$	$m_i \times 10^3$ mole. l^{-1}	$(m_i - m_i^o) \times 10^3$ mole. l^{-1}	$(m_i - m_i^o)^{-1} \times 10^{-2}$ mole. l^{-1}	$\{(m_i - m_i^o)^{-1} - (m_i - m_i^o)^{-1}_{initial}\} \times 10^{-2}$ mole. l^{-1}	time h.
Run. 269$_t$						
3.003	5.66	5.34	4.17	2.398	0	0
2.918	5.71	5.17	4.05	2.469	0.071	0.5
2.878	5.74	5.06	4.00	2.500	0.102	1
2.787	5.75	4.88	3.89	2.571	0.173	2
2.637	5.79	4.21	3.71	2.695	0.297	3
2.131	5.82	3.34	3.04	3.289	0.891	5.5
1.380	6.32	2.54	2.17	4.611	2.213	12
1.030	6.68	2.11	1.37	7.320	4.922	22
$1/R \times 10^3$	Λ					
Run. 270$_t$						
11.790	–	5.340	4.167	2.400	0	0
11.410	93.36	5.[illegible]	3.[illegible]	2.[illegible]	0.[illegible]	[illegible]
10.960	94.16	4.916	3.743	2.672	0.272	4
9.970	95.66	4.478	3.305	3.026	0.626	6
7.790	99.27	3.514	2.341	4.272	1.872	10
6.290	101.85	2.894	1.721	5.811	3.411	15
5.500	103.27	2.760	1.587	6.301	3.901	20
5.160	103.87	2.448	1.275	7.843	5.443	24

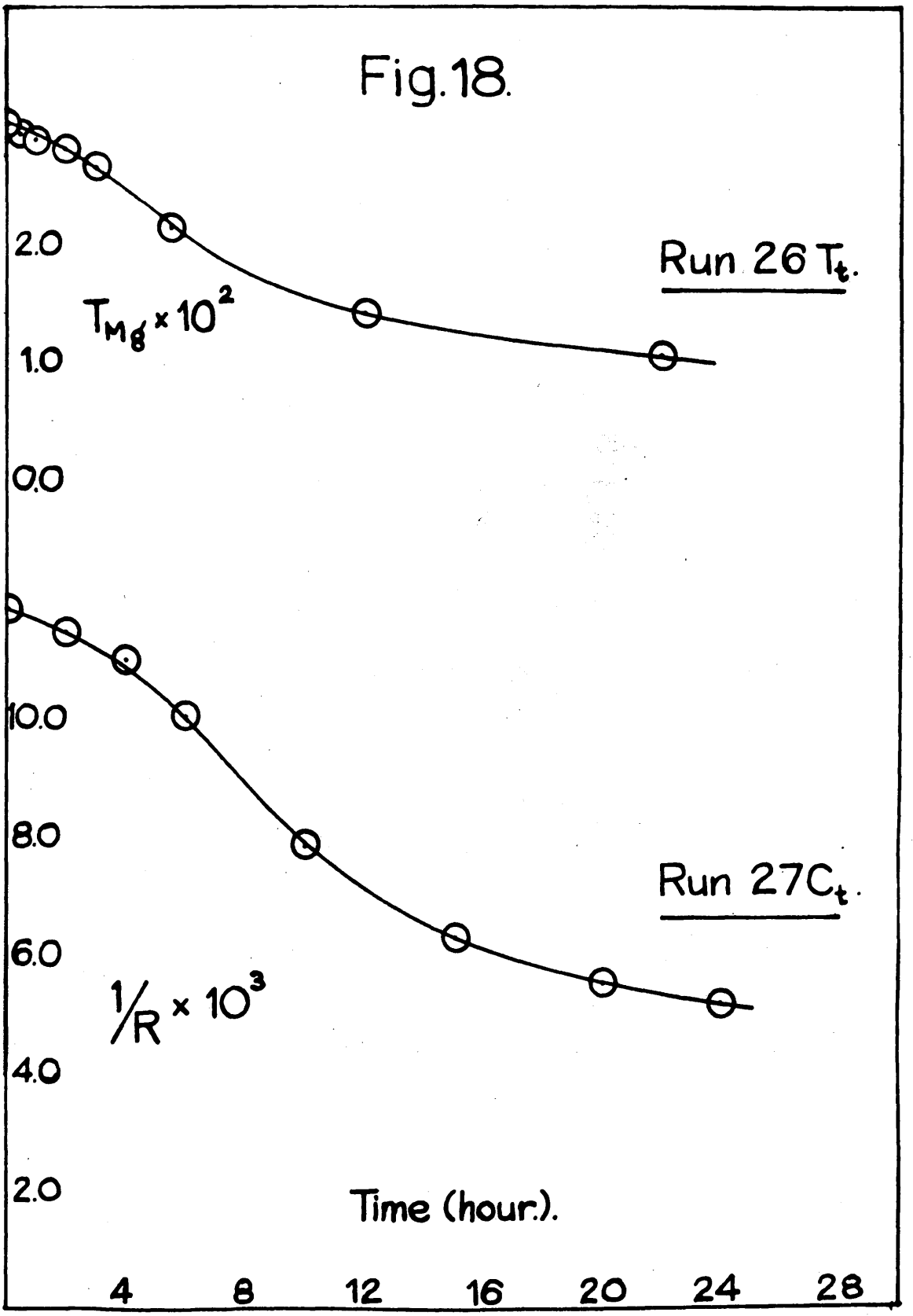
Fig.18.
2.0
1.0
0.0
$T_{Mg} \times 10^2$
Run 26 T_t.
10.0
8.0
6.0
4.0
2.0
$1/R \times 10^3$
Run 27 C_t.
Time (hour.).
4
8
12
16
20
24
28

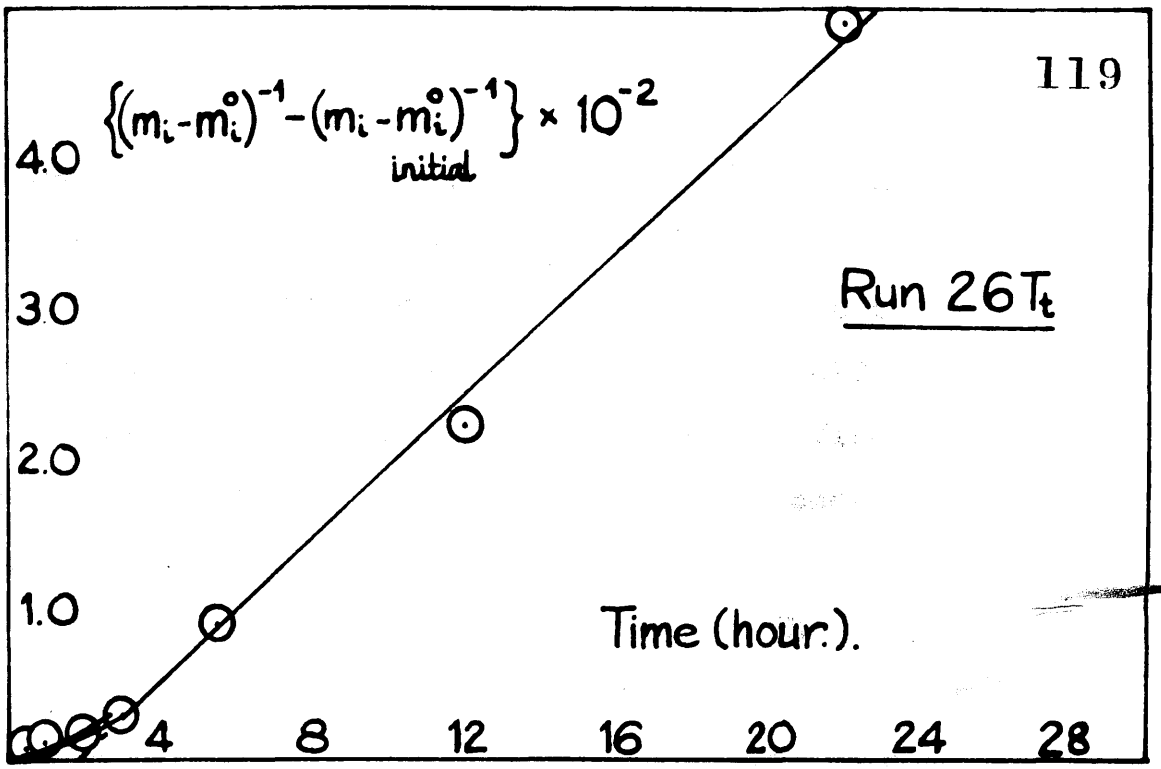
$\{(m_i-m_i^o)^{-1}-(m_i-m_i^o)^{-1}_{initial}\} \times 10^{-2}$
4.0
3.0
2.0
1.0
Run 26T$_t$
Time (hour.).
4
8
12
16
20
24
28

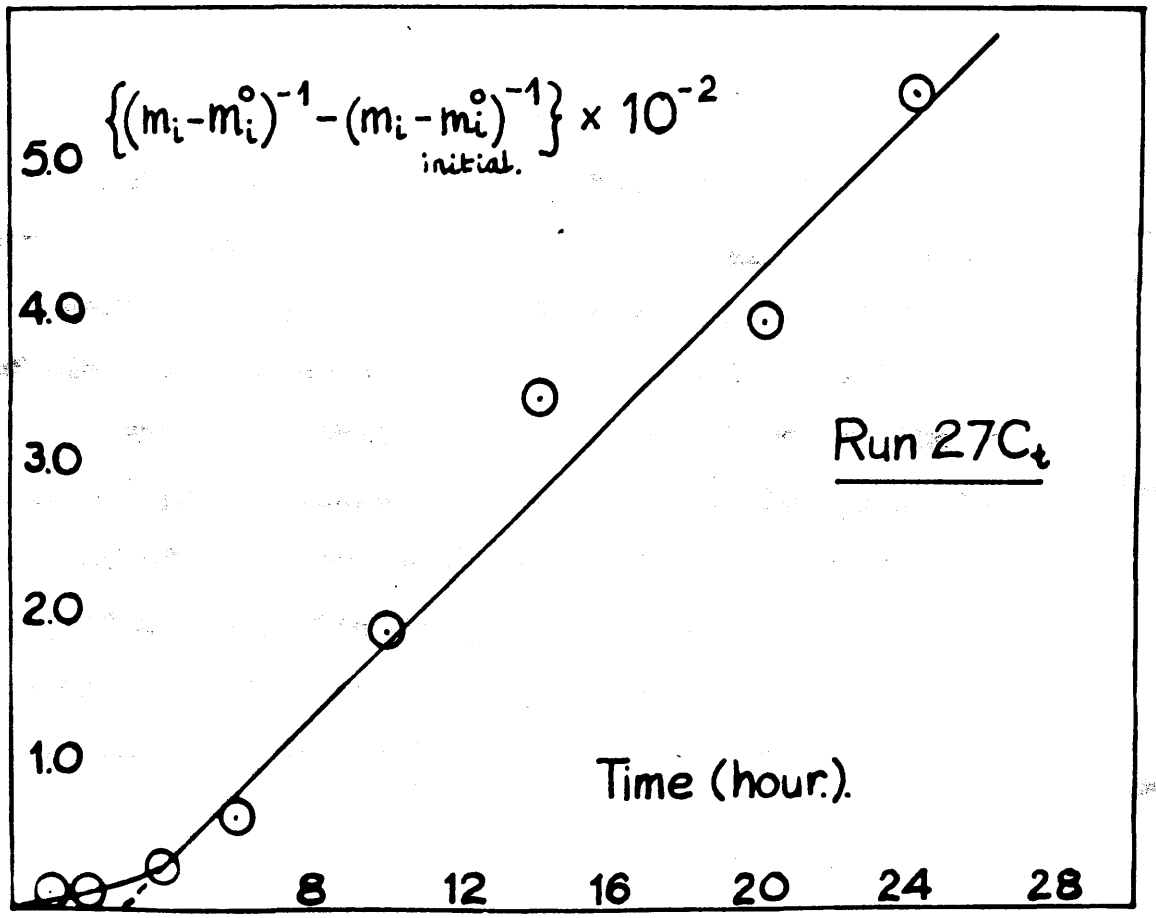
$\{(m_i-m_i^o)^{-1}-(m_i-m_i^o)^{-1}_{initial.}\} \times 10^{-2}$
5.0
4.0
3.0
2.0
1.0
Run 27C$_t$
Time (hour.).
8
12
16
20
24
28

Fig 19

percentage being the fraction of the total actually followed, the experiment being stopped before equilibrium was reached. It was not possible to interpret the kinetics of the induction itself and mixed mechanisms, including zero order and first order, and first order and second order were unsuccessfully applied.

Photomicroscopic examination showed that inoculation of growth with seed crystals was accompanied by nucleation, Plate 2 (c,d); growth continued on all the crystals present. As well as complicating the overall kinetics of growth, nucleation would not allow very good reproducibility, since it is very different to reporduce the conditions for heterogeneous nucleation. In spite of this experiments 26 Tt and 27 Ct, Fig. 19, show very good agreement and consistency for both techniques, as also do 38 Ct and 41 Tt in Fig. 21.

It was found that nucleation and therefore the induction period could be eliminated completely by the addition of a larger amount of inoculating crystals, Figs. 22 and 24. The straight line plot for the integrated form of equation (7) passes through the origin for runs 67 Ts, 68 Ts, 69 Ts and 70 Ts.

TABLE. 20.

$\frac{1}{R} \times 10^3$	Λ	$m_i \times 10^3$ mole.l^{-1}	$(m_i - m_i^o) \times 10^3$ mole.l^{-1}	$(m_i - m_i^o)^{-1} \times 10^{-2}$ mole.l^{-1}	$\{(m_i - m_i^o)^{-1} - (m_i - m_i^o)^{-1}_{initial}\}$ $\times 10^{-2}$.mole.l^{-1}	time h.
Run. 380.						
13.076	88.70	6.677	5.504	1.817	0	0
12.843	89.12	6.530	5.357	1.867	0.050	1
12.605	89.56	6.376	5.203	1.922	0.105	2
12.389	89.98	6.230	5.063	1.975	0.158	2.75
11.655	91.36	5.779	4.606	2.171	0.354	5
11.127	92.36	5.456	4.283	2.335	0.518	6
10.721	93.17	5.214	4.041	2.475	0.658	6.75
7.522	99.62	3.420	2.247	4.550	2.633	20.50
$T_m \times 10^2$	$f_2 \times 10$					
Run. 41T.						
2.939	5.616	5.416	4.243	2.414	0	0
2.793	5.665	5.130	3.957	2.527	0.113	1
2.669	5.707	4.970	3.797	2.634	0.220	2
2.535	5.856	4.793	3.621	2.762	0.348	3
2.286	5.851	4.461	3.288	3.041	0.627	5
2.006	5.971	4.075	2.902	3.446	1.032	7
1.889	6.025	3.808	2.635	3.655	1.241	8
1.052	6.612	2.610	1.437	6.959	4.545	19.25
1.003	6.573	2.535	1.362	7.344	4.930	20.25

TABLE. 21.

$T_m \times 10^2$ mole. l^{-1}	$f_2 \times 10$	$m_i \times 10^3$ mole. l^{-1}	$(m_i - m_i^o) \times 10^3$ mole. l^{-1}	$(m_i - m_i^o)^{-1} \times 10^{-2}$ mole. l^{-1}	$\{(m_i - m_i^o)^{-1} - (m_i - m_i^o)^{-1}_{initial}\}$ $\times 10^{-2}$ mole. l^{-1}	time h.
Run. 42T.						
2.926	3.699	7.649	5.499	1.818	0	0
2.843	3.706	7.510	5.360	1.866	0.048	0.5
2.761	3.714	7.372	5.222	1.914	0.097	1.5
2.613	3.725	7,169	5.019	1.992	0.174	2.5
2.414	3.748	6.767	4.617	2.166	0.384	4
2.345	3.756	6.643	4.493	2.226	0.408	5
2.258	3.765	6.485	4.335	2.307	0.489	6
2.079	3.786	6.152	4.002	2.499	0.681	7.5
1.212	3.899	4.351	2.201	4.544	2.726	19
1.126	3.912	4.148	1.998	5.005	3.187	21
1.046	3.926	3.954	1.804	5.543	3.725	23.5
-	4.057	2.150	0	-	-	∞

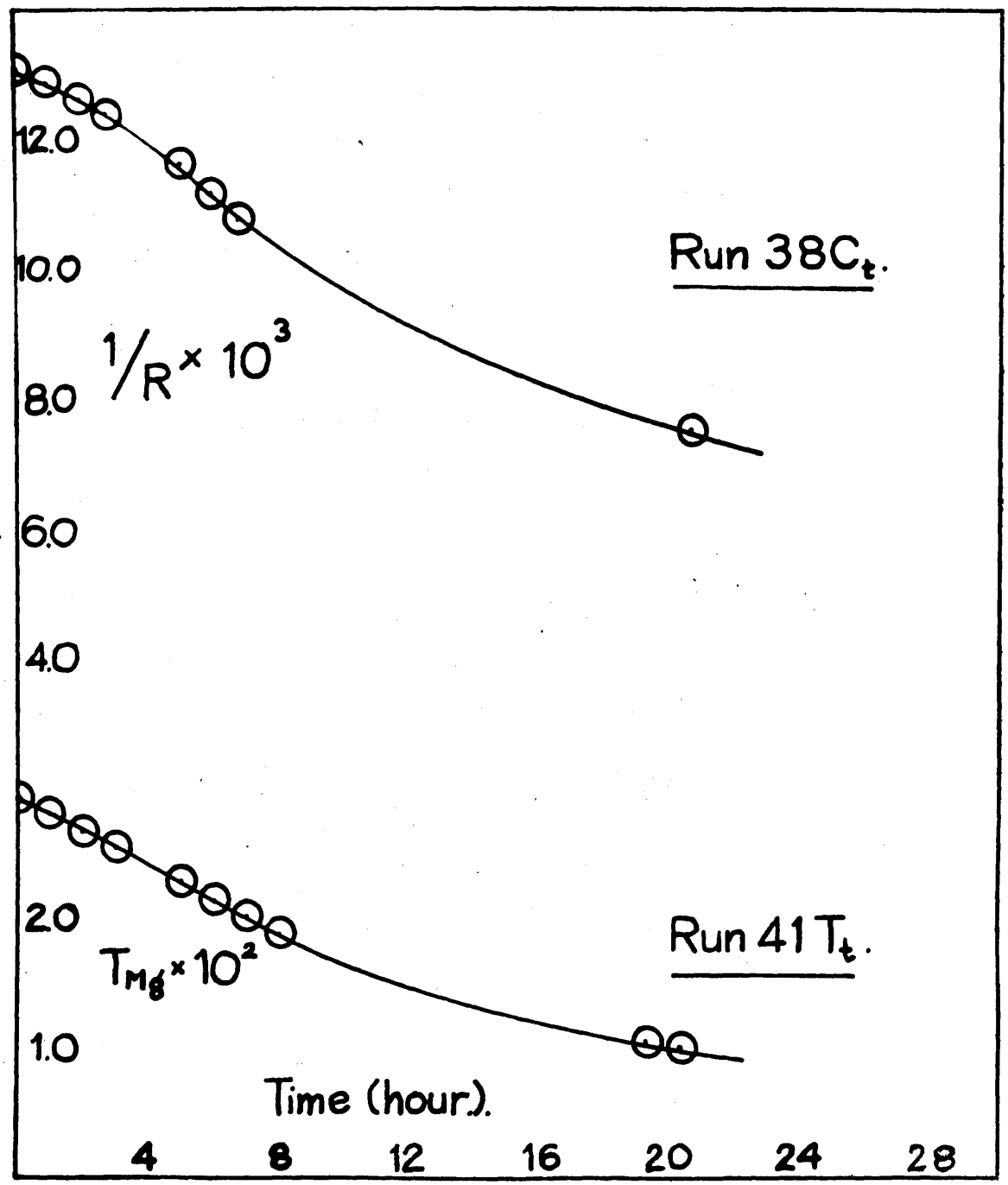
12.0
10.0
8.0
6.0
4.0
2.0
1.0
1/R × 10³
Run 38Ct.
TMg × 10²
Run 41 Tt.
Time (hour).
4
8
12
16
20
24
28

Fig. 20.

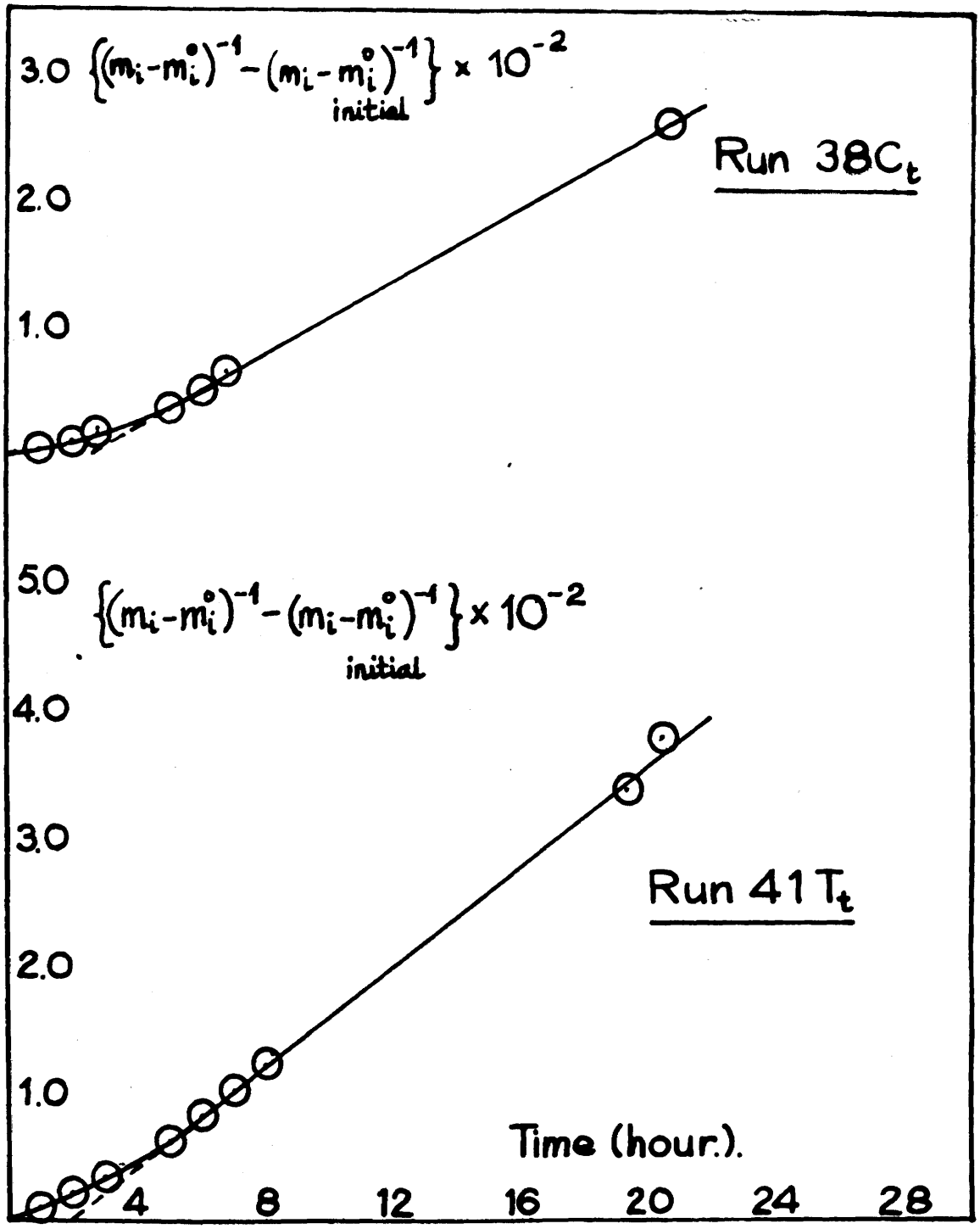
3.0
2.0
1.0
$\{(m_i-m_i^\circ)^{-1}-(m_i-m_i^\circ)^{-1}_{initial}\} \times 10^{-2}$
Run 38C$_t$
5.0
4.0
3.0
2.0
1.0
$\{(m_i-m_i^\circ)^{-1}-(m_i-m_i^\circ)^{-1}_{initial}\} \times 10^{-2}$
Run 41 T$_t$
Time (hour.).
4
8
12
16
20
24
28

Fig. 21.

TABLE. 22.

$T_m \times 10^2$ mole.l^{-1}	$f_2 \times 10$	$m_i \times 10^3$ mole.l^{-1}	$(m_i - m_i^o) \times 10^3$ mole.l^{-1}	$(m_i - m_i^o)^{-1} \times 10^{-2}$ mole.l^{-1}	$\{(m_i - m_i^o)^{-1} - (m_i - m_i^o)^{-1}_{initial}\}$ $\times 10^{-2}$ mole.l^{-1}	time h.
Run. 67T.						
3.167	5.545	5.603	4.430	2.257	0	0
2.971	5.606	5.357	4.184	2.390	0.133	0.5
2.620	5.725	4.906	3.733	2.679	0,422	1.0
2.419	5.788	4.700	3.507	2.852	0,595	1.5
2.014	5.967	4.086	2.913	3.433	1.176	3.25
1.605	6.171	3.494	2.321	4.308	2.051	5.5
1.356	6.318	3.113	1.940	5.155	2.898	8.5
0.753	6.806	2.086	1.913	10.953	8.696	23.0
Run. 68T.				$\times 10^{-1}$	$\times 10^{-1}$	
6.130	2.930	14.246	11.547	8.661	0	0
5.672	2.945	13.575	10.876	9.195	0.534	0.5
4.616	2.981	11.943	9.244	10.819	2.158	1.75
3.052	3.046	9.221	6.522	15.332	6.671	3.25
1.768	3.117	6.522	3.823	26.160	17.499	5.50
0.771	3.198	3.775	1.076	92.944	84. 283	23.0
-	3.232	2.699	0	-	-	∞

TABLE. 23.

$T_m \times 10^2$ mole.l^{-1}	$f_2 \times 10$	$m_i \times 10^3$ mole.l^{-1}	$(m_i - m_i^o) \times 10^3$ mole.l^{-1}	$(m_i - m_i^o)^{-1} \times 10^{-2}$ mole.l^{-1}	$\left\{(m_i - m_i^o)^{-1} - (m_i - m_i^o)^{-1}_{initial}\right\}$ $\times 10^{-2}$ mole.l^{-1}	time h.
Run. 69T$_s$						
3.212	3.592	8.274	6.064	1.649	0	0
2.874	3.611	7.710	5.500	1.818	0.169	1
2.719	3.634	7.443	5.233	1.911	0.262	1.75
2.391	3.644	6.859	4.649	2.151	0.502	3.25
1.933	3.711	5.989	3.779	2.646	0.997	5.50
0.860	3.858	3.546	1.336	7.482	5.833	23.50
-	3.948	2.210	0	-	-	∞
Run. 70T$_s$						
3.212	3.592	8.274	6.064	1.649	0	0
2.449	3.659	6.964	4.754	2.103	0.454	0.5
1.900	3.715	5.924	3.714	2.693	1.044	1.75
1.500	3.763	5.091	2.881	3.471	1.822	3.25
1.344	3.797	4.512	2.302	4.343	2.694	5.50
0.664	3.894	2.987	0.777	12.871	11.222	23.50

Fig. 22.

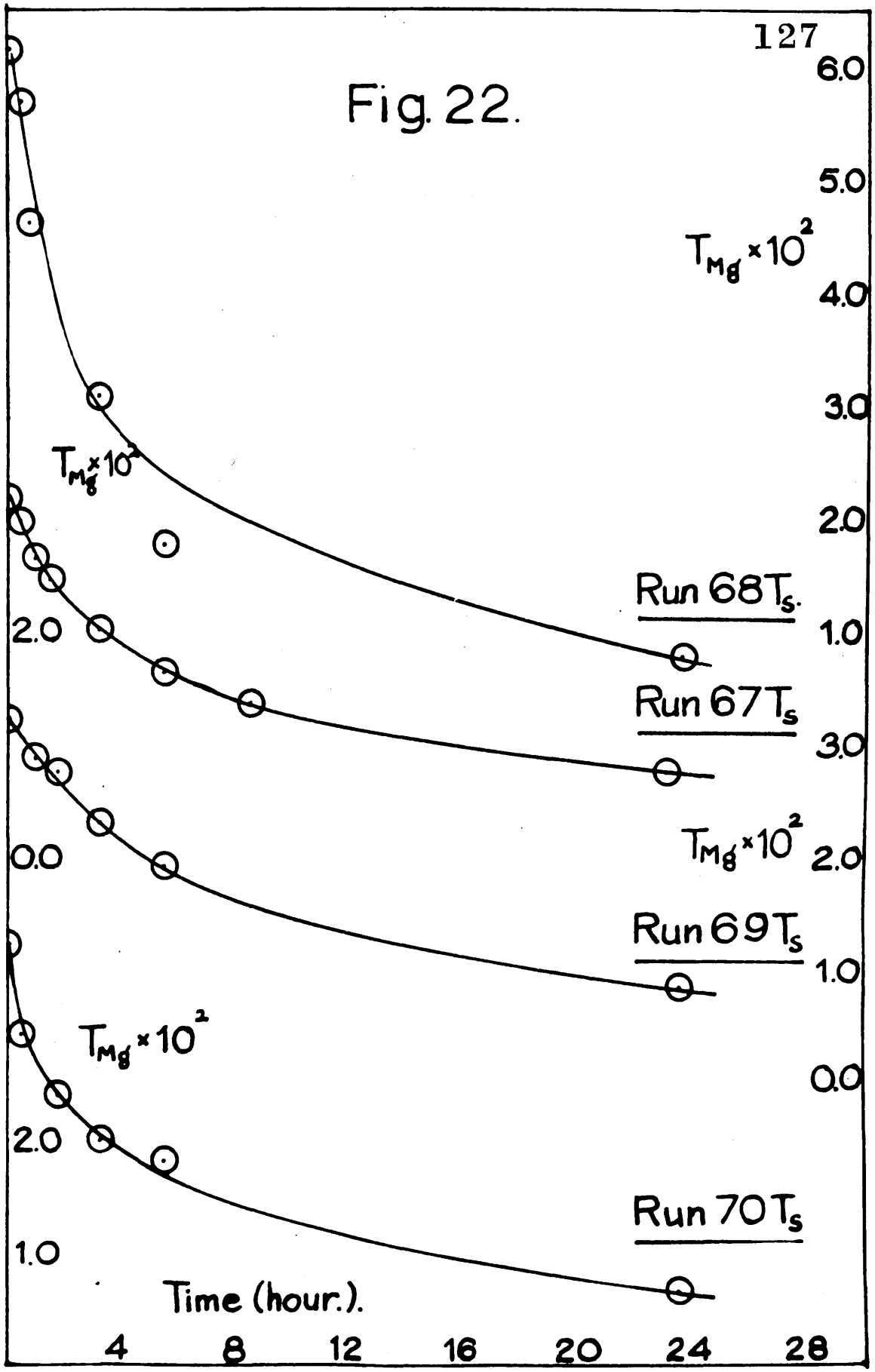
6.0
5.0
$T_{Mg} \times 10^2$
4.0
3.0
$T_{Mg} \times 10^2$
2.0
Run 68 T_s.
1.0
2.0
Run 67 T_s
3.0
$T_{Mg} \times 10^2$
0.0
2.0
Run 69 T_s
1.0
$T_{Mg} \times 10^2$
0.0
2.0
Run 70 T_s
1.0
Time (hour.).
4
8
12
16
20
24
28

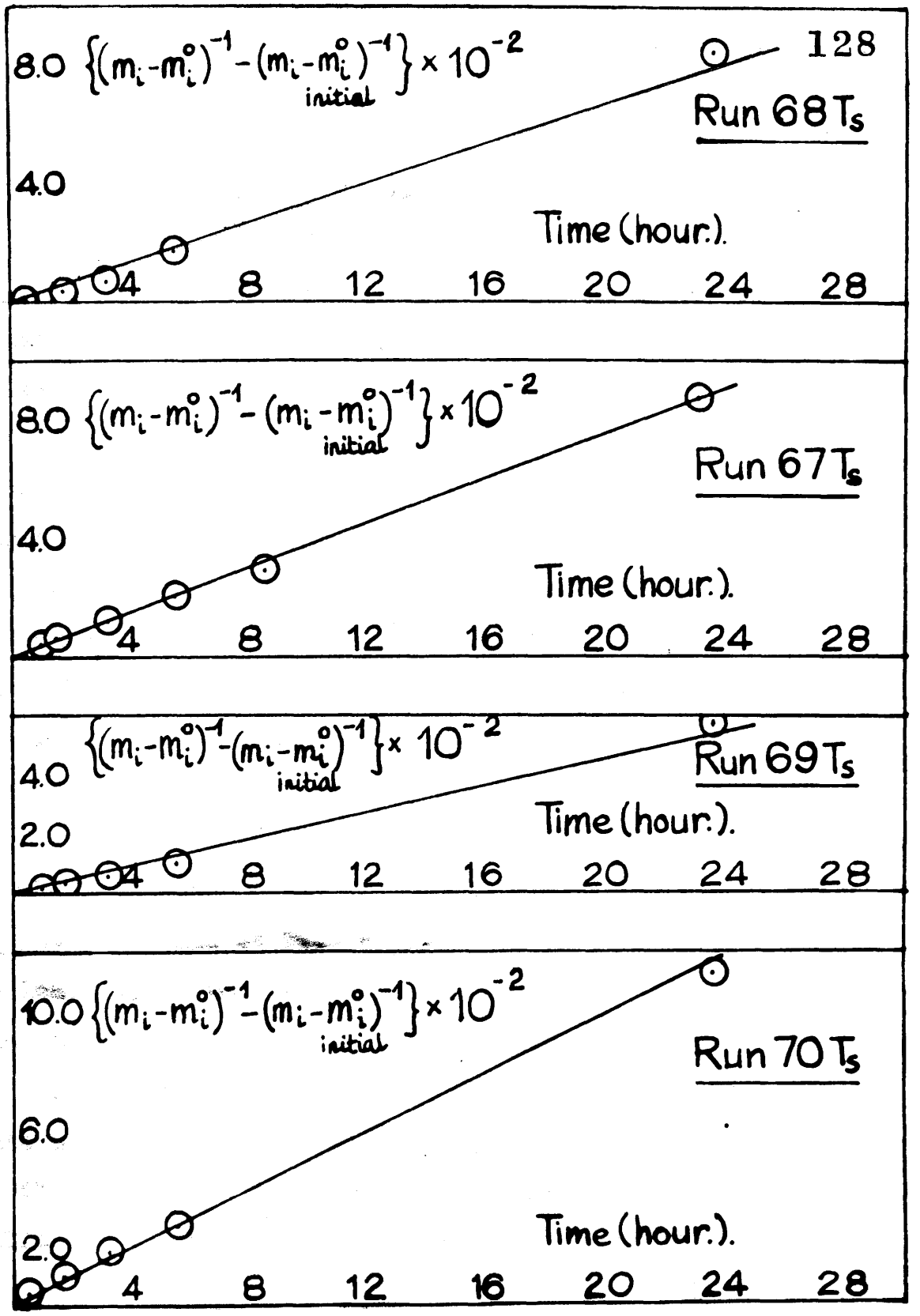
8.0 $\{(m_i-m_i^o)^{-1}-(m_i-m_i^o)_{initial}^{-1}\}\times 10^{-2}$
Run 68 Ts
4.0
Time (hour.).
4 8 12 16 20 24 28
8.0 $\{(m_i-m_i^o)^{-1}-(m_i-m_i^o)_{initial}^{-1}\}\times 10^{-2}$
Run 67 Ts
4.0
Time (hour.).
4 8 12 16 20 24 28
4.0 $\{(m_i-m_i^o)^{-1}-(m_i-m_i^o)_{initial}^{-1}\}\times 10^{-2}$
Run 69 Ts
2.0
Time (hour.).
4 8 12 16 20 24 28
10.0 $\{(m_i-m_i^o)^{-1}-(m_i-m_i^o)_{initial}^{-1}\}\times 10^{-2}$
Run 70 Ts
6.0
2.0
Time (hour.).
4 8 12 16 20 24 28

Fig. 23.

Fig. 23 and runs 71 Ts and 72 Ts, Fig. 25. Thus, in Table 11, the seed concentration in experiment 69 Ts is about twice that in 42 Tt and the long induction period has been removed even though the initial concentration is higher in 69 Ts.

A number of experiment at non equivalent ionic concentrations were made at ratios of Tmg/Tox of 2 and 4. Table 26. The plots of Δ against time are shown in Fig. 28. The rate constants k_3 were obtained after an induction period of about 3 hours. Data is given in tables 27 and 28 and good straight line plots according to the equation

$$-\frac{d\Delta}{dt} = k_3(s)\Delta^2$$

in the integrated form are seen in Fig. 29 for experiments 47 Tt, 48 Tt and 49 Tt. Reproducibility, in spite of nucleation, is very good for runs 47 Tt and 48 Tt, and the value of k_3 falls off considerably on increasing the ratio.

The effect of the addition of foreign ions upon the rate of growth in solutions of equivalent concentrations is illustrated by the data in Table 29. The value of k_1 falls as the concentration of the dodecylsulphate ion is

TABLE. 24.

$T_m \times 10^2$ mole.l^{-1}	$f_2 \times 10$	$m_i \times 10^3$ mole.l^{-1}	$(m_i - m_i^0) \times 10^3$ mole.l^{-1}	$(m_i - m_i^0)^{-1} \times 10^{-2}$ mole.l^{-1}	$\{(m_i - m_i^0)^{-1} - (m_i - m_i^0)^{-1}_{initial}\}$ $\times 10^{-2}$ mole.l^{-1}	time h.
Run. 71T_s						
2.087	4.106	5.761	3.806	2.627	0	0
1.819	4.146	5.275	3.320	3.012	0.385	0.5
1.676	4.170	5.004	3.049	3.280	0.653	1.0
1.412	4.215	4.482	2.527	3.957	1.330	3.0
1.186	4.258	4.005	2.050	4.878	2.251	6.0
0.797	4.343	3.094	1.139	8.780	6.153	22.5
-	4.463	1.955	0	-	-	∞
Run. 72T_s						
2.045	4.130	5.667	3.722	2.687	0	0
1.714	4.181	5.052	3.107	3.219	0.532	0.5
1.536	4.213	4.714	2.769	3.611	0.924	1.0
1.224	4.267	4.075	2.130	4.695	2.008	3.0
0.964	4.325	3.490	1.545	6.473	3.786	6.0
0.671	4.400	2.752	0.807	12.392	9.705	22.5
-	4.485	1.945	0	-	-	∞

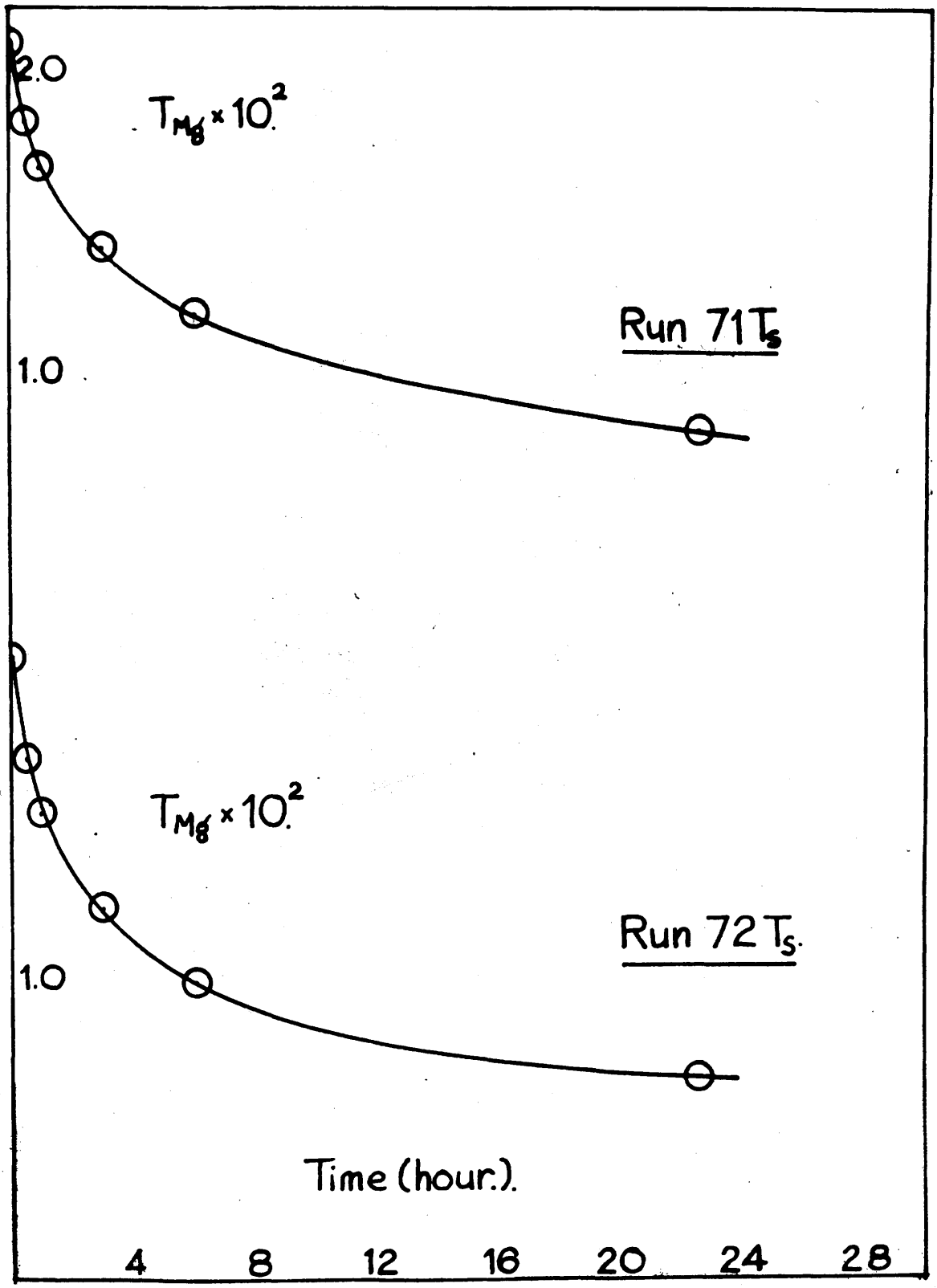
2.0
$T_{Mg} \times 10^2$
Run 71 T_s
1.0
$T_{Mg} \times 10^2$
Run 72 T_s.
1.0
Time (hour.).
4
8
12
16
20
24
28

Fig. 24.

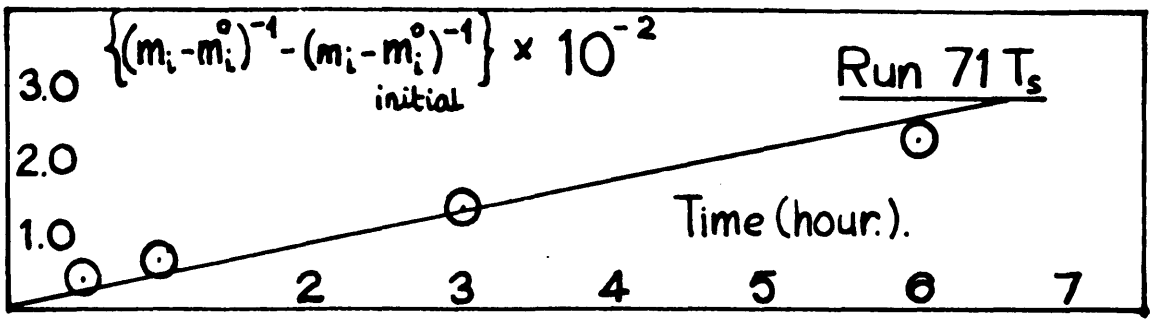
$\{(m_i-m_i^o)^{-1}-(m_i-m_i^o)^{-1}_{initial}\} \times 10^{-2}$
Run 71 T_s
3.0
2.0
1.0
Time (hour.).
2
3
4
5
6
7

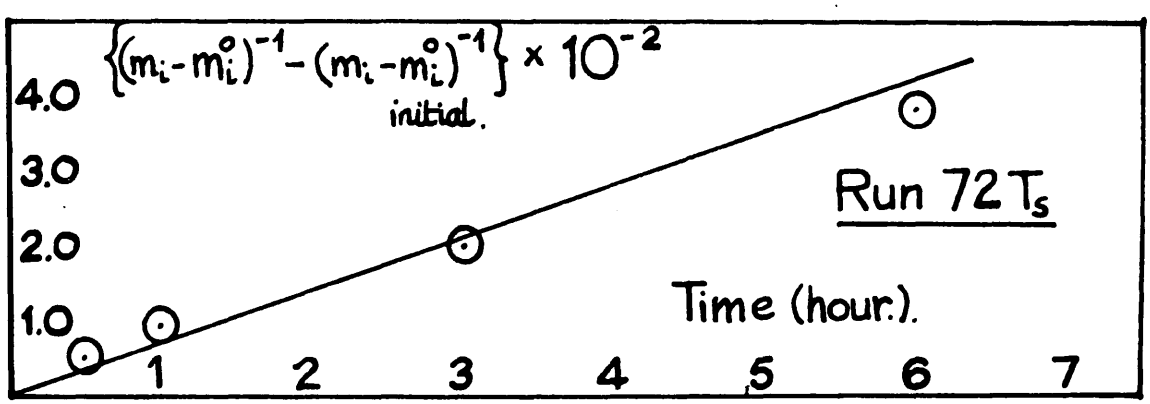
$\{(m_i-m_i^o)^{-1}-(m_i-m_i^o)^{-1}_{initial.}\} \times 10^{-2}$
Run 72 T_s
4.0
3.0
2.0
1.0
Time (hour.).
1
2
3
4
5
6
7

Fig. 25.

TABLE. 25.

time h.	$(T_m-T_m^o)$ $\times 10^2$ mole.l^{-1}	$(T_m-T_m^o)^2$ $\times 10^4$ mole^2.l^{-2}	$(m_i-m_i^o)$ $\times 10^3$ mole.l^{-1}	W_x	$\left(\frac{W_1}{W_2}\right)^{\frac{2}{3}}$	$\frac{dT_m}{dt}\times 10^2$ mole.l^{-1} h^{-1}	$\left(\frac{W_1}{W_2}\right)^{\frac{2}{3}} \times (T_m-T_m^o)^2$ $\times 10^4$	$\frac{dm_i}{dt}$ $\times 10^2$	$\left(\frac{W_1}{W_2}\right)^{\frac{2}{3}}(m_i-m_i^o)^2$ mole^2.l^{-2}
Run. 67T$_s$									
0	2.844	8.088	1.962	50.00	1.00	0.62	-	0.84	1.962
0.5	2.648	7.012	1.751	63.50	0.84	0.53	-	0.74	1.464
1.0	2.297	5.276	1.394	98.96	0.61	0.42	-	0.60	0.849
1.5	2.126	4.520	1.230	113.90	0.55	0.34	-	0.49	0.677
3.3	1.691	2.859	0.849	152.66	0.45	0.20	-	0.29	0.381
5.5	1.282	1.634	0.539	189.08	0.39	0.13	-	0.18	0.209
8.5	1.033	1.067	0.376	205.22	0.36	0.09	-	0.11	0.135
23	0.430	0.185	0.083	254.92	0.32	0.02	-	0.03	0.026
Run. 70T$_s$									
0	2.785	7.756	-	50.00	1.00	1.88	7.756	-	-
0.5	2.022	4.088	-	118.00	0.57	0.88	2.336	-	-
1.8	1.473	2.170	-	167.00	0.45	0.39	0.973	-	-
3.3	1.073	1.151	-	202.00	0.40	0.18	0.457	-	-
5.5	0.817	0.667	-	225.00	0.36	0.09	0.243	-	-
24.	0.237	0.562	-	277.00	0.32	0.02	0.180	-	-

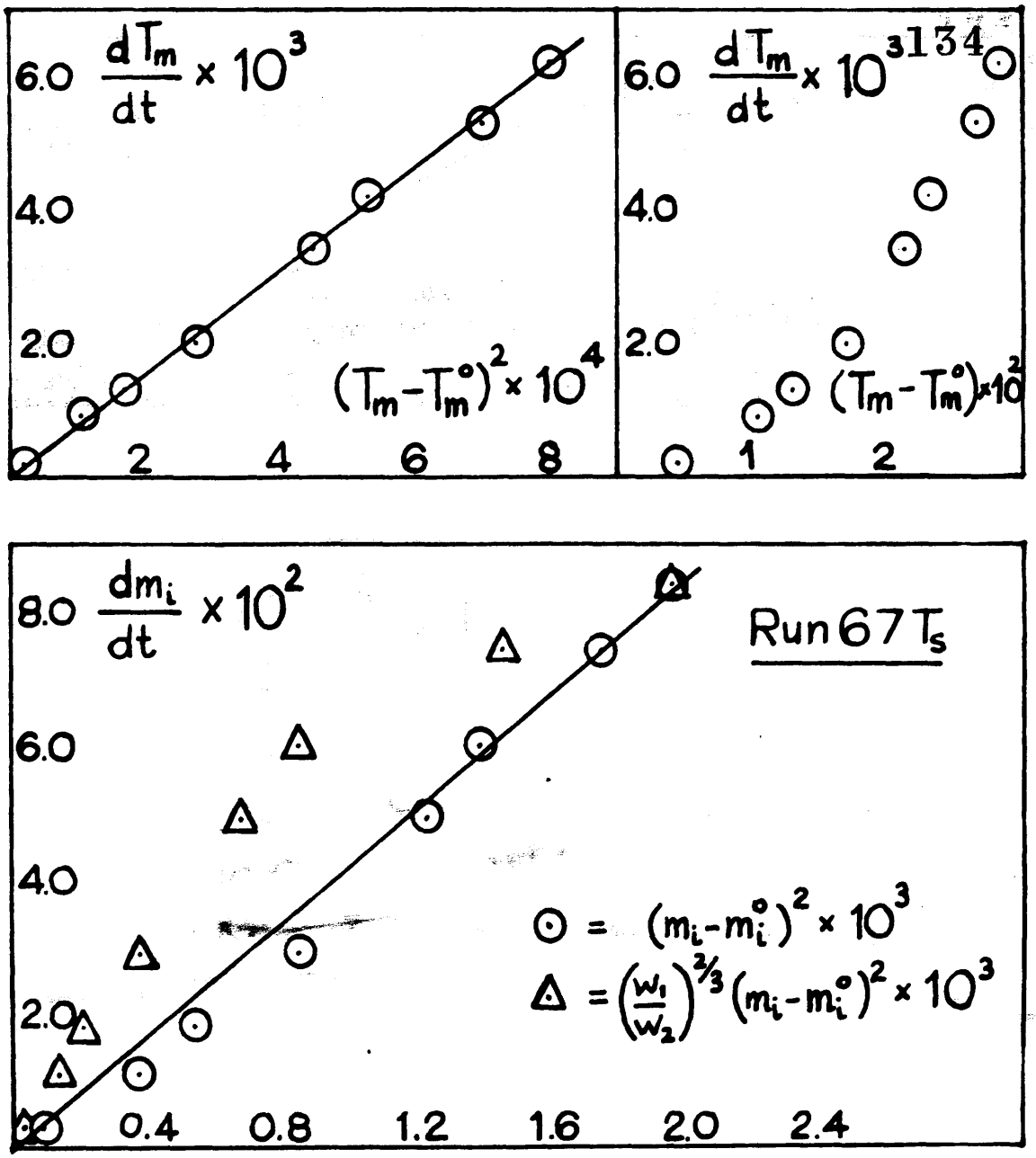
6.0
4.0
2.0
$\frac{dT_m}{dt} \times 10^3$
$(T_m - T_m^\circ)^2 \times 10^4$
2
4
6
8
6.0
4.0
2.0
$\frac{dT_m}{dt} \times 10^3$
$(T_m - T_m^\circ) \times 10^2$
1
2
8.0
6.0
4.0
2.0
$\frac{dm_i}{dt} \times 10^2$
Run 67 T_s
$\odot = (m_i - m_i^\circ)^2 \times 10^3$
$\triangle = \left(\frac{w_1}{w_2}\right)^{2/3} (m_i - m_i^\circ)^2 \times 10^3$
0.4
0.8
1.2
1.6
2.0
2.4

Fig. 26.

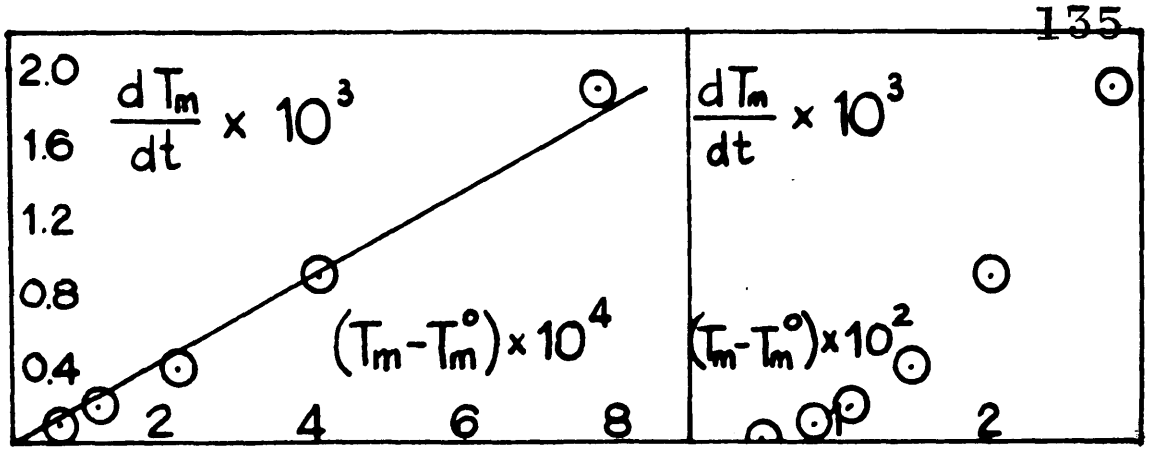

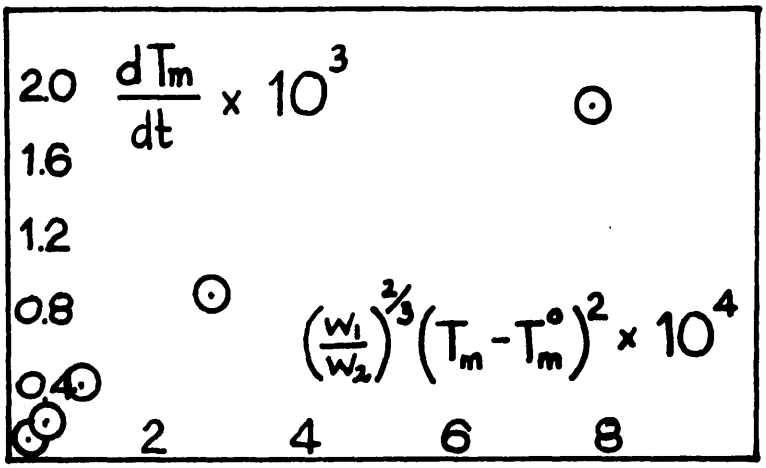

Run 70T_s

Fig. 27.

TABLE. 26.

Crystallisation Experiments at 25°C. $[Mg^{2+}]/[Ox^{2-}] \neq 1$.

Seed F, concentration approx. 25mg. per 100ml. solution

Expt. no.	$\Delta_{initial}$ x 10^2 mole.l^{-1}	I x10^2	T_{Mg}/T_{Ox}	k_3 *** l.mole.h^{-1}.
60_t	0.173	7.04	2	13
$47T_t$	0.199	11.34	2	26
$48T_t$	0.167	6.89	2	30
$49T_t$	0.069	11.88	4	2.5

*** k_3 is the second order rate constant after an induction period of about 3 hours.

TABLE. 27.

$\frac{1}{R}\times10^3$	Λ	$\delta(\Delta)\times10^5$ mole.l^{-1}	$\Delta\times10^3$ mole.l^{-1}	$\Delta^{-1}\times10^{-2}$ mole.l^{-1}	$(\Delta^{-1}-\Delta^{-1}_{initial})$ $\times10^{-2}$ mole.l^{-1}	time h.
Run. 46C$_t$						
46.355	-	0	0.1726	5.794	0	0
46.338	108.10	0.83	0.1643	6.086	0.292	2
46.270	108.28	1.12	0.1614	6.196	0.402	3
46.110	108.67	1.78	0.1584	6.460	0.666	5
46.028	108.87	2.12	0.1514	6.605	0.811	6
45.379	110.54	4.76	0.1250	8.000	2.206	17
45.339	110.94	5.34	0.1192	8.389	2.595	20
45.095	111.31	5.89	0.1137	8.795	3.001	24
44.468	113.11	8.32	0.0894	11.186	5.392	41.75
44.448	113.17	8.39	0.0887	11.273	5.479	43

$T_{mg}\times10^2$	$T_{ox}\times10^2$	$m_{i\,mg}\times10^2$	$m_{i\,ox}\times10^2$	$f_2\times10$	$\Delta\times10^2$	$\Delta^{-1}\times10^{-2}$	$(\Delta^{-1}-\Delta^{-1}_{init.})\times10^{-2}$	time.
Run. 47T$_t$								
4.147	1.999	2.376	0.228	3.480	0.199	5.03	0	0
4.053	1.920	2.367	0.219	3.480	0.185	5.41	0.38	1.5
3.941	1.827	2.357	0.209	3.486	0.180	5.56	0.53	3
3.870	1.730	2.347	0.199	3.488	0.170	5.88	0.85	4.5
3.656	1.511	2.322	0.174	3.497	0.146	6.85	1.82	8
3.493	1.348	2.304	0.156	3.508	0.128	7.81	2.78	11
2.986	0.888	2.252	0.104	3.529	0.076	13.16	8.13	22.75
2.698	0.541	2.212	0.064	3.546	0.036	27.78	22.75	34.5

TABLE. 28.

$T_{mg} \times 10^2$ mole.l^{-1}	$T_{ox} \times 10^2$ mole.l^{-1}	$m_{i\,mg} \times 10^2$ mole.l^{-1}	$m_{i\,ox} \times 10^2$ mole.l^{-1}	$f_2 \times 10$	$\Delta \times 10^2$ mole.l^{-1}	$\Delta^{-1} \times 10^{-2}$ mole.l^{-1}	$(\Delta^{-1} - \Delta^{-1}_{init}) \times 10^{-2}$ mole.l^{-1}	time h.
Run. 48T$_t$								
4.109	2.052	2.241	0.184	4.083	0.167	5.99	0	0
4.035	1.969	2.234	0.177	4.091	0.159	6.29	0.30	1
3.980	1.900	2.227	0.170	4.097	0.149	6.71	0.72	2
3.867	1.812	2.219	0.162	4.101	0.140	7.14	1.15	3.5
3.783	1.727	2.212	0.156	4.110	0.134	7.46	1.47	5
3.669	1.588	2.201	0.144	4.115	0.123	8.13	2.14	7
3.516	1.447	2.187	0.130	4.127	0.104	9.61	3.62	9.5
2.981	0.914	2.140	0.083	4.163	0.062	16.13	10.14	21.5
Run. 49T$_t$								
4.165	1.021	3.234	0.090	3.428	0.069	1.449	0	0
4.140	0.999	3.232	0.088	3.428	0.067	1.493	0.044	1
4.114	0.976	3.230	0.086	3.429	0.066	1.515	0.066	2.25
4.091	0.960	3.229	0.085	3.430	0.064	1.563	0.126	4
4.071	0.934	3.226	0.082	3.430	0.062	1.613	0.164	6
4.043	0.902	3.224	0.080	3.431	0.060	1.667	0.218	8
3.949	0.800	3.216	0.072	3.434	0.052	1.923	0.474	23

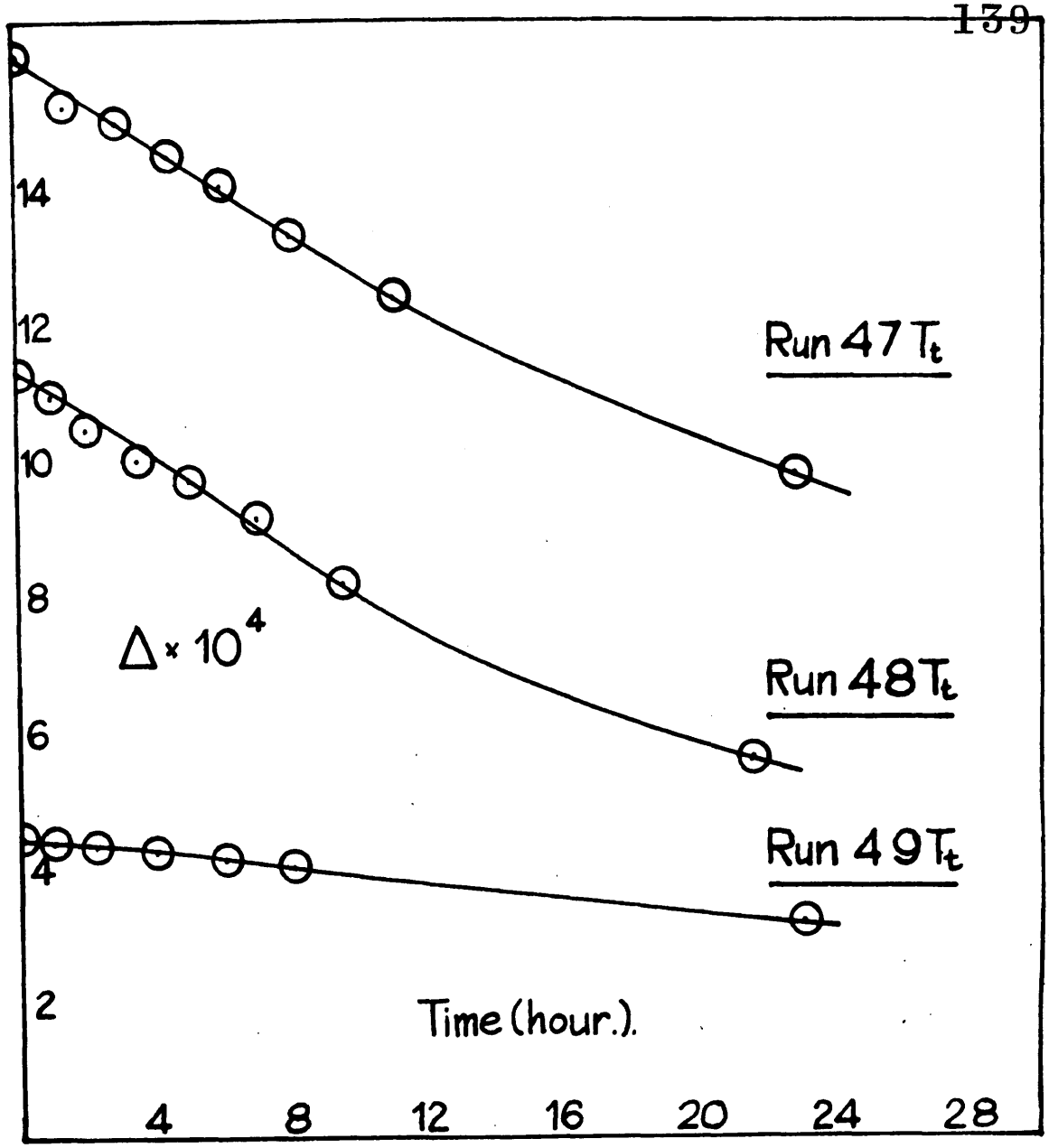
14
12
10
8
6
4
2
Δ × 10^4
Run 47 Tt
Run 48 Tt
Run 49 Tt
Time (hour.).
4
8
12
16
20
24
28

Fig.28.

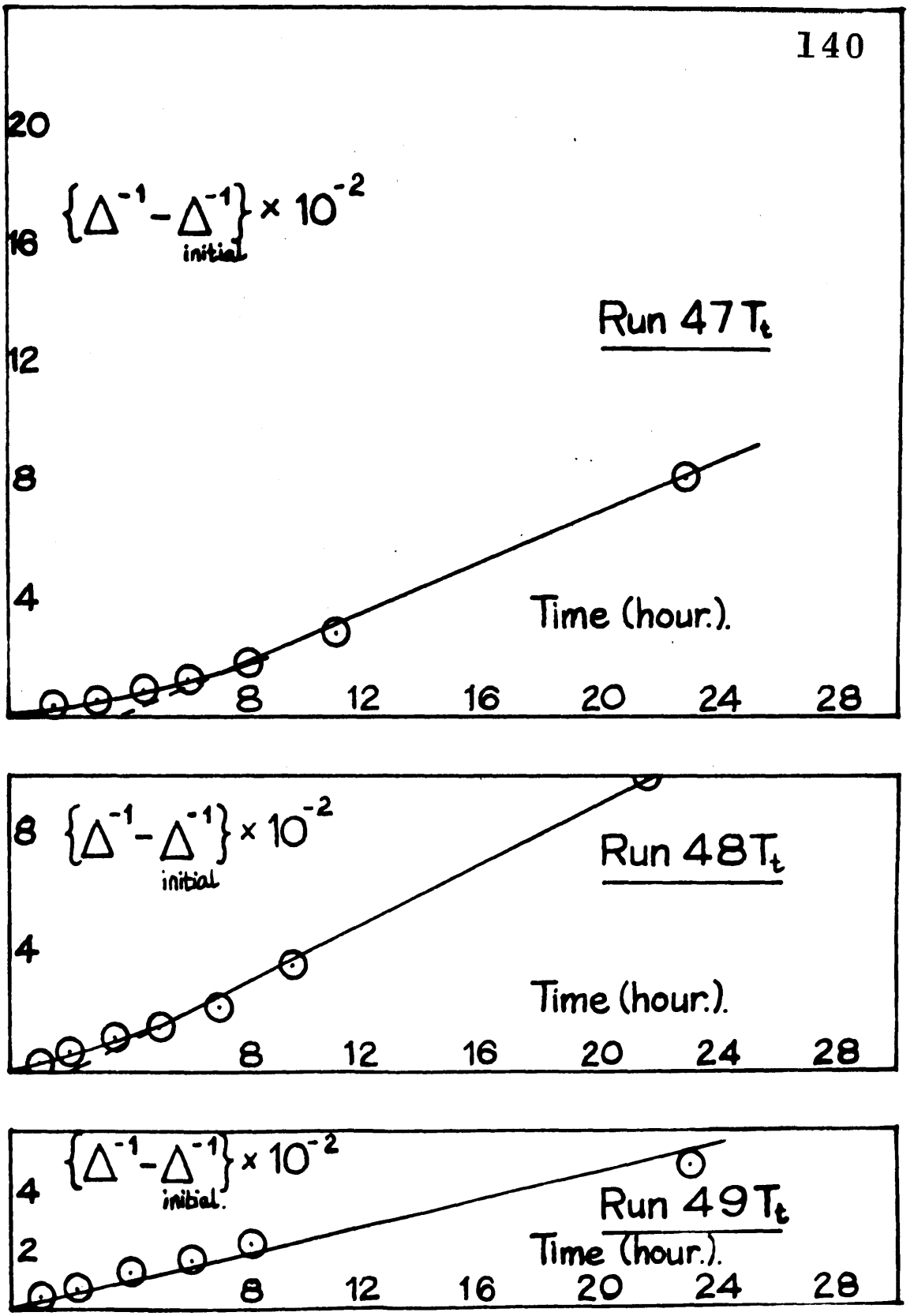
20
16
12
8
4
$\{\Delta^{-1} - \Delta^{-1}_{initial}\} \times 10^{-2}$
Run 47 T_t
Time (hour.).
8
12
16
20
24
28
8
4
$\{\Delta^{-1} - \Delta^{-1}_{initial}\} \times 10^{-2}$
Run 48 T_t
Time (hour.).
8
12
16
20
24
28
4
2
$\{\Delta^{-1} - \Delta^{-1}_{initial}\} \times 10^{-2}$
Run 49 T_t
Time (hour.).
8
12
16
20
24
28

Fig. 29.

TABLE. 29.

Crystallisation in the presence of Adsorbates: $[Mg^{2+}]/[Ox^{2-}] = 1$.

Seed F, Concentration 23mg. per 100 ml.

Expt. no.	$(m_1-m_1^0)$ x10^3 mole. l^{-1}.	I x10^2	$[A^-]$ x10^3 mole.l^{-1}.	k_1 +++ $l.mole.^{-1}$ h^{-1}.
$56T_t$	6.13	6.83	0	3.48
$55T_t$	6.12	6.91	1.029	1.95
$57T_t$	6.03	6.89	2.031	1.63
$58T_t$	5.84	7.34	9.572	1.51
$60T_t$	4.52	2.28	0	5.04
$52T_t$	4.57	2.42	1.029	4.73
***$63C_t$	4.52	2.32	0.425	1.40

*** $[A^-]$ = eosin ion, all others have sodium dodecyl sulphate present

+++ k_1 is the second order rate constant after an induction period of about 4 hours.

TABLE. 30.

$T_m \times 10^2$ mole. l^{-1}	$f_2 \times 10$	$m_i \times 10^3$ mole. l^{-1}	$(m_i - m_i^o) \times 10^3$ mole. l^{-1}	$(m_i - m_i^o)^{-1} \times 10^{-2}$ mole. l^{-1}	$\{(m_i - m_i^o)^{-1} - (m_i - m_i^o)^{-1}_{initial}\} \times 10^{-2}$ mole. l^{-1}	time h.
Run. 56T$_t$						
3.246	3.581	8.345	6.129	1.632	0	0
3.002	3.601	7.941	5.725	1.747	0.115	2
2.681	3.629	7.390	5.174	1.933	0.301	4
2.335	3.661	6.769	4.553	2.196	0.564	6
2.120	3.682	6.365	4.149	2.410	0.778	7
1.292	3.784	4.618	2.402	4.157	2.525	12
0.970	3.832	3.846	1.630	6.140	4.508	18
0.786	3.861	3.349	1.133	8.826	7.194	25.25
-	3.937	2.216	0	-	-	∞
Run. 55T$_t$						
3.233	3.572	8.344	6.120	1.634	0	0
2.972	3.593	7.910	5.696	1.759	0.125	2
2.736	3.613	7.505	5.261	1.894	0.260	4
2.448	3.640	6.992	4.668	2.097	0.463	6
2.153	3.668	6.444	4.220	2.370	0.736	8
1.923	3.693	5.996	3.772	2.651	1.017	10
1.575	3.738	5.063	2.839	3.522	1.888	14
1.375	3.768	4.652	2.428	4.117	2.483	17
1.090	3.798	4.160	1.946	5.165	3.531	22
-	3.923	2.224	0	-	-	∞

TABLE. 31.

$T_m \times 10^2$ mole.l^{-1}	$f_2 \times 10$	$m_i \times 10^3$ mole.l^{-1}	$(m_i - m_i^0) \times 10^3$ mole.l^{-1}	$(m_i - m_i^0)^{-1} \times 10^{-2}$ mole.l^{-1}	$\{(m_i - m_i^0)^{-1} - (m_i - m_i^0)^{-1}_{initial}\} \times 10^{-2}$ mole.l^{-1}	time h.
Run. 57T$_t$						
3.181	3.577	8.257	6.034	1.657	0	0
2.969	3.594	7.904	5.681	1.760	0,013	2
2.703	3.617	7.446	5.223	1.915	0.258	4
2.351	3.649	6.814	4.591	2.178	0.521	6
2.192	3.665	6.517	4.294	2.329	0.672	7
2.022	3.681	6.182	3.959	2.525	0.868	8
1.300	3.768	4.662	2.439	4.100	2.443	18
1.225	3.794	4.465	2.242	4.452	2.795	20
Run. 58T$_t$						
3.032	3.529	8.124	5.856	1.708	0	0
2.848	3.544	7.808	5.540	1.805	0.097	2
2.670	3.559	7.495	5.227	1.913	0,205	4
2.425	3.580	7.050	4.782	2.091	0.383	6
2.245	3.605	6.521	4.253	2.351	0.643	8
1.811	3.703	5.642	3.384	2.956	1.248	12
1.584	3.736	5.123	2.855	3.504	1.796	16
1.375	3.768	4.654	2.386	4.212	2.504	20
1.041	3.836	4.094	1.826	4.740	3.032	23

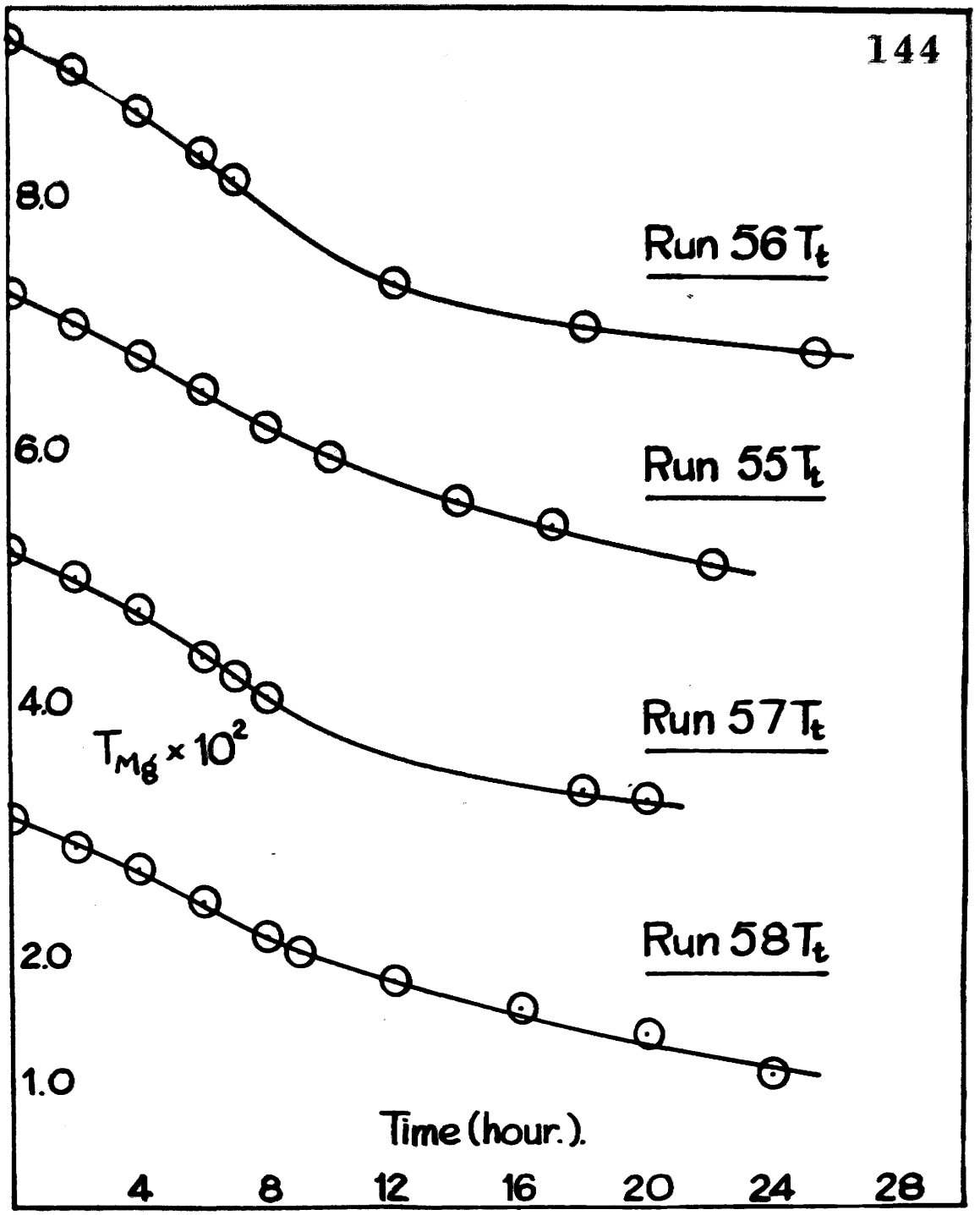
8.0
6.0
4.0
2.0
1.0
$T_{Mg} \times 10^2$
Run 56 T_t
Run 55 T_t
Run 57 T_t
Run 58 T_t
Time (hour.).
4
8
12
16
20
24
28

Fig. 30.

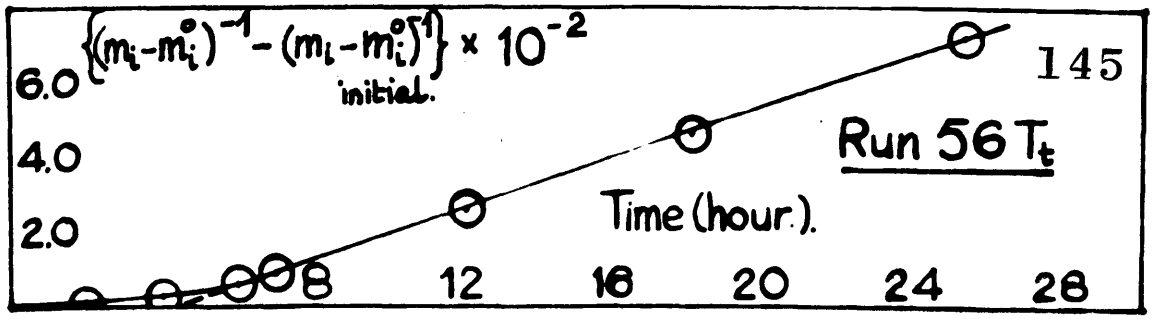
$\{(m_i-m_i^o)^{-1}-(m_i-m_i^o)^{-1}_{initial}\} \times 10^{-2}$
6.0
4.0
2.0
Run 56 T_t
Time (hour.).
8
12
16
20
24
28

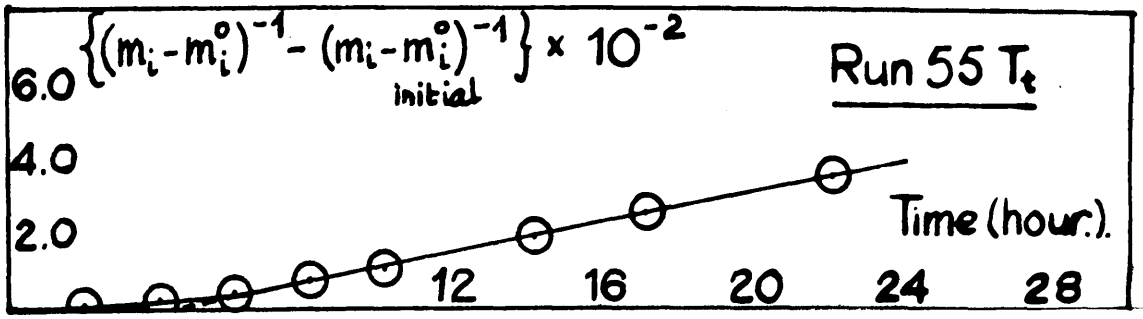
$\{(m_i-m_i^o)^{-1}-(m_i-m_i^o)^{-1}_{initial}\} \times 10^{-2}$
6.0
4.0
2.0
Run 55 T_t
Time (hour.).
12
16
20
24
28

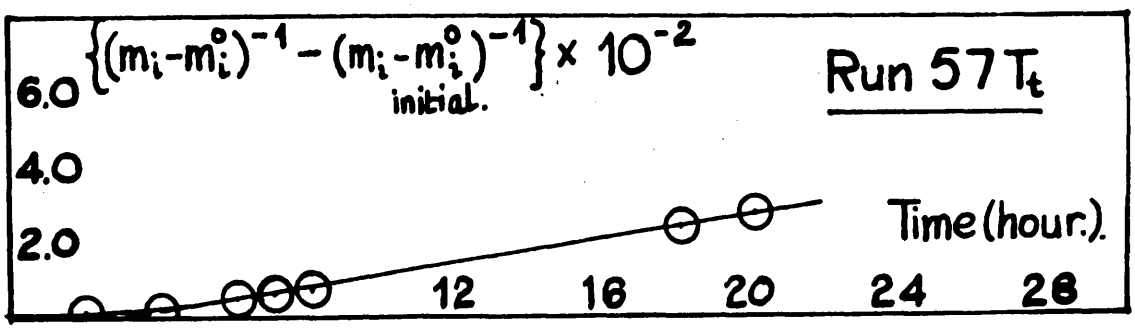
$\{(m_i-m_i^o)^{-1}-(m_i-m_i^o)^{-1}_{initial}\} \times 10^{-2}$
6.0
4.0
2.0
Run 57 T_t
Time (hour.).
12
16
20
24
28

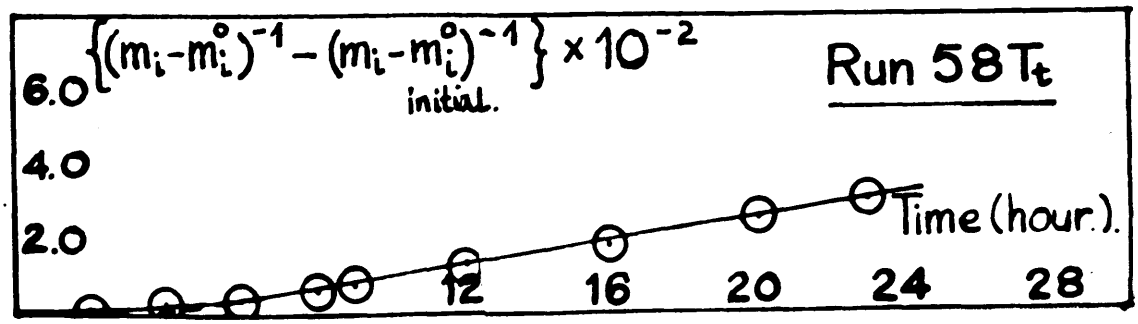
$\{(m_i-m_i^o)^{-1}-(m_i-m_i^o)^{-1}_{initial}\} \times 10^{-2}$
6.0
4.0
2.0
Run 58 T_t
Time (hour.).
12
16
20
24
28

Fig. 31.

TABLE. 32.

$T_m \times 10^2$ mole.l^{-1}	$f_2 \times 10$	$m_i \times 10^3$ mole.l^{-1}	$(m_i - m_i^o) \times 10^3$ mole.l^{-1}	$(m_i - m_i^o)^{-1} \times 10^{-2}$ mole.l^{-1}	$\{(m_i - m_i^o)^{-1} - (m_i - m_i^o)^{-1}_{initial}\}$ $\times 10^{-2}$. mole.l^{-1}	time h.
Run. 60T$_t$						
3.238	5.525	5.690	4.517	2.214	0	0
2.926	5.622	5.299	4.126	2.424	0.210	2
2.318	5.839	4.504	3.331	3.002	0.788	5
1.648	6.148	3.558	2.385	4.193	1.979	8
1.294	6.358	3.015	1.842	5.429	3.215	11
1.078	6.513	2.662	1.489	6.716	4.502	14
0.927	6.638	2.402	1.229	8.136	5.922	17
0.808	6.750	2.188	1.015	9.851	7.637	20
0.703	6.861	1.991	0.818	12.225	10.011	23
Run. 52T$_t$						
3.255	5.443	5.784	4.573	2.187	0	0
2.947	5.533	5.596	4.185	2.389	0.202	2
2.530	5.670	4.854	3.643	2.746	0.559	4
2.052	5.853	4.201	2.990	3.345	1.158	6
1.665	6.030	3.640	2.429	4.117	1.930	8
1.078	6.529	2.578	1.367	7.317	5.130	14
0.786	6.617	2.190	0.979	10.216	8.029	20.5
0.709	6.691	2.043	0.832	12.020	9.833	24.25

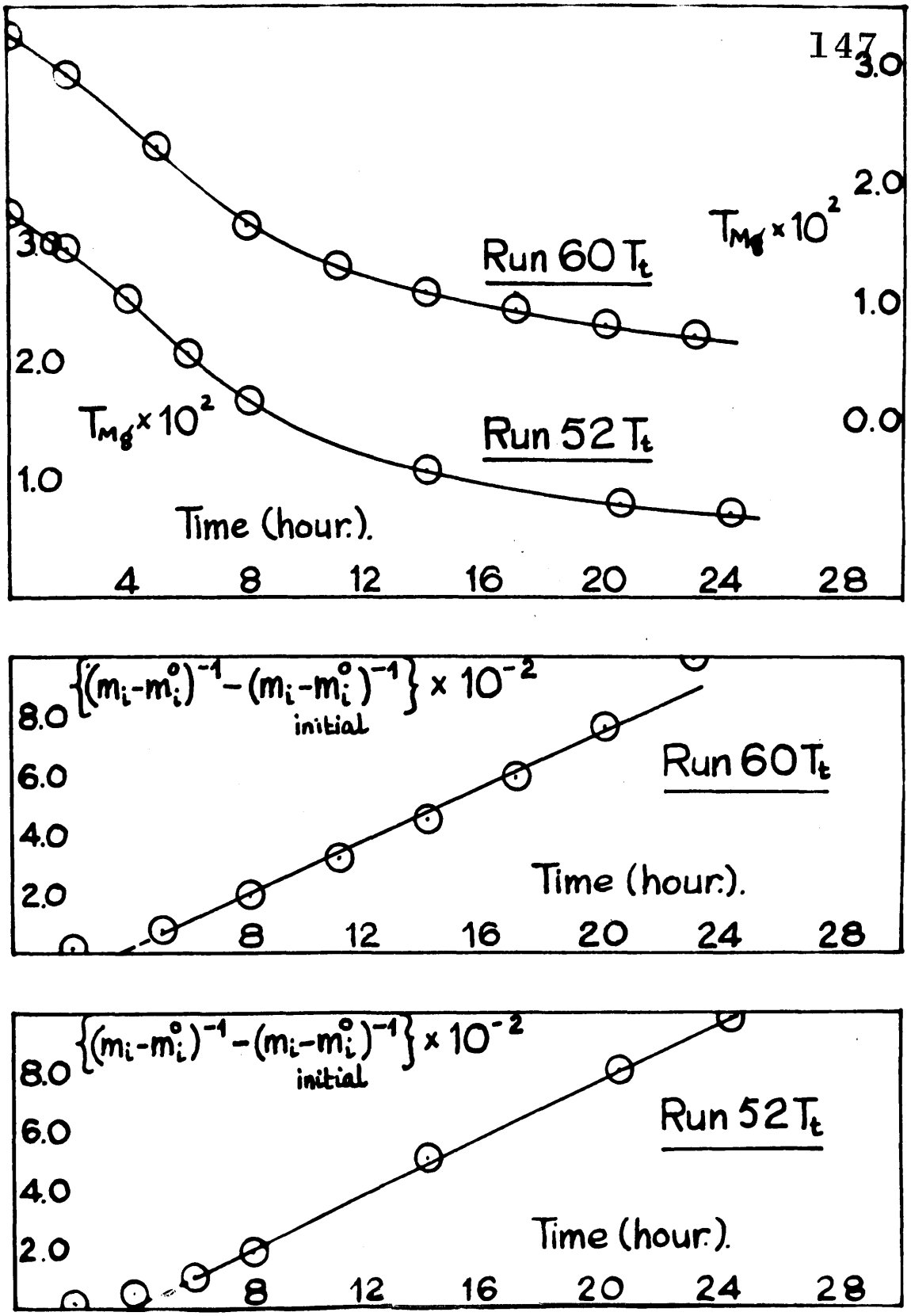
Run 60 T_t
$T_{Mg} \times 10^2$
Run 52 T_t
$T_{Mg} \times 10^2$
Time (hour.).
3.0
2.0
1.0
0.0
4
8
12
16
20
24
28
$\{(m_i-m_i^o)^{-1}-(m_i-m_i^o)^{-1}_{initial}\} \times 10^{-2}$
Run 60 T_t
Time (hour.).
8.0
6.0
4.0
2.0
$\{(m_i-m_i^o)^{-1}-(m_i-m_i^o)^{-1}_{initial}\} \times 10^{-2}$
Run 52 T_t
Time (hour.).

Fig. 32.

increased. The straight line kinetic plots all show a time intercept of about 4 hours in Fig. 31. The greater efficiency of Eosin in retarding the growth rate is illustrated by experiment 63 Ct, Fig. 33.

TABLE. 33.

$\frac{1}{R} \times 10^3$	Λ	$m_i \times 10^3$ mole. l^{-1}	$(m_i - m_i^o) \times 10^3$ mole. l^{-1}	$(m_i - m_i^o)^{-1} \times 10^{-2}$ mole. l^{-1}	$\{(m_i - m_i^o)^{-1} - (m_i - m_i^o)^{-1}_{initial}\}$ $\times 10^{-2}$ mole. l^{-1}	time h.
Run. 630.						
12.261	-	5.693	4.520	2.212	0	0
11.899	92.30	5.486	4.313	2.319	0.107	1
11.495	92.92	5.291	4.118	2.428	0.216	2
11.007	93.68	5.058	3.885	2.574	0.362	3
10.449	94.57	4.796	3.623	2.760	0.548	4.25
10.068	95.16	4.621	3.448	2.900	0.688	5
9.563	95.96	4.391	3.218	3.108	0.896	6
9.101	96.71	4.185	3.012	3.320	1.108	7
8.652	97.44	3.988	2.815	3.552	1.340	8
6.946	100.27	3.266	2.093	4.778	2.566	18.5
6.919	100.31	3.254	2.081	4.805	2.593	19
6.884	100.38	3.240	2.067	4.838	2.626	19.5
-	-	1.173	0	-	-	∞

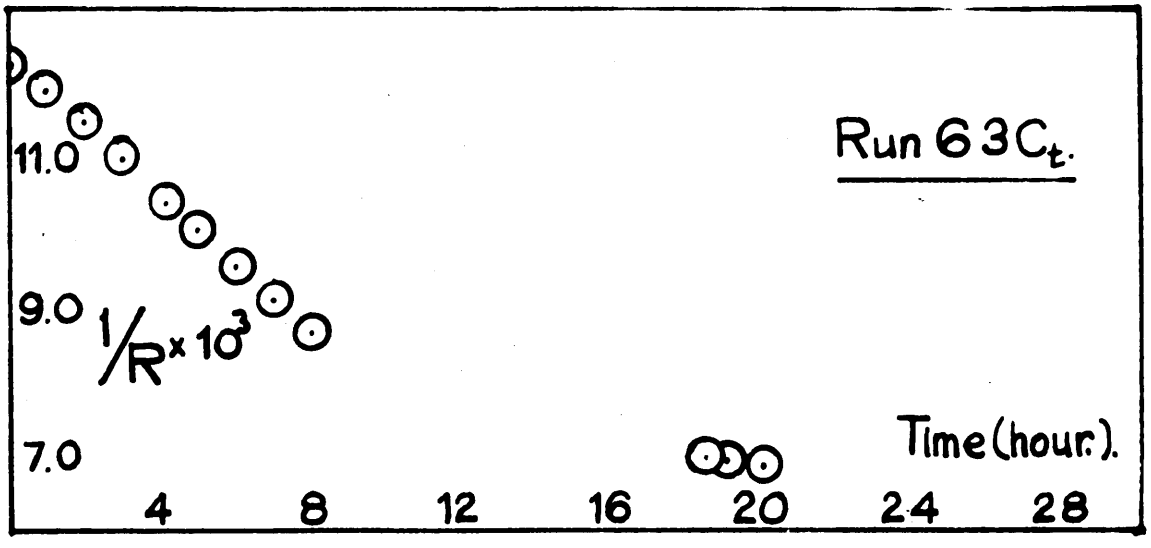
Run 63C$_t$.
11.0
9.0
7.0
$1/R \times 10^3$
Time (hour).
4
8
12
16
20
24
28

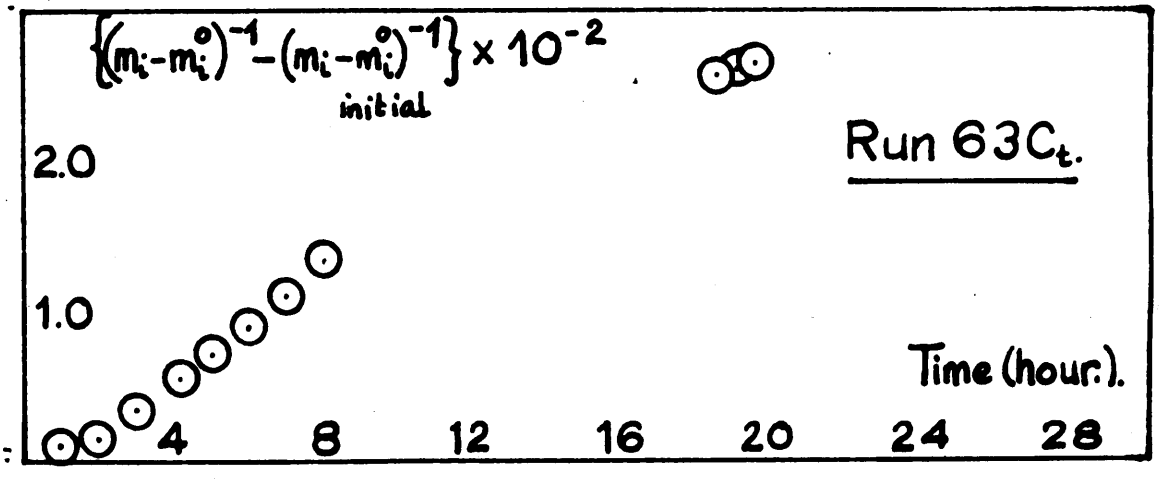
$\{(m_i-m_i^o)^{-1}-(m_i-m_i^o)^{-1}_{initial}\} \times 10^{-2}$
Run 63C$_t$.
2.0
1.0
Time (hour).
4
8
12
16
20
24
28

Fig. 33.

Discussion:

The kinetics of crystallisation of magnesium oxalate, a 2-2 electrolyte of quite a high solubility, agreed with the second order rate equation already described for silver chloride, under conditions of equivalent and non equivalent ion concentrations, and in the presence of surface active reagents.

Above a certain concentration product limit for a known weight of added seed crystals, spontaneous crystallisation was initiated, an effect which could be eliminated by increasing the weight of seed added. Spontaneous nucleation would occur if an insufficient number of suitable growth sites were added to accommodate the initial growth surge as fast as it was provided by diffusion. Normal second order growth according to equation (6) began immediately when spontaneity was eliminated.

From the plot of the gradient $\frac{-d\,Tm}{dt}$ against $(Tm - Tm^{o})$, Figs. 26 and 27, for runs 67 Ts and 70 Ts respectively, first order kinetics in total oxalate, suggested by Brescia and Peisach[84], did not describe the growth mechanism. Their experiments were made in high concentrations of sodium sulphate and they did

not take into account complexes such as $MgSO_4$ from the equilibrium

$$Mg^{2+} + SO_4^{2-} \rightleftharpoons Mg\,SO_4,$$

which must contibute to the equation for total magnesium. The concentration of this ion pair would be appreciable,[97] the association constant

$$K = \frac{[MgSO_4]}{[Mg^{2+}][SO_4^{2-}]f_2^2} = 179$$

However from the same figures, the second order equation in total concentration

$$-\frac{dTm}{dt} = k_2(s)\,(Tm - Tm^o)^2 \qquad (7)$$

was seen to be obeyed closely. The two interpretations were compatible since:

$$\frac{k_1}{k_2} = (5.4 \times 10^3 f_2^2\, m_1 + 1)(m_1 - m_1^o)^2 / (Tm - Tm^o)^2$$

and the ratio varied by only 1 or 2% during an experiment.

In order to test for a diffusion controlled process the dependence of k_1 on the rate of stirring, reported by Lichstein and Bresoia [85], was investigated. In run 40 Ct the rate of stirring was increased very

considerably (at points indicated by the arrows in Fig. 13) without any discontinuity in the growth curve. Furthermore a good agreement in K_2 was observed for experiments 40 Ct (Table 11) and 69 Ts (Table 16) where completely different modes of stirring were employed. Growth would appear, therefore, not to be diffusion controlled.

The theoretical dependence of the rate of growth on increasing surface area was not observed in this system. The crystals were observed to enlarge considerably during growth. The calculated increase in weight from direct measurement of photographs after 23 hours agreed to within 10% of the weight deposited calculated from concentration changes, assuming the crystals to be cubic. This was true only for runs without nucleation. Plate 2 (c, d) shows the spontaneous growth which initially occurred in 68 Ts and the subsequent multitude of crystal sizes.

The good linearity in Figs. 26 and 27 for 67 Ts and 70 Ts show that the second order rate constant is independent of the increasing surface area. Doremus[72] has suggested for some systems, that the rate constant K_1 depends only upon the number of growth sites available initially. Assuming that the availability

of suitable growth sites is constant for each specimen of the same seed, the rate constant k_1 would therefore depend upon the weight of crystals added. The observed rate constants for experiments 69 T_s and 70 T_s are proportional to the seed concentration, Table 16. This is also true for experiments 71 T_s and 72 T_s Table 16., and is consistent with the idea that no new growth sites are formed during crystallisation. The rate constants for runs 70 T_s and 71 T_s, although from solutions of different supersaturations, agree very well as would be expected from the rate equation.

In solutions of non equivalent concentrations the second order growth equation was obeyed, and the rate constant k_3 was seen to decrease as the ratio of T_{Mg}/T_{Ox} was increased. This was also true of silver chloride, where ratios of ionic concentrations were considered, but a comparison between the relative retarding powers of the cation or anion in excess could not be drawn because of the absence of runs with oxalate in excess; when higher complexes of the type $Mg(Ox)_2^{2-}$ would be formed. The association constants of these types are not known and the results could not be calculated.

In the presence of surface active agents, the second order growth equation was obeyed. The experiments were done in solutions of high initial

concentration which gave induction periods in the regioncf four hours.

Analysis of the rate constants in terms of the Langmuir Adsorption Isotherm indicated that as the concentration of sodium dodecyl sulphate was increased the rate constant was not reduced to zero but approached a limiting value. An exactly similar result was obtained with silver chloride[22], and may be due to adsorption of surface active ions at only some of the growth sites.

The Langmuir adsorption treatment is applicable if it is presumed that the retarding action is exerted in the monolayer in contact with the crystal surface. Suppose that a fraction α of the available sites is occupied by the added ion when its molar concentration is $[A]$. If the rate of adsorption is written $k'[A](1-\alpha)$, and the rate of desorption is k'' then

$$\alpha = k'[A]/(k'[A] + k'').$$

Let k_0 be the rate constant for crystallisation in the absence of the contaminant, $b\,k_0$ its limiting value with contaminant present. Then

$$k = k_0 - \alpha k_0(1-b).$$

and substituting for α,

$$\frac{k_o}{k_o - k} = \frac{1}{(1 - b)} + \frac{k''}{(1-b)\,k'[A]}$$

A plot of $k_o / k_o - k$ against $1 / [A]$ is shown for the dodecylsulphate results, Fig. 34.

TABLE. 14.

k	$k_o - k$	$k_o / k_o - k$	$[A^-] \times 10^2$	$[A^-]^{-1}$.
3.48	0	-	0	-
1.95	1.53	2.28	1.029	97.3
1.63	1.85	1.88	2.031	49.3
1.51	1.97	1.77	9.572	10.5

This treatment is only very approximate because spontaneous crystallisation was induced in the experiments and conditions were not entirely reproducible. However a tendency to alinear adsorption isotherm was observed.

In conclusion of part 2a, the interpretation advanced for the crystallisation of 1-1 and 1-2 electrolytes is also applicable to a very much more soluble 2-2 electrolyte. In spite of the very substantial increase in the surface area, the second order rate constant are independent of this and appear to depend upon the number of growth sites available initially.

———oOo———

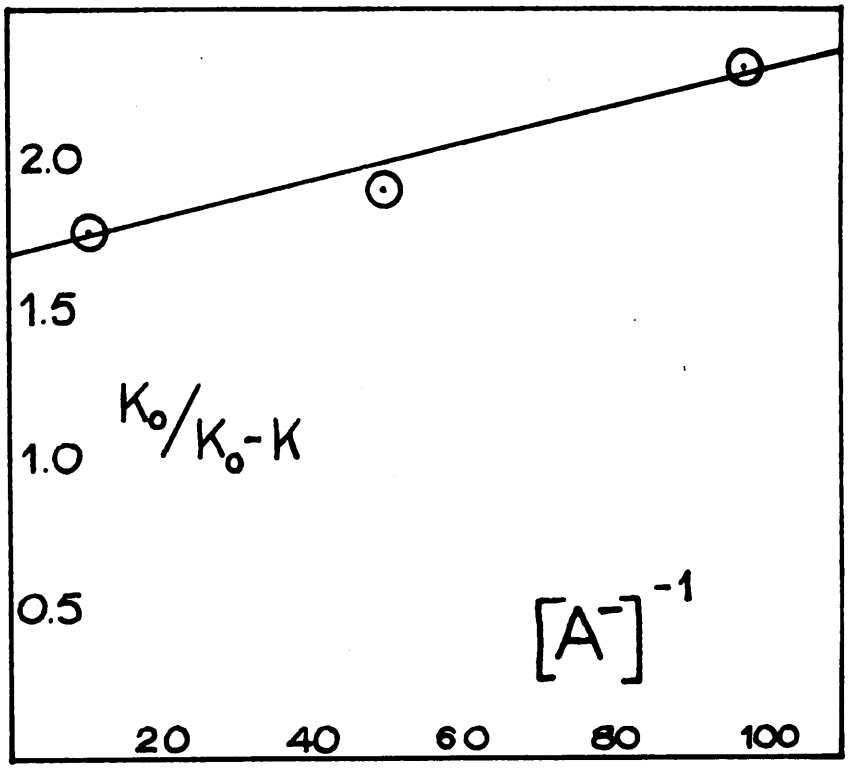

Fig. 34.

Part. 2b.

The Crystallisation of Barium Sulphate from Supersaturated Aqueous Solutions.

THE KINETICS OF CRYSTALLISATION OF BARIUM SULPHATE.

Barium sulphate is a 2-2 electrolyte but unlike magnesium oxalate does not form a stable complex in solution, and is very much more insoluble.

The conductivity technique already described was used and various attempts were made to eliminate the possible sources of error to be described. Crystallisation was observed under conditions of equivalent and non equivalent ionic concentrations of Ba^{2+} and SO_4^{2-} ions.

Spontaneous crystallisation has been studied by many workers because of the importance of barium sulphate gravimetrically, and many explanations of the mechanism of nucleation and growth have been suggested[7,11-16,18,65,69-71] (p. 1-8).

In this work inoculation of growth by seed crystals provided evidence for the same second order rate equation already observed for silver chloride[2] and magnesium oxalate.

Extensive studies of the crystal form have been made involving X-ray examination and electron microscopy, and many features were observed which present complications to a quantitative study of growth. Barium sulphate on crystallisation occludes other ions from the mother

liquor into the lattice, as well as the mother liquor itself, to produce a solid solution[98], and in an electron microscope study of colloidal barium sulphate Dawson and McGaffney[99], observed that the crystal surface was porous and capable of including solvent or dissolved solute. The dimensions of the pores varied in the range 15 to 70Å and it is possible that extensive inclusion occurs.

Takiyama[100] in an electron microscope study of the spontaneous crystallisation of barium sulphate observed the formation of two types of crystal shapes above and below a critical concentration limit of 5×10^{-4} mole.l^{-1} in barium ion concentration above the limit dendritic crystals were produced and below, regular orthorhombic platelets. In an earlier publication Takiyama[101] described the effect of adding seed crystals, when as well as enlargement of the seed crystals, new smaller crystals were obtained which were removed on ageing. This phenomenon is easily explained by the observation made in part 2a that probably an insufficient number of seed crystals were added. Perhaps it might be necessary to inoculate supersaturated solutions with seed crystals

of the same shape as those which would have been produced had the supersaturated solution crystallised spontaneously.

Experimental.

Preparation of Solutions.

Analar reagents were used throughout without further prefication. Cell solutions for experiments in which a supporting electrolyte was present were prepared by mixing dilute solutions of barium chloride and sodium sulphate in situ, as already described. The technique for carrying out the experiments and the apparatus have already been described in detail in the silver chloride section. The cell was washed between experiments with 3% hydrochloric acid or simply by a rapid stream of distilled water.

To prevent ion occlusion in the crystal lattice cell solutions were also prepared by mixing together dilute solutions of sulphuric acid and barium hydroxide. Saturated baryta, approximately 0.35N, was prepared according to Cumming and Kay[102], and a dilute solution prepared in an automatic 10 ml. burette fitted with soda lime guard tubes to exclude carbon dioxide. The concentration of the solution was such that around 10 m.l. of solution were sufficient to give the final barium ion concentration in the cell, and equivalance

with the sulphuric acid already present in the cell was obtained by a conductimetric titration performed in situ. In this way contact of the barium hydroxide with the air was avoided.

Preparation of Seed Crystals.

Attempts to prepare pure specimens of barium sulphate crystals by recrystallisation on a large scale were unsuccessful because of the very low temperature coefficient of solubility of the salt. Hence the general method of slow precipitation from hot solutions was used and seed suspensions were prepared by the method described by Cuming and Schulman[103]. Equimolar proportions of a barium salt and a sulphate were added simultaneously to normal hydrochloric acid or to water heated in an asbestos-lagged beaker to 90°C on a hot plate. The solution was stirred throughout the addition and a further period, about five hours, was allowed for digestion. The crystals were washed 20 times with distilled water and conductivity water by decantation before being transferred to pyrex stock flasks and stored in a water thermostat at 25°C.

Suspension A. - The crystals were regular rhombs about 8-12μ in size and were prepared from 50ml. portions of 0.5M barium chloride and 0.5M sulphuric acid added to 500ml. N. hydrochloride acid.

Concentration = 57mg. solid (ml. suspension)$^{-1}$.

Suspension B. - More dilute solutions (0.05M) than those used in A gave more perfect rhombs of size 10-20μ.

Concentration = 3mg. solid (ml. suspension)$^{-1}$.

Suspension C. - Suspension A was diluted ten times.

Concentration = 6mg. solid (ml. suspension)$^{-1}$.

Suspension D. - Prepared as in B, this sample was very regular in size and shape but too dilute to give measurable changes in conductivity readings when used in experiments.

Suspension E. - 0.1M Solutions were used, and regular rhombs of size 10μ were obtained.

Concentration = 50mg. solid. (ml. suspension)$^{-1}$.

Suspension E (a). - A portion of suspension E was allowed to grow from a supersaturated solution similar in concentration to that in the cell, and aged for one month before use.

Concentration = 16mg. solid (ml. suspension)$^{-1}$.

Suspension E (b). - A portion of E was allowed to age for one month in excess barium ion of a concentration similar to that used in the cell.
Concentration = 6mg. solid (ml. suspension)$^{-1}$.

Suspension F and G. - 0.01M solutions of barium hydroxide and sulphuric acid were added to water, and the crystals digested for 6 hours. Regular rhombs were obtained.
Concentration (F) = 9mg. solid (ml. suspension)$^{-1}$.
Concentration (G) = 4mg. solid (ml. suspension)$^{-1}$.

Suspension F (b). - A portion of suspension F was allowed to age in the presence of a slightly supersaturated solution of barium sulphate.
Concentration = 2mg. solid (ml. suspension)$^{-1}$.

The experimental conditions of precipitation assured that all the seed suspensions were prepared from solutions of concentrations below the transition limit observed by the Japanese, and all were seen to be orthorhombic in shape. The crystals could safely be used to inoculate the solutions used in this study since all initial cell concentrations were less than 5×10^{-4} mole.l^{-1}.

Solubility Value.

Many values for the solubility have been reported as might be anticipated from the uncertainty in producing a pure sample ~~from~~ of the solid. The literature values range from 9.55×10^{-6} mole.l^{-1} to 1.636×10^{-5} mole.l^{-1} and the values found in this work by allowing growth and dissolution experiments to proceed to equilibrium was 1.043×10^{-5}, and agreed very well with the value given by Rossoinsky[104] of 1.0385×10^{-5} mole.l^{-1} and this value was used throughout. The thermodynamic solubility product K given by

$$K = \left[Ba^{2+}\right] . \left[SO_4^{2-}\right] f_2^2$$

is equal to 1.014×10^{-10} mole^2.l^{-2}.

The Davies equation (p.) was used to evalute f_2.

All the crystals were above 10μ in size, and could be considered to have the same solubility value.

Mobility Value.

The equivalent conductivity of barium sulphate is given by

$$\Lambda_{BaSO_4} = \Lambda^{o} - b\sqrt{2m}.$$

Where m is the ionic concentration in mole.l^{-1}, Λ^{o} = 143.64 and b = 501.09 at 25°C.[95]

The activity of the solution was taken to be equal to the concentration, so that over the very small concentration changes observed the value of Λ was considered constant, and taken as 141.32 at the concentration 2 x 10^{-5} mole.l^{-1}. The change in concentration in solutions of equivalent concentration was evaluated by the equation

$$\Delta m = \Delta 1/R \times F$$

$$\text{where } F = \frac{10^3 \times \text{cell constant}}{\Lambda}$$

The treatment of results at non equivalent concentrations is as in section 2a (p.91) except that Λ is constant.

Results.

Experiments at equivalent and non equivalent ionic concentrations are summarised in Tables 35 and 41 respectively. The concentration of the cell solution in equivalent concentration work was always about twice the solubility value. The ionic products varied between 4.07×10^{-10} and 4.25×10^{-10} $mole^2.l^{-2}$ and in non equivalent concentration work, the initial ionic product was within this range.

Smooth curves of $1/R$ against time are shown in Figs. 35 and 40. The growth was usually followed for a period of two to three hours corresponding to about 20% of the total growth. In experiment 28, growth was followed for 15 hours and the smooth plot is shown which corresponds to 60% of the total growth.

Integrated plots of the second order equation

$$-\frac{dm}{dt} = k(s)(m - mo)^2$$

are shown for equivalent concentrations in Figs. 36 to 39 and all plots are good straight lines after an abnormally fast initial period. The results for non equivalent concentration experiments are similar, Figs. 41 to 43, where the integrated forms of the equation

$$-\frac{d\Delta}{dt} = kl(s)\Delta^2$$

TABLE. 35.

Crystallisation Experiments at 25°C. $[Ba^{2+}]/[SO_4^{2-}] = 1$.

Expt. no.	$[Ba^{2+}] \times 10^5$ mole. l^{-1}.	$[SO_4^{2-}] \times 10^5$ mole. l^{-1}.	$[Ba^{2+}][SO_4^{2-}]$ 10^{10} mole.l^{-1}	Seed Susp.	Seed conc. mg.	Initial Period (min.)	k $\times 10^7$ $l.mole^{-1}$ min^{-1}
15	2.0183	2.0183	4.0735	A	285	30	0.220
16	2.0180	2.0180	4.0723	C	29	70	0.021
18	2.0253	2.0253	4.1018	C	29	60	0.026
28	2.0409	2.0409	4.1653	E	150	30	0.173
29	2.0558	2.0558	4.2263	G	20	50	0.013
30	2.0629	2.0629	4.2556	G	20	45	0.016
32	2.0628	2.0628	4.2551	E(b)	30	25	0.120
33	2.0630	2.0630	4.2560	F(b)	10	40	0.028
34	2.0505	2.0505	4.2046	E(a)	80	30	0.184
35	2.0530	2.0530	4.2148	G(a)	?	30	0.025

Solubility product = 1.014×10^{-10} $mole^2 . l^{-2}$.

Fig 35.

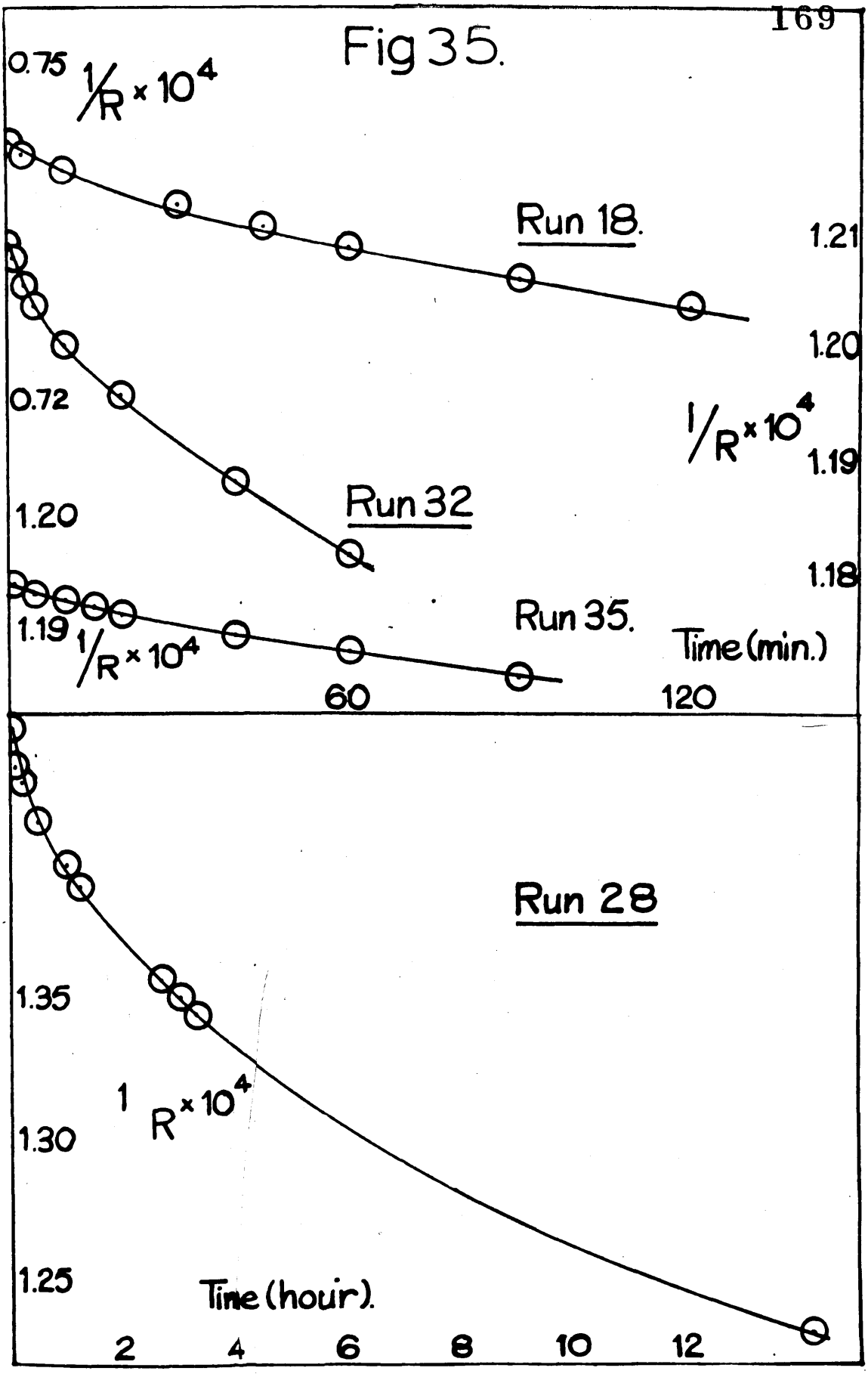
0.75
1/R × 10^4
Run 18.
1.21
1.20
0.72
1/R × 10^4
1.19
Run 32
1.20
1.18
Run 35.
1.19
1/R × 10^4
Time (min.)
60
120
Run 28
1.35
1/R × 10^4
1.30
1.25
Time (hour).
2
4
6
8
10
12

TABLE. 36.

time min.	$1/R \times 10^4$ ohm^{-1}	$\Delta m \times 10^5$ mole.l^{-1}	$m \times 10^5$ mole.l^{-1}	$(m-m_0) \times 10^5$ mole.l^{-1}	$\{(m-m_0)^{-1} - (m_{initial}-m_0)^{-1}\} \times 10^{-5}$ mole.l^{-1}
Experiment 15. - Cell B. (F = 0.29097).					
0	1.36620	0	2.0183	0.9798	0
5	1.36083	0.0156	2.0027	0.9642	0.0165
10	1.35705	0.0266	1.9917	0.9532	0.0285
20	1.34984	0.0487	1.9696	0.9311	0.0534
30	1.34285	0.0679	1.9504	0.9119	0.0760
50	1.33083	0.1050	1.9133	0.8784	0.1178
70	1.31895	0.1375	1.8808	0.8423	0.1666
90	1.30814	0.1689	1.8494	0.8109	0.2126
120	1.29421	0.2095	1.8088	0.7703	0.2776
Experiment 16. - Cell B. (F = 0.29097).					
0	1.35971	0	2.0180	0.9795	0
5	1.35849	0.0036	2.0144	0.9759	0.0038
10	1.35732	0.0070	2.0110	0.9625	0.0072
20	1.35544	0.0124	2.0056	0.9671	0.0131
30	1.35416	0.0162	2.0018	0.9633	0.0172
60	1.35112	0.0250	1.9930	0.9545	0.0268
90	1.34885	0.0316	1.9864	0.9479	0.0341
105	1.34786	0.0345	1.9835	0.9450	0.0373
120	1.34709	0.0367	1.9813	0.9428	0.0398

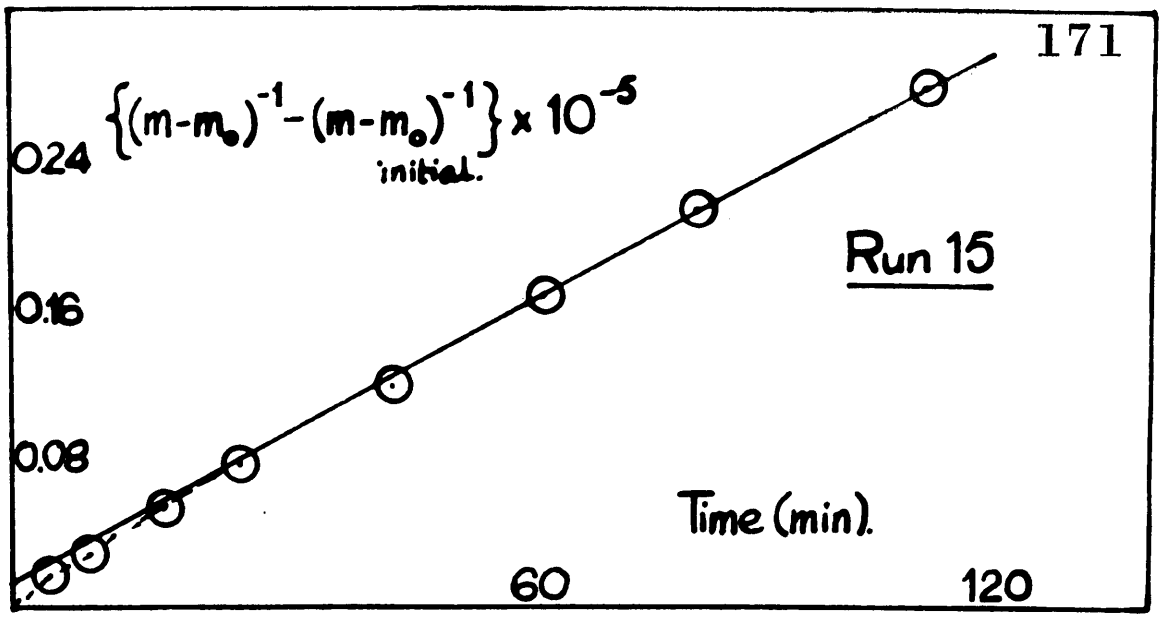
$\{(m-m_0)^{-1}-(m-m_0)^{-1}_{initial}\} \times 10^{-5}$
0.24
0.16
0.08
Run 15
Time (min).
60
120

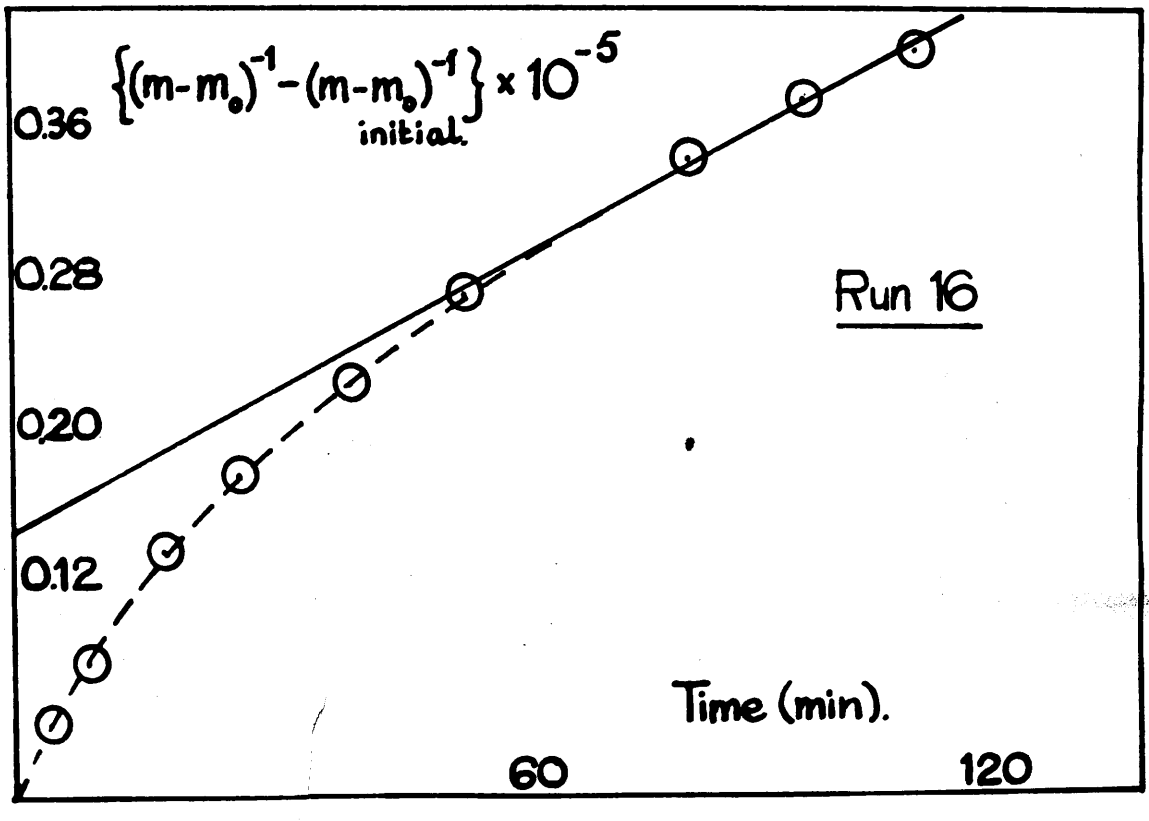
$\{(m-m_0)^{-1}-(m-m_0)^{-1}_{initial}\} \times 10^{-5}$
0.36
0.28
0.20
0.12
Run 16
Time (min).
60
120

Fig. 36.

TABLE. 37.

time min.	$1/R \times 10^4$ ohm.$^{-1}$	$\Delta m \times 10^5$ mole. l^{-1}	$m \times 10^5$ mole. l^{-1}	$(m-m_0) \times 10^5$ mole. l^{-1}	$\{(m-m_0)^{-1} - (m-m_0)^{-1}_{initial}\} \times 10^{-5}$ mole. l^{-1}
Experiment 18. - Cell B. (F = 0.29097).					
0	0.74320	0	2.0253	0.9868	0
3	0.74192	0.0037	2.0216	0.9831	0.0038
10	0.74046	0.0080	2.0173	0.9788	0.0083
30	0.73747	0.0167	2.0086	0.9701	0.0174
60	0.73379	0.0247	1.9979	0.9594	0.0289
90	0.73088	0.0358	1.9895	0.9510	0.0381
120	0.72843	0.0430	1.9823	0.9438	0.0461
150	0.72628	0.0492	1.9761	0.9376	0.0532
180	0.72432	0.0549	1.9704	0.9319	0.0597
Experiment 28. - Cell C. (F = 0.27381).					
0	1.44530	0	2.0409	1.0024	0
5	1.43191	0.0367	2.0042	0.9657	0.0379
10	1.42624	0.0522	1.9887	0.9502	0.0584
20	1.41902	0.0720	1.9689	0.9304	0.0772
40	1.40703	0.1048	1.9361	0.8976	0.1165
60	1.39676	0.1329	1.9080	0.8695	0.1525
75	1.38949	0.1528	1.8881	0.8496	0.1794
155	1.35744	0.2406	1.8003	0.7618	0.3151
180	1.34913	0.2633	1.7776	0.7391	0.3554

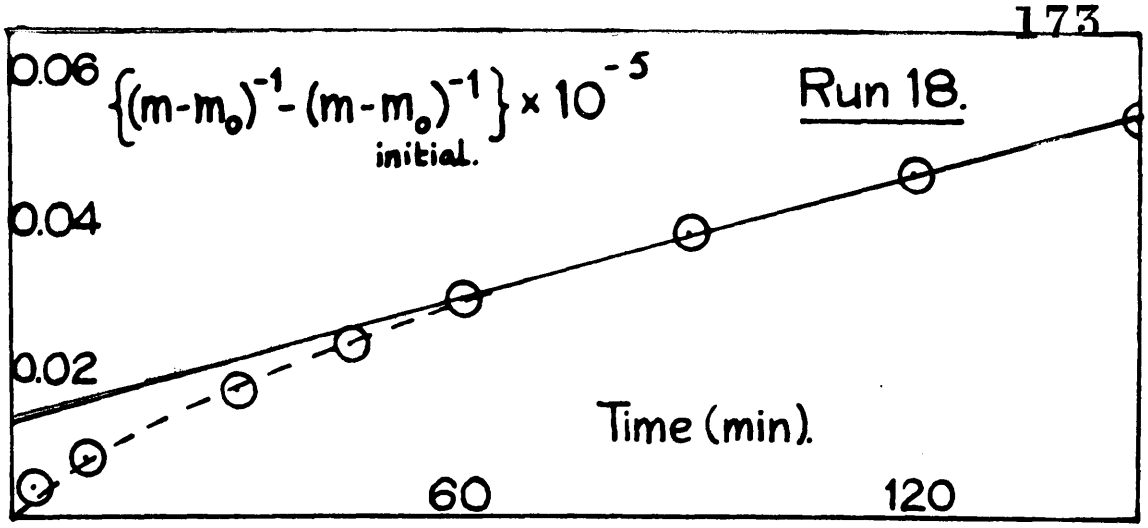
0.06
0.04
0.02
$\{(m-m_o)^{-1}-(m-m_o)^{-1}_{initial.}\} \times 10^{-5}$
Run 18.
Time (min).
60
120

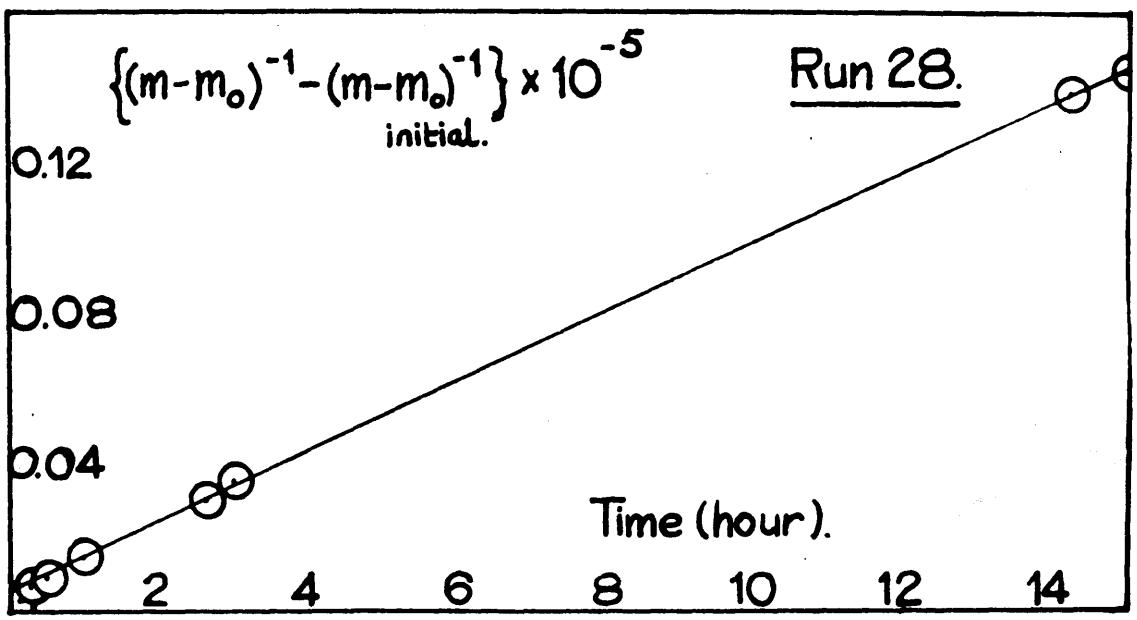
$\{(m-m_o)^{-1}-(m-m_o)^{-1}_{initial.}\} \times 10^{-5}$
Run 28.
0.12
0.08
0.04
Time (hour).
2
4
6
8
10
12
14

Fig. 37.

TABLE. 38.

time min	$1/R \times 10^4$ ohm^{-1}	$\Delta m \times 10^5$ mole. l^{-1}	$m \times 10^5$ mole. l^{-1}	$(m-m_0) \times 10^5$ mole. l^{-1}	$\{(m-m_0)^{-1} - (m-m_0)^{-1}_{initial}\} \times 10^5$ mole. l^{-1}.
Experiment 29. - Cell C (F = 0.27381).					
0	1.47813	0	2.0558	1.0173	0
5	1.47457	0.0097	2.0461	1.0076	0.95
10	1.47353	0.0126	2.0432	1.0047	1.23
20	1.47213	0.0164	2.0394	1.0009	1.61
40	1.46956	0.0235	2.0323	0.9938	2.32
60	1.46843	0.0268	2.0290	0.9905	2.66
90	1.46670	0.0313	2.0245	0.9860	3.12
120	1.46567	0.0341	2.0217	0.9832	3.41
150	1.46506	0.0385	2.0200	0.9815	3.58
Experiment 30. - Cell C. (F = 0.27381).					
0	1.46451	0	2.0629	1.0244	0
5	1.46227	0.0061	2.0568	1.0183	0.58
10	1.46154	0.0081	2.0548	1.0163	0.78
20	1.45972	0.0131	2.0498	1.0113	1.26
40	1.45718	0.0201	2.0428	1.0043	1.95
60	1.45574	0.0240	2.0389	1.0004	2.34
90	1.45471	0.0268	2.0361	0.9976	2.62
120	1.45206	0.0341	2.0288	0.9903	3.36

TABLE. 39.

time min.	$1/R \times 10^4$ ohm^{-1}	$\Delta m \times 10^5$ mole.l^{-1}	$m \times 10^5$ mole.l^{-1}	$(m-m_0) \times 10^5$ mole.l^{-1}	$\{(m-m_0)^{-1} - (m-m_0)^{-1}\} \times 10^{-7}$ mole.l^{-1}
Experiment 32. - Cell D (F = 0.32575).					
0	1.20922	0	2.0628	1.0243	0
1	1.20775	0.0048	2.0580	1.0195	0.46
3	1.20507	0.0135	2.0493	1.0108	1.30
5	1.20352	0.0186	2.0442	1.0057	1.80
10	1.20056	0.0282	2.0346	0.9961	2.76
20	1.19563	0.0443	2.0185	0.9800	4.41
40	1.18809	0.0688	1.9940	0.9555	7.03
60	1.18150	0.0903	1.9725	0.9340	9.44
Experiment 33. - Cell D (F = 0.32575).					
0	1.19581	0	2.0630	1.0245	0
1	1.19544	0.0012	2.0618	1.0233	0.11
3	1.19457	0.0040	2.0590	1.0205	0.38
5	1.19380	0.0065	2.0565	1.0180	0.62
10	1.19279	0.0098	2.0532	1.0147	0.94
20	1.19154	0.0139	2.0491	1.0106	1.34
40	1.18909	0.0219	2.0411	1.0026	2.13
60	1.18756	0.0269	2.0361	0.9976	2.59
90	1.18527	0.0343	2.0287	0.9902	3.39

TABLE. 40.

time min	$1/R \times 10^4$ ohm^{-1}	$\Delta m \times 10^5$ mole. l^{-1}	$m \times 10^5$ mole. l^{-1}	$(m-m_0) \times 10^5$ mole. l^{-1}	$\{(m-m_0)^{-1} - (m-m_0)^{-1}_{initial}\} \times 10^{-7}$ mole. l^{-1}
Experiment 34. - Cell D (F = 0.32575).					
0	1.18961	0	2.0505	1.0120	0
1	1.18790	0.0056	2.0449	1.0064	0.55
3	1.18379	0.0190	2.0325	0.9930	1.89
10	1.17775	0.0386	2.0119	0.9734	3.92
20	1.17089	0.0610	1.9895	0.9510	6.34
30	1.16539	0.0789	1.9716	0.9331	8.36
50	1.15485	0.1132	1.9379	0.8988	12.45
75	1.14427	0.1477	1.9028	0.8643	16.89
90	1.13826	0.1673	1.8832	0.8447	19.58
Experiment 35. - Cell D (F = 0.32575).					
0	1.1942	0	2.0530	1.0145	0
1	1.1939	0.0010	2.0520	1.0135	0.10
5	1.1932	0.0033	2.0497	1.0112	0.32
10	1.1924	0.0059	2.0471	1.0086	0.58
15	1.1918	0.0078	2.0452	1.0067	0.76
20	1.1911	0.0101	2.0429	1.0044	0.99
40	1.1894	0.0156	2.0374	0.9989	1.54
60	1.1880	0.0202	2.0328	0.9943	2.00
90	1.1856	0.0280	2.0250	0.9865	2.80

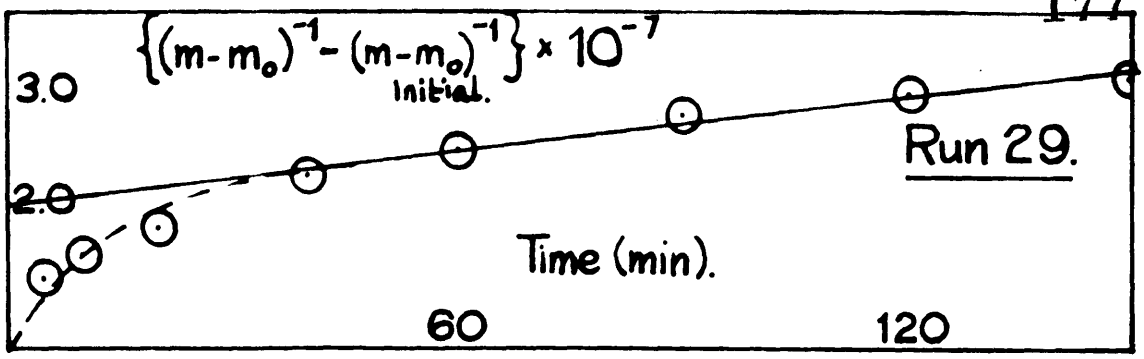
$\{(m-m_o)^{-1}-(m-m_o)^{-1}_{initial.}\}\times 10^{-7}$
3.0
2.0
Run 29.
Time (min).
60
120

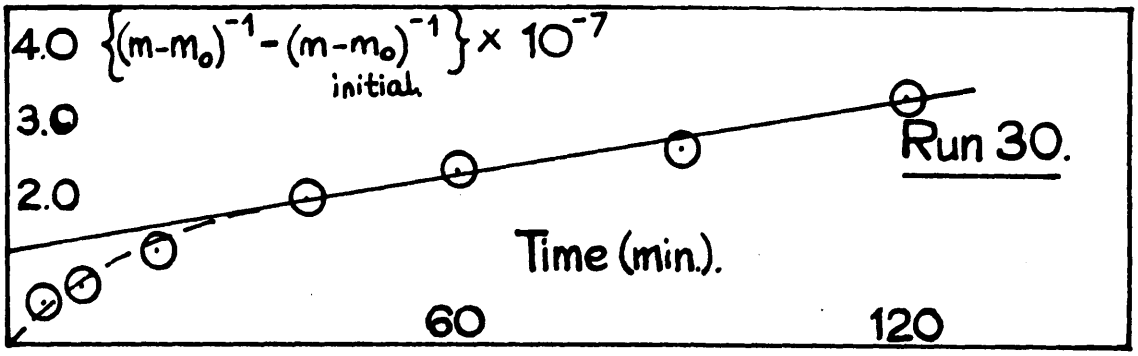
4.0 $\{(m-m_o)^{-1}-(m-m_o)^{-1}_{initial.}\}\times 10^{-7}$
3.0
2.0
Run 30.
Time (min.).
60
120

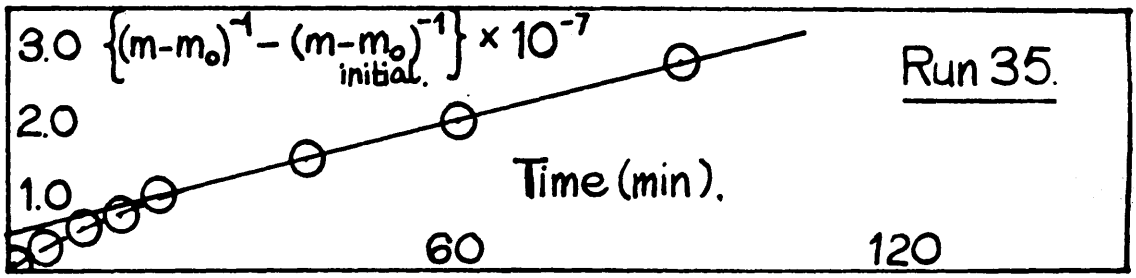
3.0 $\{(m-m_o)^{-1}-(m-m_o)^{-1}_{initial.}\}\times 10^{-7}$
2.0
1.0
Run 35.
Time (min).
60
120

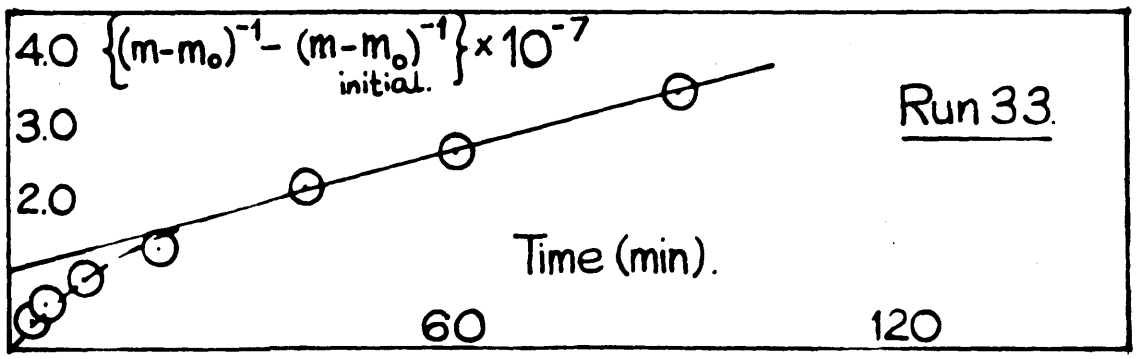
4.0 $\{(m-m_o)^{-1}-(m-m_o)^{-1}_{initial.}\}\times 10^{-7}$
3.0
2.0
Run 33.
Time (min).
60
120

Fig. 38.

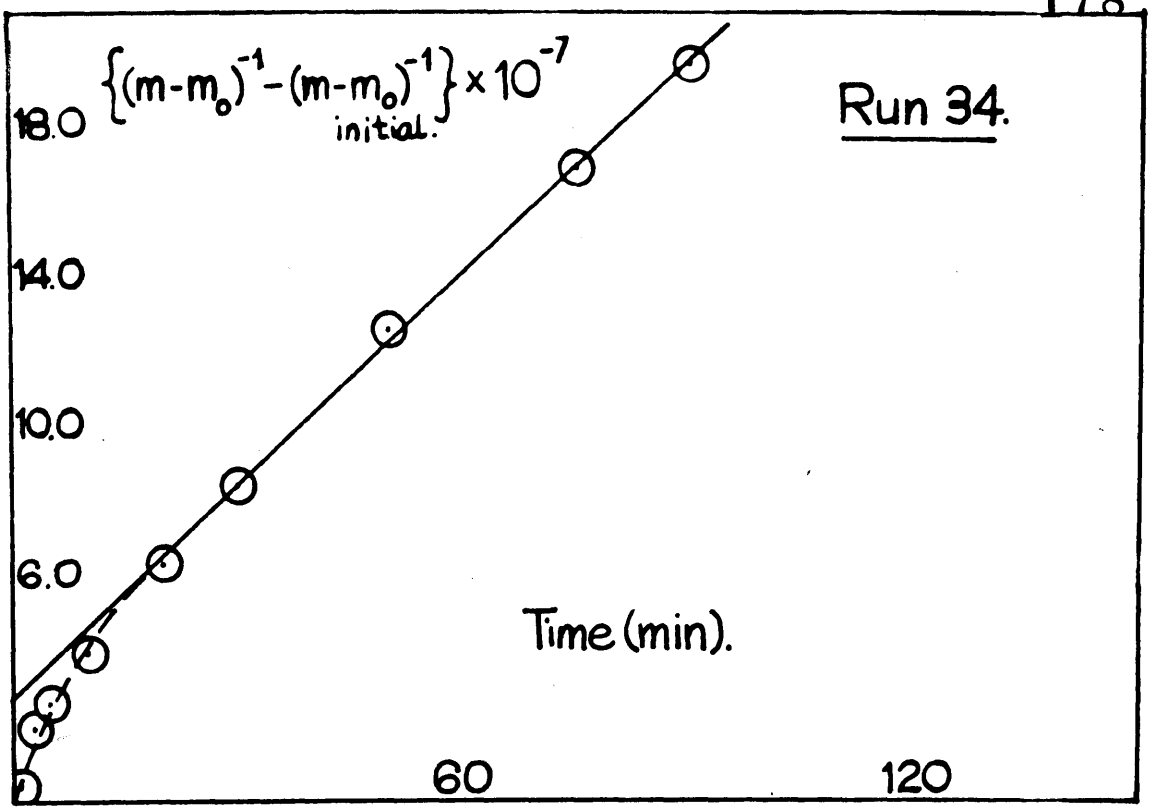
$\{(m-m_o)^{-1}-(m-m_o)^{-1}_{initial}\} \times 10^{-7}$
Run 34.
18.0
14.0
10.0
6.0
Time (min).
60
120

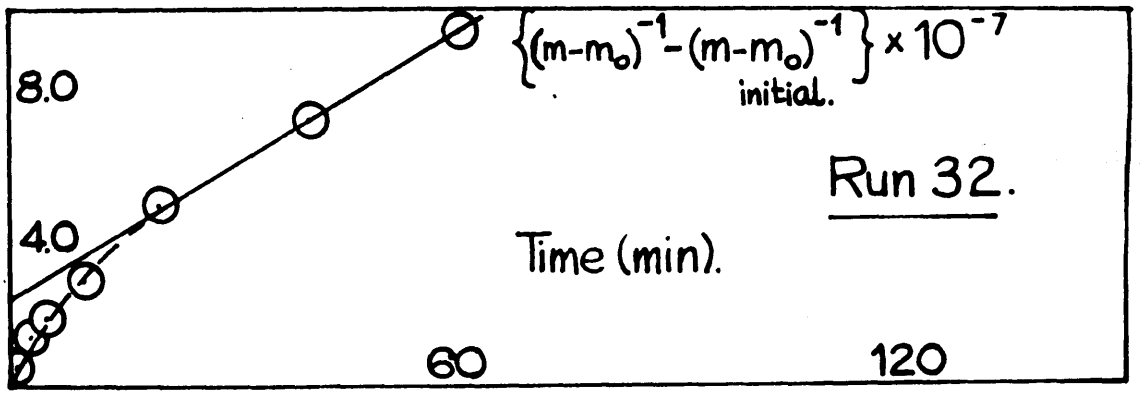
$\{(m-m_o)^{-1}-(m-m_o)^{-1}_{initial}\} \times 10^{-7}$
Run 32.
8.0
4.0
Time (min).
60
120

Fig. 39.

are shown. Δ is the concentration of ions which remain to be precipitated from solution. The data for the construction of these figures are given in Tables 36 to 40 and 42 to 44 respectively.

The reproducibility of the method is illustrated by experiments 29 and 30, and 20, 21 and 24. Good agreement between seed A and seed C is shown by experiments 15 and 16, where the ratio of rate constants is equal to the ratio of seed concentrations. This consistency is not observed between any other seed suspensions (e.g. A and E) and probably reflects the irreproducibility of pure products.

In experiment 16, the cell solution was prepared by mixing barium chloride and sodium sulphate solutions, and from a mixture of barium hydroxide and sulphuric acid in 18. The rate constants are seen to be very similar.

Experiment 32 was inoculated with seed E(b) which had been aged in excess barium ions; in Fig. 39 the initial fast part is still observed. This is also true of experiments 33 and 34, in which the seed crystals added had been aged in excess barium sulphate for a considerable length of time.

Experiment 35 is singularly interseting in that crystallisation was initiated by seed crystals which

TABLE. 41.

Crystallisation Experiments at 25°C. $[Ba^{2+}]/[SO_4^{2-}] \neq 1$.

Expt. no.	$[Ba^{2+}]\times10^5$ mole. l^{-1}	$[SO_4^{2-}]\times10^5$ mole. l^{-1}	$[Ba^{2+}][SO_4^{2-}]$ $\times10^{10}$ mole^2. l^{-2}	$\frac{[Ba^{2+}]}{[SO_4^{2-}]}$	Seed Susp.	Seed Conc. mg.	Initial Period min.	$k\times10^7$ l.mole^{-1} min^{-1}
20	2.8612	1.4304	4.0927	2.0	A	285	50	0.140
21	2.8642	1.4339	4.1070	2.0	A	285	45	0.130
22	1.4237	2.8658	4.0799	0.5	A	285	60	0.090
23	1.4317	2.8637	4.0998	0.5	A	285	65	0.100
24	2.8647	1.4327	4.1043	2.0	A	285	50	0.140
27	2.8648	1.4328	4.1047	2.0	B	150	25	0.184

TABLE. 42.

time min.	$1/R \times 10^4$ ohm^{-1}	$\delta\Delta \times 10^5$ mole. l^{-1}	$\Delta \times 10^5$ mole. l^{-1}	$\{\Delta^{-1} - \Delta^{-1}_{initial}\} \times 10^{-5}$ mole. l^{-1}
Experiment 20. - Cell B. (F = 0.29097).				
0	1.48126	0	0.9108	0
5	1.47684	0.0120	0.8979	0.0158
15	1.46999	0.0328	0.8780	0.0411
30	1.46196	0.0562	0.8546	0.0722
45	1.45525	0.0757	0.8351	0.0996
60	1.44978	0.0916	0.8192	0.1228
90	1.44057	0.1184	0.7924	0.1641
120	1.43333	0.1395	0.7713	0.1986
Experiment 21. - Cell B. (F = 0.29097).				
0	1.49631	0	0.9141	0
5	1.48967	0.0193	0.8949	0.0236
10	1.48651	0.0285	0.8856	0.0352
20	1.48198	0.0443	0.8698	0.0557
30	1.47641	0.0579	0.8562	0.0740
40	1.47262	0.0689	0.8452	0.0892
60	1.46621	0.0876	0.8265	0.1159
90	1.45898	0.1089	0.8052	0.1479
120	1.45128	0.1310	0.7631	0.1830

TABLE. 43.

time min.	$1/R \times 10^4$ ohm^{-1}	$\delta\Delta \times 10^5$ mole. l^{-1}	$\Delta \times 10^5$ mole. l^{-1}	$\{\Delta^{-1} - \Delta^{-1}_{initial}\} \times 10^{-5}$ mole. l^{-1}
Experiment 22. – Cell B (F = 0.29097).				
0	1.36988	0	0.9063	0
10	1.36407	0.0169	0.8894	0.0210
20	1.35966	0.0297	0.8766	0.0374
30	1.35627	0.0396	0.8667	0.0504
40	1.35325	0.0490	0.8573	0.0631
50	1.35018	0.0573	0.8490	0.0745
110	1.33553	0.0997	0.8066	0.1364
150	1.32796	0.1220	0.7843	0.1716
180	1.32277	0.1371	0.7692	0.1967
Experiment 23. – Cell B (F = 0.29097).				
0	1.37409	0	0.9122	0
10	1.36793	0.0179	0.8943	0.0219
20	1.36328	0.0315	0.8807	0.0392
40	1.35527	0.0548	0.8574	0.0700
60	1.34896	0.0731	0.8391	0.0955
80	1.34358	0.0885	0.8237	0.1171
100	1.33907	0.1019	0.8103	0.1378
120	1.33465	0.1148	0.7974	0.1578
140	1.33089	0.1257	0.7865	0.1752

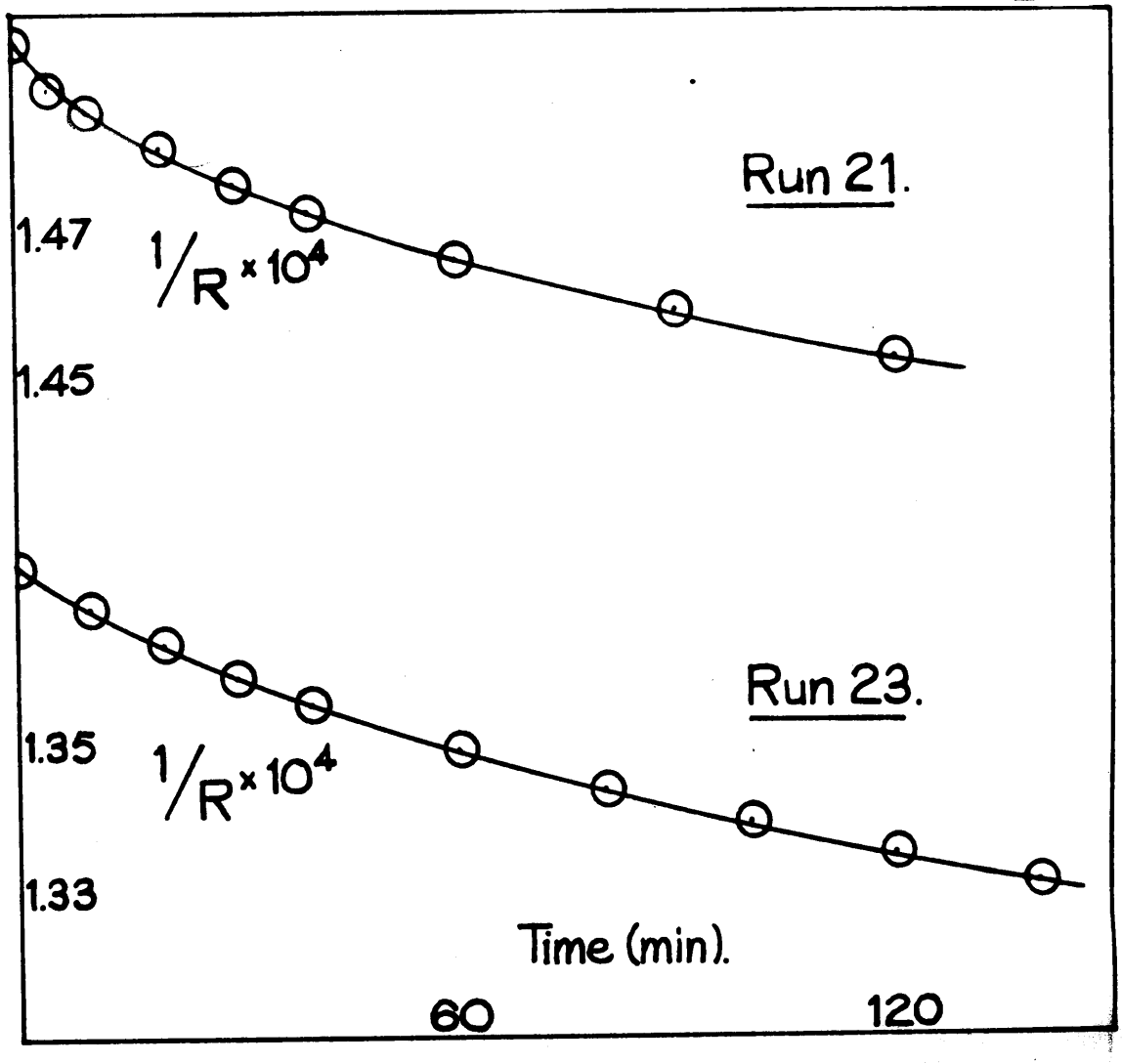

Fig.40.

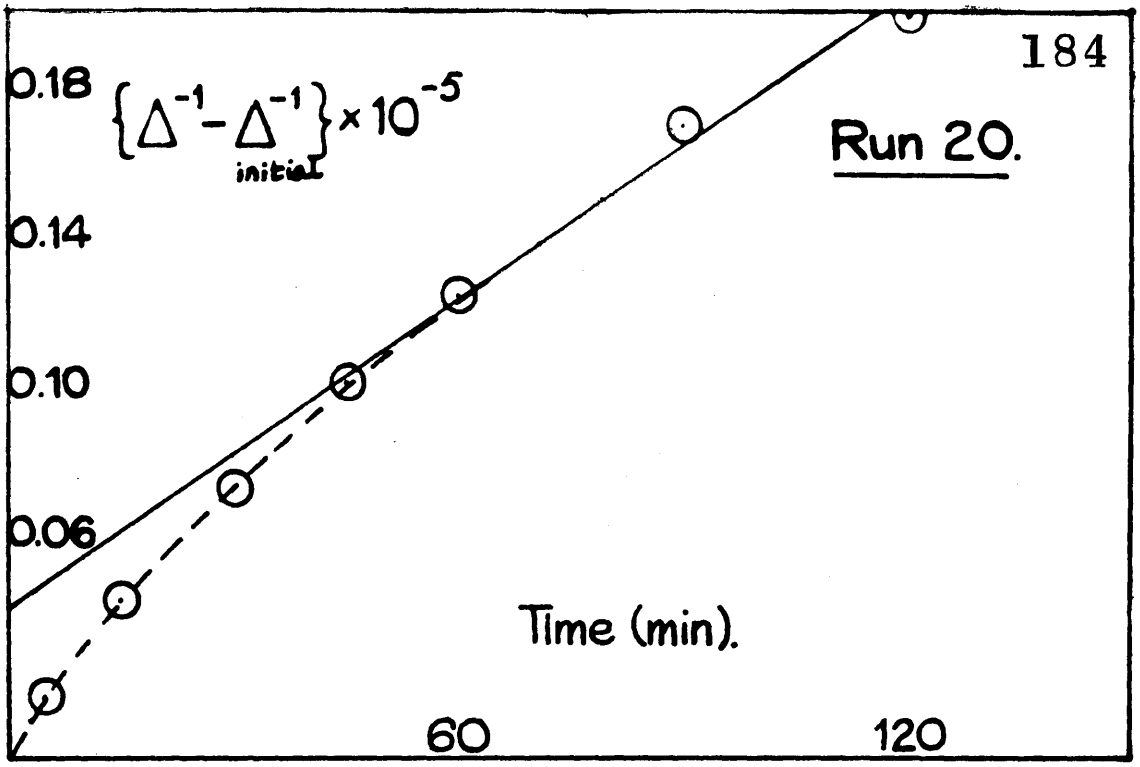
0.18
0.14
0.10
0.06
$\{\Delta^{-1} - \Delta^{-1}_{initial}\} \times 10^{-5}$
Run 20.
Time (min).
60
120

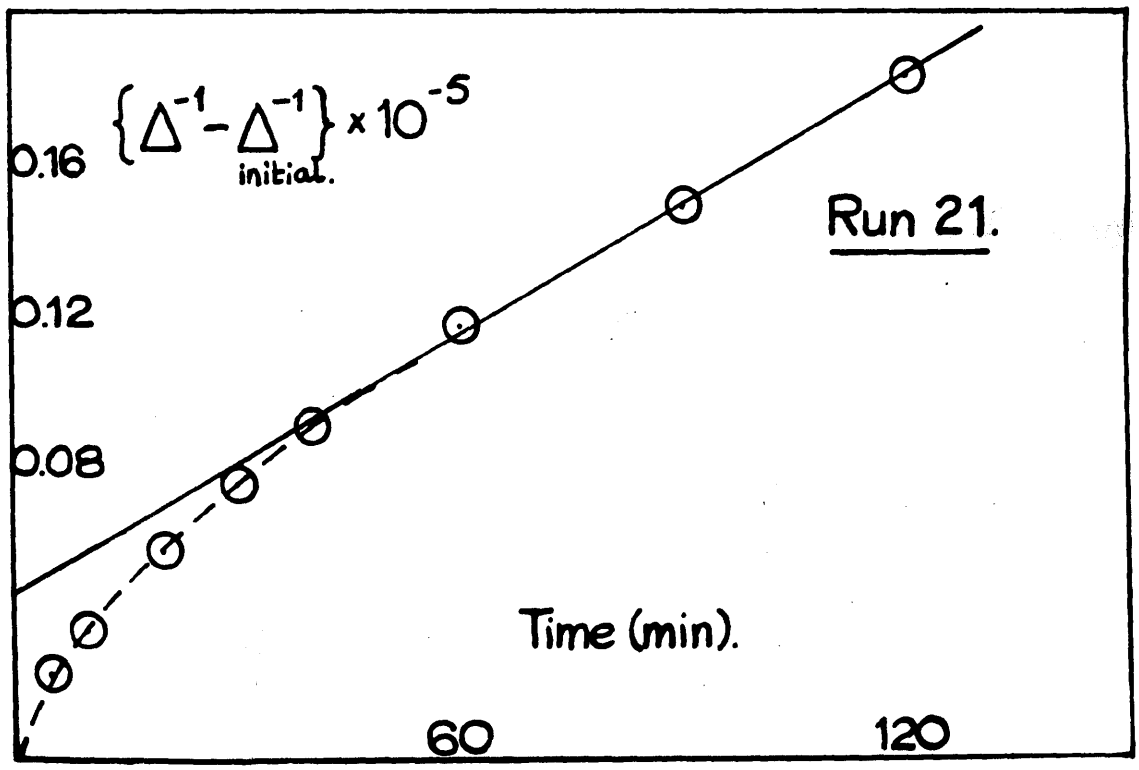
0.16
0.12
0.08
$\{\Delta^{-1} - \Delta^{-1}_{initial.}\} \times 10^{-5}$
Run 21.
Time (min).
60
120

Fig. 41.

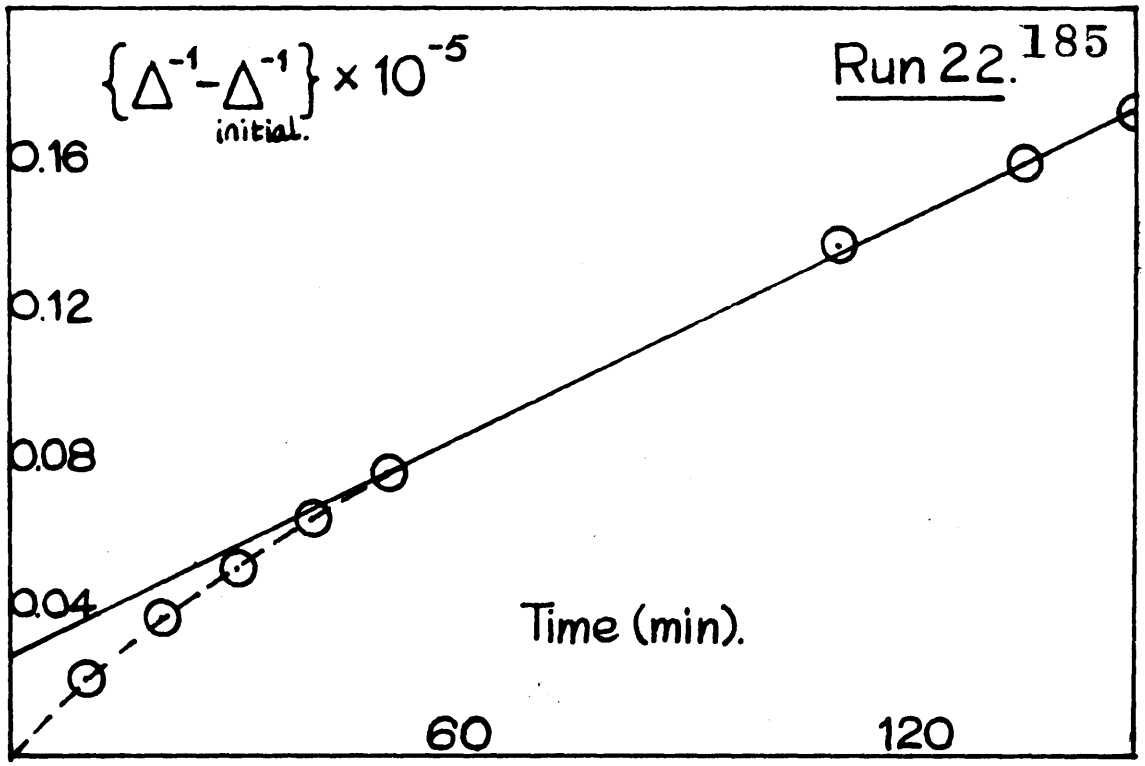
$\{\Delta^{-1} - \Delta^{-1}_{initial.}\} \times 10^{-5}$
Run 22.
0.16
0.12
0.08
0.04
Time (min).
60
120

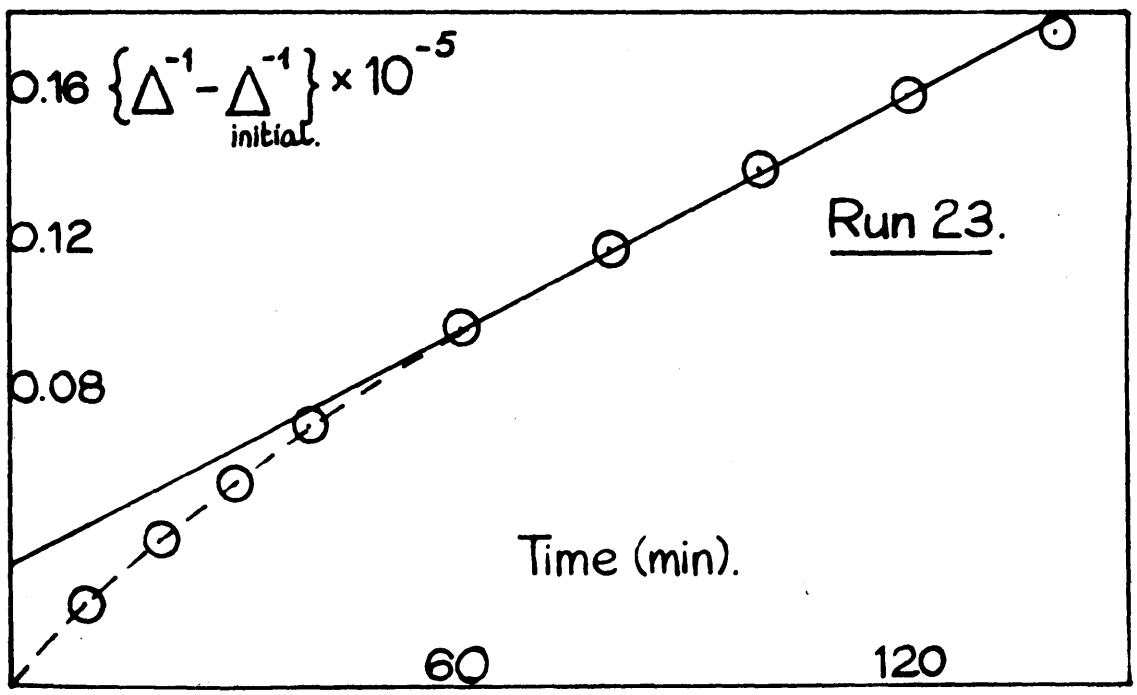
0.16 $\{\Delta^{-1} - \Delta^{-1}_{initial.}\} \times 10^{-5}$
Run 23.
0.12
0.08
Time (min).
60
120

Fig. 42.

TABLE. 44.

time min.	$\frac{1}{R} \times 10^4$ ohm^{-1}	$\delta\Delta \times 10^5$ mole. l^{-1}	$\Delta \times 10^5$ mole. l^{-1}	$\{\Delta^{-1} - \Delta^{-1}_{initial}\} \times 10^{-5}$ mole. l^{-1}
Experiment 24. - Cell B (Γ = 0.29097).				
0	1.46694	0	0.9132	0
10	1.45791	0.0263	0.8869	0.0324
20	1.45098	0.0464	0.8668	0.0586
30	1.44577	0.0616	0.8516	0.0792
40	1.44099	0.0755	0.8377	0.0986
60	1.43356	0.0971	0.8161	0.1308
90	1.42418	0.1244	0.7888	0.1726
120	1.41616	0.1478	0.7654	0.2114
150	1.40894	0.1688	0.7444	0.2483
Experiment 27. - Cell C (Γ = 0.27381).				
0	1.54792	0	0.9133	0
10	1.52915	0.0514	0.8619	0.0653
20	1.52264	0.0692	0.8441	0.0898
40	1.51263	0.0966	0.8167	0.1295
60	1.50369	0.1211	0.7922	0.1674
80	1.49545	0.1437	0.7696	0.2045
100	1.48781	0.1646	0.7847	0.2407
120	1.48096	0.1833	0.7300	0.2750
150	1.47121	0.1833	0.7033	0.3271

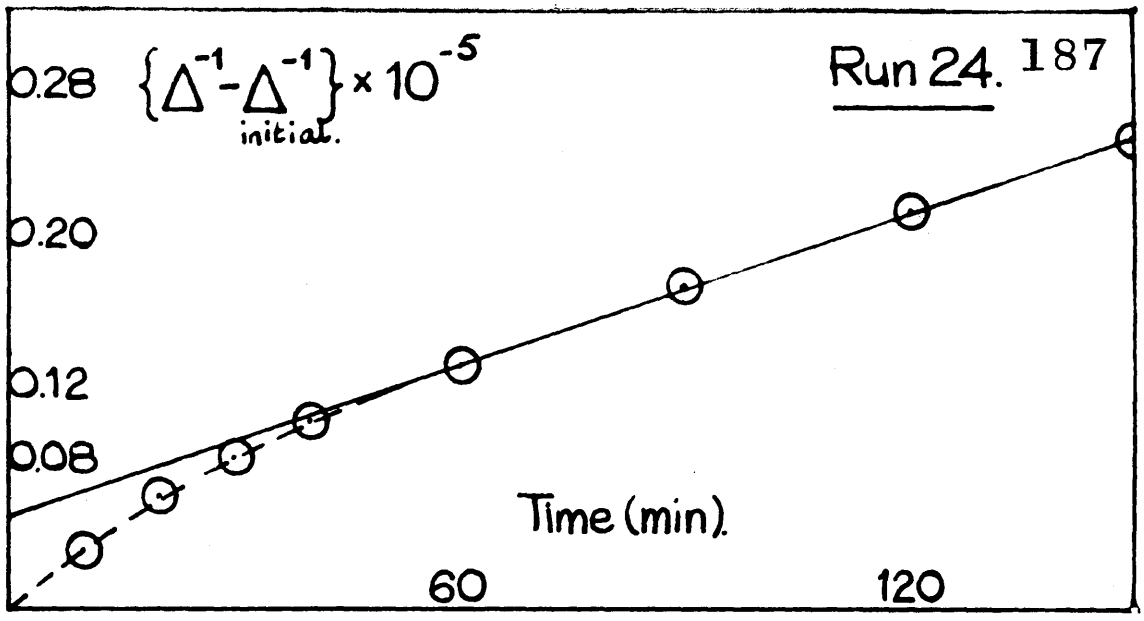
$\{\Delta^{-1}-\Delta^{-1}_{initial.}\}\times 10^{-5}$
Run 24.
0.28
0.20
0.12
0.08
Time (min).
60
120

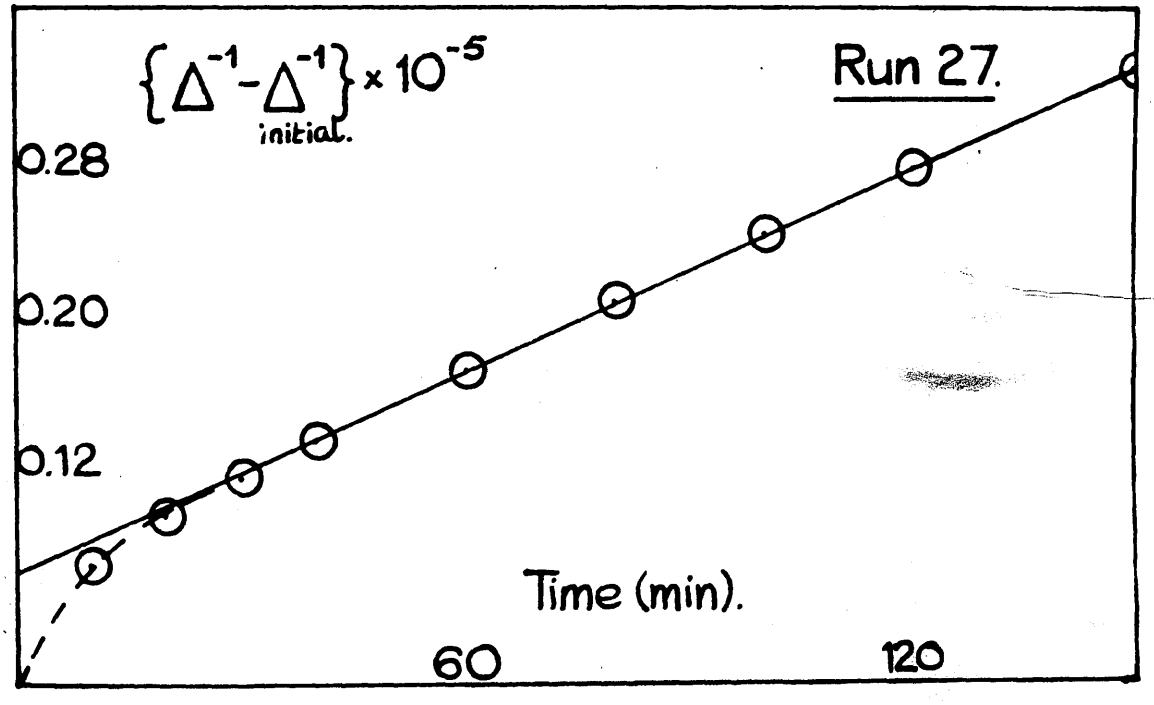
$\{\Delta^{-1}-\Delta^{-1}_{initial.}\}\times 10^{-5}$
Run 27.
0.28
0.20
0.12
Time (min).
60
120

Fig 43.

were allowed to seed another supersaturated solution and to grow for two hours before addition. However the initial fast period of growth was still observed, Fig. 38.

Although no quantitative study was made of the effects of altering the stirring rates, the changes in speed of the vibratory stirrer did not affect the rate of growth.

Discussion.

Apart from the abnormally fast initial growth rate, the growth of barium sulphate seed crystals from supersaturated solutions follows the second order rate equation suggested by Davies and Jones for at least 60% of the total reaction. The duration of the initial period varies between a few minutes to an hour and the amount of solid desposited corresponds to about 3% of the total in solutions of equivalent concentrations and to about 8% in solutions of non equivalent concentrations.

Various unsuccessful attempts have been made to explain this fast period of growth. From Table 17 no correlation between the length of time of the surge and the seed concentration can be drawn. The previous

histories of the seed suspensions provide no additional information.

When chloride and potassium ions are occluded into the crystal lattice, the observed change in conductivity is not entirely due to the removal of the lattice ions. Such a process might have explained the initial surge, but experiment 18 was a replica of 16 and the effect is considered negligible.

Writing

$$\frac{-dm}{dt} = k(s)(m-m_0)^n$$

and taking logarithms throughout, the graph of log $(\frac{dm}{dt})$ against log $(m - m_0)$ would be a straight line, whose gradient would be equal to n. Such a plot was constructed for experiment 28 from the data in Table 45 and is shown in Fig.44. The graph consists of two intersecting straight lines A and B, the slope of the latter being equal to 2. Therefore second order kinetics exist in the slower part of the growth. The slope of A is equal to 20 and no possible mechanism can be suggested at present.

It was thought that the fast rate might be explained by the "filling in" of surface pores on the seed crystals 99. The attempts to fill in the pores with excess barium sulphate solution and excess Ba^{2+}

TABLE. 45.

time min.	$\frac{\Delta 1/R}{\Delta t} \times 10^7$ ohm^{-1}.min^{-1}	$\frac{dm}{dt} \times 10^7$ mole.l^{-1}.min^{-1}	$-\log \frac{dm}{dt}$	$(m-m_0) \times 10^5$ mole.l^{-1}	$-\log(m-m_0)$
Experiment 28.					
0	4.30	1.18	6.93	1.0024	5.000
1	2.90	0.79	7.10	0.9970	5.001
3	2.22	0.60	7.22	0.9737	5.012
5	1.72	0.47	7.32	0.9657	5.015
10	1.08	0.30	7.52	0.9502	5.022
20	0.66	0.18	7.74	0.9304	5.031
40	0.54	0.15	7.82	0.8976	5.047
60	0.49	0.14	7.85	0.8695	5.061
75	0.46	0.13	7.89	0.8496	5.071
155	0.41	0.11	7.96	0.7618	5.118
15h.	0.10	0.03	8.52	0.4064	5.391
11					

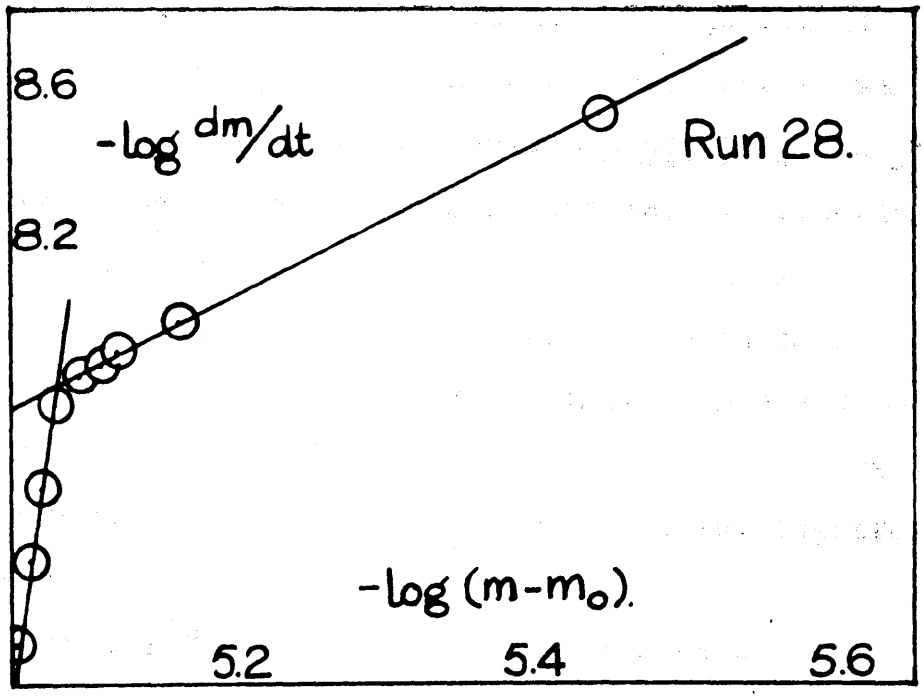

Fig. 44.

ions alone did not eliminate the fast period of growth. The effect of ageing the crystals may have meant that the crystals of seed suspensions E(a), E(b) and F(b) resorted to their original condition. In experiment 35, seed crystals, which had been growing in a supersaturated solution of similar concentration to the working solution for two hours, when added to the solution in the cell failed to eliminate the initial fast rate. Such a simple explanation is, therefore, incorrect.

Meisen[11], in his work on spontaneous crystallisation reported that the order of the nucleation step in the overall growth was 8. The very high order of A in Fig.44 might suggest nucleation as a possible step in the mechanism, but nucleation steps are necessarily slow steps and by analogy with the magnesium oxalate results of the present work the likelihood of simultaneous or induced nucleation is not feasible.

In experiments of non equivalent concentrations, the observed second order rate constant k^1 is lower than that k for crystallisation under equivalent concentration conditions. This retardation is general and is due to the increase in the potential

difference which is always present at the surface of the crystal from a disparity in ion concentrations. The value of $\underline{k}^1$ is lower when sulphate rather than barium ion is in excess. This was observed by Davies[21] in the crystallisation of silver chloride and it is probable that the rate of adsorption of the anion is greater than that of the cation in both systems.

In conclusion, therefore, it has been shown that in the crystallisation, of barium sulphate, a very insoluble 2-2 electrolyte, the general theory of growth suggested by Davies and Jones is followed for most of the reaction. It is clearly desirable to supplement these observations by further crystallisation and dissolution work in the presence of adsorbates, in particular sodium triphosphate[59], and at a variety of temperatures.

BIBLIOGRAPHY.

(1). BIRCUMSHAW & RIDDIFORD, Quart. Rev., 1952, 6, 157.

(2). DAVIES & JONES, Trans. Far. Soc., 1955, 51, 812.

(3). BURTON, CABRERA & FRANK, Disc. Far. Soc., 1951, 24, 299.

(4). SEARS, J. Chem. Phys., 1960, 32, 1317.

(5). DE VRIES & SEARS, ibid., 1961, 34, 616.

(6). JOHNSON & O'ROURKE, Anal. Chem., 1955, 27, 1699.

(7). NIELSEN, Acta. Chem. Scand., 1959, 13, No.4.

(8). BECKER & DORING, Ann. Phys., 1938, 32, 128.

(9). OSTWALD, Z. Physik. Chem., 1897, 22, 289.

(10). VON WEIMARN, Chem. Revs., 1925, 2, 217.

(11). CHRISTIANSEN & NIELSEN, Acta. Chem. Scand., 1951, 5, 673.

(12). TURNBULL, Acta. Met., 1953, 1, 684.

(13). FISCHER, Anal. Chem. Acta., 1960, 22, 501.

(14). FISCHER & RHINEHAMMER, ibid, 1953, 25, 1544.
ibid, 1954, 26, 244.

(15). FISCHER, Ibid, 1960, 22, 508.

(16). COLLINS & LEINEWEBER, J. Phys. Chem., 1956, 60, 389.

(17). DUNNING & NOTLEY, Z. Elektrochem., 1957, 61, 55.

(18). CHRISTIANSEN & NIELSEN, Acta. Chem. Scand., 1951, 5, 674.

(19). TOVBERG JENSEN, Z. Physik. Chem. A., 1937, 108, 93.

(20). KOLTHOFF, J. Phys. Chem., 1959, 63, 817.

(21). DAVIES & NANCOLLAS, Trans. Far. Soc., 1955, 51, 818.
(22). DAVIES & NANCOLLAS, ibid., 1955, 51, 823.
(23). DAVIES, JONES & NANCOLLAS, ibid., 1955, 51, 1232.
(24). HOWARD & NANCOLLAS, ibid., 1957, 53, 1449.
(25). JONES & JOSEPH, J. Amer. Chem. Soc., 1928, 50, 1049.
(26). SHEDLOVSKY, ibid., 1930, 52, 1793.
(27). CALVERT et. al. J. Phys. Chem., 1958, 62, 47.
(28). NAIR & NANCOLLAS, J. Chem. Soc., 1958, 4144.
(29). HARTLEY & BARRETT, ibid., 1913, 786.
(30). HOWARD, Ph.D. Thesis, Glasgow, 1958.
(31). DAVIES & NANCOLLAS, Chem. & Ind., 1950, 129.
(32). KOHLRAUSCH, "Textbook of Analytical Chemistry", Treadwell & Hall, 5th. Ed., New York, 1924.
(33). VOGEL, "Quantitative Inorganic Analysis", 1947, p. 222.
(34). FRAZER & HARTLEY, Proc. Roy. Soc., A. 1925, 109, 355.
(35). SHEDLOVSKY, J. Amer. Chem. Soc., 1932, 54, 1411.
(36). DAVIES, Trans. Far. Soc., 1929, 25, 1129.
(37). BUCKLEY, "Crystal Growth", Wiley, New York, 1951, Chap.9.
(38). NOYES & WHITNEY, Z. physik, Chem., 1897, 23, 689.
(39). KING & BRAVERMAN, J. Amer. Chem. Soc., 1932, 54, 1744.
(40). KING & SCHACK, ibid., 1935, 57, 1212.
(41). NERNST, Z. phys. Chem., 1904, 47, 52.
(42). BRUNNER, ibid., 1904, 47, 56.
(43). VAN NAME & EDGAR, Amer. J. Sci., 1910, 29, 237.
Z. phys. Chem., 1910, 73, 97.

(44). GARRETT & COOPER, J. Phys. Colloid Chem., 1950, 54, 437.

(45). JOHNSON & McDONALD, J. Amer. Chem. Soc., 1950, 72, 666.

(46). BIRCUMSHAW & RIDDIFORD, J. Chem. Soc., 1952, 698.

(47). CENTNERSZWER & ZABLOCKI, Z. phys. Chem., 1926, 122, 455.

(48). CENTNERSZWER, ibid., 1928, 137, 352.

(49-52). MARC, Z. phys. Chem., 1908, 61, 385.
ibid., 1909, 67, 470.
ibid., 1909, 68, 104.
ibid., 1910, 73, 685.

(53). MOELWYN-HUGHES, "The Kinetics of Reactions in Solution". 2nd. Edition, Cambridge, 1947, p. 357.

(54). PAGE & TOWNEND, Proc. Roy. Soc. A., 1932, 135, 656.

(55). JABLCZYNSKI & ST. JABLONSKI, Z. phys. Chem., 1911, 75, 503.

(56). VAN NAME & HILL, Amer. J. Sci., 1913, 36, 543.

(57). KING & LIU, J. Amer. Chem. Soc., 1933, 55, 1928.

(58). KING, ibid., 1935, 57, 828.

(59). OTANI, Bull. Chem. Soc. Jap., 1960, 33, 1543, 1549.

(60). KING & CATHCART, J. Amer. Chem. Soc., 1937, 59, 63.

(61). RUCKEN, Z. Elektrochem., 1932, 38, 341.

(62). KING, Trans. N.Y. Acad. Sci., 1948, II, 10, 262.

(63). VAN NAME, Amer. J. Sci., 1917, 43, 449.

(64). HOWARD, MANCOLLAS & PURDIE, Trans. Far. Soc., 1960, 56, 278.

(65). FISCHER, Anal. Chem., 1951, 23, 1667.

(66). HAUNERT & KLEBER, Kolloid Z., 1959, 162, 36.

(67). KOLTHOFF & BOYERS, J. Amer. Chem. Soc., 1954, 76, 1503.

(68). ALEXANDER, J. Phys. Chem., 1957, 61, 1563.

(69). HARBURG, ibid., 1946, 50, 190.

(70). TURKEVICH, J. Amer. Chem. Soc., 1960, 82, 4502.

(71). NIELSEN, J. Colloid Sci., 1955, 10, 576.

(72). DORSEUS, J. Phys. Chem., 1958, 62, 1068.

(73). KLISNAKOV & KIRKOVA, Z. phys. Chem.,(Leipzig)., 1957, 206, 271.

(74). HOAR, J. Appl. Chem., 1953, 3, 502.

(75). MICHAELS & COLVILLE, J. Phys. Chem., 1960, 64, 13.

(76). SEARS, J. Chem. Phys., 1958, 29, 1045.

(77). SMITH & PUDDINGTON, Cand. J. Chem,, 1960, 3973.

(78). GILES et. al. J. Chem. Soc., 1960, 3973.

(79). PEDERSON, Trans. Far. Soc., 1939, 35, 277.

(80). HAMMERSTON, Compt. Rend. Trav. Lab. Carlsburg., 1928, 17, No.11.

(81). SCHAFER, Z. anorg. Chem., 1905, 45, 293.

(82). BARNEY, J. Amer. Chem..Soc., 1951, 73, 3785.

(83). DAVIES, Trans. Far. Soc., 1927, 23, 351.

(84). BRESCIA & PEISACH, J. Amer. Chem. Soc., 1954, 76, 5946.

(85). LICHSTEIN & BRESCIA, ibid., 1957, 79, 1391.

(86). VOGEL, "Quantitative Inorganic Analysis", 1947, p. 340.

(87). SCHWARZENBACH, "Complexometric Titrations", English Translation by H. Irving, 1957, p.62.

(88). WYN WILLIAMS, Ph.D. Thesis, U.C.W. Aberystwyth, 1959.

(89). SEIDELL, "Solubility of Inorganic & Metal Organic Compounds", 2nd. Ed., New York, 1919.

(90). MIYAMOTO, Bull. Chem. Soc. Jap., 1960, 33, 371.

(91). UENO et. al., J. Chem. Soc. Jap., 1923, 35, 1368.

(92). NIELSEN, Acta. Chem. Scand., 1960, 14, 1654.

(93). NIELSEN, J. Phys. Chem., 1961, 65, 46.

(94). DAVIES, J. Chem. Soc., 1938, 2093.

(95). HARNED & OWEN, "Physical Chemistry of Electrolytic Solutions", Reinhold Publishing Corporation, New York, 1943, p. 127.

(96). SCHIEKHOLZ, Cand. J. Chem.,1958, 1057.

(97). NAIR & NANCOLLAS, J. Chem. Soc., 1958, 3706.

(98). WALTON & WALDEN, J. Amer. Chem. Soc., 1946, 68, 1742.

(99). DAWSON & McGAFFNEY, (4th. International Conference on Electron Microscopy, Berlin, 1958.).

(100). TAKIYAMA, Bull, Chem. Soc. Jap., 1959, 32, 68.

(101). TAKIYAMA, ibid., 1954, 27, 123.

(102). CUMMING & KAY, "Quantitative Chemical Analysis", 1948,p.86

(103). CUMING & SCHULMAN, Austr. J. Chem., 1959, 12, 413.

(104). ROSSEINSKY, Trans. Far. Soc., 1958, 54, 116.

Offprinted from the *Transactions of the Faraday Society*,
No. 446, Vol. 56, Part 2, February, 1960

THE PRECIPITATION OF SILVER CHLORIDE FROM AQUEOUS SOLUTIONS

PART 6.—KINETICS OF DISSOLUTION OF SEED CRYSTALS

Since the total amount of silver chloride dissolved during a run was only about 4 % of the weight of seed crystals present, changes in surface area, s, could be neglected.

A number of experiments were made in which the initial ionic ratio $[Ag^+]/[Cl^-]$ was not unity. Some of these are summarized in table 2 and in fig. 3, the rates of solution are plotted against Δ, the amount of silver chloride to be dissolved before equilibrium is

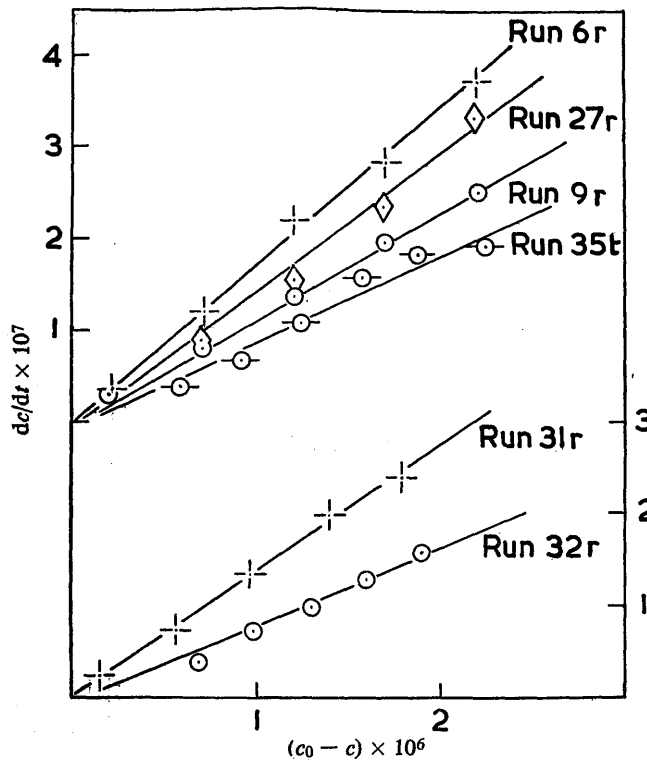

FIG. 2.—Rate of dissolution of silver chloride plotted against (c_0-c); $[Ag^+] = [Cl^-]$.

reached; when $[Ag^+] = [Cl^-]$, $\Delta = (c_0-c)$. The equation $dc/dt = k's\Delta$ is followed in a number of cases but there is a tendency for the rate to fall off during dissolution.

TABLE 2.—DISSOLUTION AT 25°C; $[Ag^+]/[Cl^-] \neq 1$

expt. no	initial concentrations (mole/l.)			ionic ratio	seed susp.	% sub-saturation
	$[Ag^+]\times 10^5$	$[Cl^-]\times 10^5$	$[Ag^+][Cl^-]\times 10^{10}$			
12_r	1·577	0·789	1·244	2·0	A	30
13_r	0·789	1·577	1·244	0·5	A	30
10_t	1·696	0·850	1·458	2·0	E	19
33_t	1·577	0·789	1·244	2·0	H	30
31_t	1·930	0·652	1·258	3·0	H	29
30_t	0·652	1·930	1·258	0·3	H	29
32_t	0·652	1·930	1·258	0·3	H	29
34_t	2·231	0·558	1·248	4·0	H	30
20_t	0·592	2·366	1·400	0·25	F	22
21_t	0·592	2·366	1·400	0·25	F	22

The results of experiments at 15 and 35° are given in table 3. As is seen in fig. 2, eqn. (1) is again obeyed.

Three runs were made of the dissolution of silver chromate seed crystals into sub-saturated solutions of silver chromate. Parallel pH runs exactly analogous to those in the

crystallization work [7] were carried out, and it was found that for dissolution as well as for crystallization, the pH was constant to within ±0·01 during the run. From the pH of the cell solution at the end of each dissolution experiment, $\alpha = [HCrO_4^-]/[CrO_4^{2-}]$ was obtained

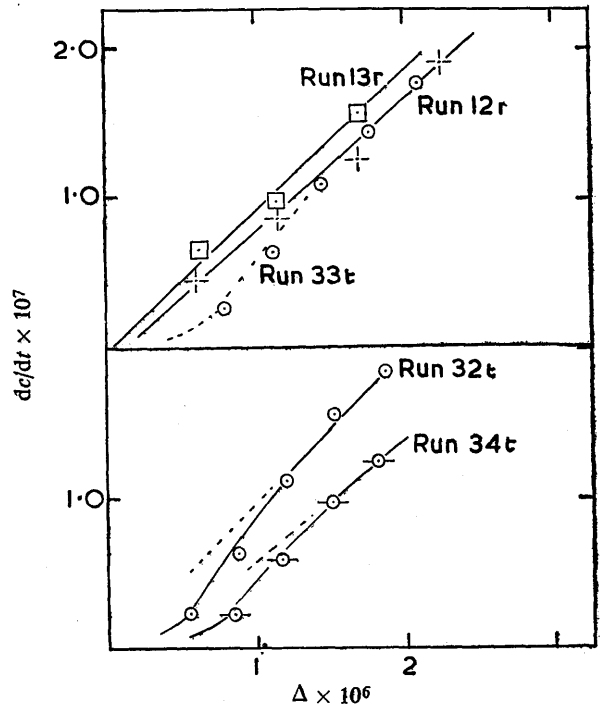

FIG. 3.—Rate of dissolution of silver chloride plotted against Δ; $[Ag^+] \neq [Cl^-]$.

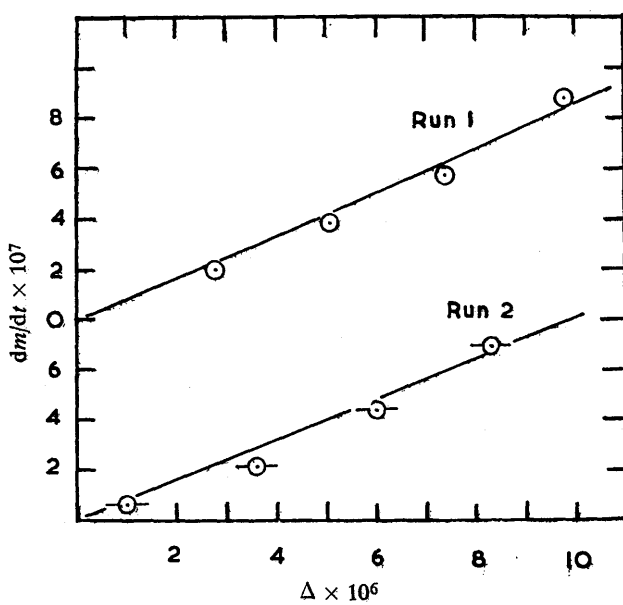

FIG. 4.—Rate of dissolution of silver chromate plotted against Δ.

and the changes in ionic concentrations $\delta[Ag^+]$ and $\delta[CrO_4^{2-}]$ during dissolution were calculated from the observed specific conductivity as described previously.[7] The data are given in table 4 and plots of dm/dt against Δ are shown in fig. 4. It is seen that for silver chromate the dissolution also follows first-order kinetics.

TABLE 3.—DISSOLUTION AT 15 AND 35°

expt. no.	temp.	initial concentrations (mole/l.)			seed susp.	% sub-saturation
		$[Ag^+]\times 10^5$	$[Cl^-]\times 10^5$	$[Ag^+][Cl^-]\times 10^{10}$		
32_r	15	0·618	0·618	0·382	C	0·080
33_r	15	0·618	0·618	0·382	C	0·088
29_r	35	1·800	1·800	3·240	C	0·141
31_r	35	1·813	1·814	3·289	C	0·138

TABLE 4.—DISSOLUTION OF SILVER CHROMATE AT 25°

expt. no.	pH	initial concentrations (mole/l.)			% sub-saturation
		$[Ag^+]\times 10^4$	$[CrO_4^{2-}]\times 10^4$	$[Ag^+]^2[CrO_4^{2-}]\times 10^{12}$	
1	7·6	1·60	0·74	1·89	31
2	7·2	1·66	0·69	1·91	30
3	6·9	1·71	0·61	1·78	35

DISCUSSION

Although crystallization of silver chloride and silver chromate under similar conditions has been found to follow second- and third-order equations respectively,[6, 7] the dissolution of both salts is a first-order reaction. This is in conformity with the results of most other workers which point to dissolution being a diffusion controlled process. The rate is proportional to the total surface area of seed crystals present. Assuming the seed crystals to be uniform cubes, the rate constant, 0·140, of expt. 27, becomes 0·120 when corrected for the difference in surface area of seed crystals used in expt. 26 and 27. This compares favourably with the value 0·126 found for expt. 26.

Previous study of the solution of silver chloride seed crystals into water [5] gave 3/2-order kinetics at 25° and it was suggested that this may have been due to the concentration gradient surrounding the particles being a significant fraction of the mean distance between particles. In the present work, when the initial sub-saturation was increased to about 70 % the process tended to follow a kinetic equation of a higher order then unity and it would seem that this effect may be dependent upon the size of the concentration gradient at the crystal surface, notwithstanding the Nernst assumption that the diffusion layer is of constant thickness.

It is interesting to note that the kinetics are not affected by the nature of the stirring: the vibration method indeed produces considerable turbulency. Equations relating the rotary stirring rate of diffusion controlled dissolution reactions with the rate constant k are usually of the form $k \propto (\text{rev/min})^a$, values [8] of a ranging from 0·56 to 1·0. When stirring rate was reduced from the normal 600 rev/min (expt. 6 and 8) to 320 rev/min (expt. 9), the reduction in k corresponds to $a = 0{\cdot}6_1$.

A more important test of Nernst's theory is afforded by the influence of temperature upon the rate of dissolution. The activation energy E_A may be derived graphically from the equation

$$\ln k = \ln A - (E_A/RT)$$

and the slope of the good straight line obtained on plotting log ks against $1/T$ gives an E_A of 5 kcal. This is very close to the activation energy for diffusion, 4·5 kcal and again points to diffusion being the controlling mechanism.

When either ion is in excess, it is seen from fig. 3 that the rate of dissolution falls off more rapidly than would be expected from a first-order equation; the effect is

more noticeable when Ag^+ ion is in excess. When $[Ag^+] = [Cl^-]$, however, the process follows eqn. (1) for at least 96 % of the available reaction. Adsorption of the ion in excess will begin immediately on adding the seed crystals to the subsaturated solution. Since it is unlikely that adsorption equilibrium will be maintained during the reaction, the process of dissolution will be opposed by that of adsorption and the surface will not be allowed to attain the potential necessary for the optimum release of Ag^+ and Cl^- ions in equal numbers. The result is a lowering of the rate of dissolution. Differences in the relative rates of adsorption of Ag^+ and Cl^- ions at the surface may account for the much larger lowering of dissolution rate when Ag^+ ions are in excess. Unfortunately the rates of adsorption are not known at present but it is hoped that some data may be available soon. It is interesting that the effect has not been detected previously in dissolution studies since these were usually followed for only 50-60 % of the available reaction in solutions containing stoichiometric proportions of the lattice ions.

We thank the D.S.I.R. for grants to J. R. H. and N. P.

[1] Nernst, *Z. physik. Chem.*, 1904, **47**, 52.
[2] Noyes and Whitney, *Z. physik. Chem.*, 1897, **23**, 689.
[3] e.g. King and Braverman, *J. Amer. Chem. Soc.*, 1932, **54**, 1744.
King and Schack, *J. Amer. Chem. Soc.*, 1935, **57**, 1212.
[4] King and Brodie, *J. Amer. Chem. Soc.*, 1937, **59**, 1375.
Antweiler, *Z. Elektrochem.*, 1938, **44**, 719.
[5] Davies and Nancollas, *Trans. Faraday Soc.*, 1955, **51**, 818.
[6] Davies and Jones, *Faraday Soc. Discussions*, 1949, **5**, 105.
[7] Howard and Nancollas, *Trans. Faraday Soc.*, 1957, **53**, 1449.
[8] Bircumshaw and Riddiford, *Quart. Rev.*, 1952, **6**, 157.